AFRL-AFOSR-VA-TR-2016-0066

OPTOELECTRONIC DEVICE INTEGRATION IN SILICON

Xiaodong Xu
UNIVERSITY OF WASHINGTON

10/26/2015
Final Report

Air Force Research Laboratory
AF Office Of Scientific Research (AFOSR)/ RTA1
Arlington, Virginia 22203
Air Force Materiel Command

REPORT DOCUMENTATION PAGE

Form Approved
OMB No. 0704-0188

PLEASE DO NOT RETURN YOUR FORM TO THE ABOVE ORGANIZATION.

1. REPORT DATE *(DD-MM-YYYY)*	2. REPORT TYPE	3. DATES COVERED *(From - To)*
13-10-2015	Final Technical Repoert	01 Aug 10 TO 31 Jul 15

4. TITLE AND SUBTITLE
Optoelectronic Device Integration in Silicon

5a. CONTRACT NUMBER

5b. GRANT NUMBER
FA9550-10-1-0439

5c. PROGRAM ELEMENT NUMBER

6. AUTHOR(S)
Dr. Mark Mirotznik

5d. PROJECT NUMBER

5e. TASK NUMBER

5f. WORK UNIT NUMBER

7. PERFORMING ORGANIZATION NAME(S) AND ADDRESS(ES)
University of Washington
Office of Sponsored Programs
4333 Brooklyn Ave NE
Seattle WA 98105-1016

8. PERFORMING ORGANIZATION REPORT NUMBER

9. SPONSORING/MONITORING AGENCY NAME(S) AND ADDRESS(ES)
Air Force Office of Scientific Research
875 N. Randolph St. Room 3112
Arlington VA 22203

10. SPONSOR/MONITOR'S ACRONYM(S)

11. SPONSOR/MONITOR'S REPORT NUMBER(S)

12. DISTRIBUTION/AVAILABILITY STATEMENT
Approved for public release: distribution unlimited.

13. SUPPLEMENTARY NOTES

14. ABSTRACT

This report summarizes achievements in Professor Hochberg's research group at the Universities of Washington and Delaware in the development of fundamental design tools and methodologies for optoelectronic devices in silicon photonics. We proposed to develop fundamental tools and methodologies that enable successful design of complex electronic-photonic integrated devices in silicon. We worked with a number of foundry partners, including BAE Systems, IME, and Luxtera, to develop leading-edge devices, including best-in-class modulators, couplers and detectors, and we prototyped integrated high-complexity devices that showcase these new design and layout capabilities. In particular we focused on devices that closely coupled electronics with photonics for low-loss data transmission, in order to realize multiple order-of-magnitude gains in performance and SWaP metrics. The goals of the project were to develop methodologies for designing and validating electronic-photonic integrated devices in silicon and to demonstrate leading-edge performance for a variety of device categories, including some fundamentally new device types. We developed a community of users for these processes, in order to enable the creation of a multi-project-wafer infrastructure for silicon photonics.

15. SUBJECT TERMS
Silicon photonics, electro-optical modulators, optical waveguides, optoelectronic integration, optical interconnects, photodetectors

16. SECURITY CLASSIFICATION OF:			17. LIMITATION OF ABSTRACT	18. NUMBER OF PAGES	19a. NAME OF RESPONSIBLE PERSON
a. REPORT	b. ABSTRACT	c. THIS PAGE			Mark Mirotznik
U	U	U	UU		19b. TELEPHONE NUMBER *(Include area code)* 302-831-4241

Reset

INSTRUCTIONS FOR COMPLETING SF 298

1. REPORT DATE. Full publication date, including day, month, if available. Must cite at least the year and be Year 2000 compliant, e.g. 30-06-1998; xx-06-1998; xx-xx-1998.

2. REPORT TYPE. State the type of report, such as final, technical, interim, memorandum, master's thesis, progress, quarterly, research, special, group study, etc.

3. DATES COVERED. Indicate the time during which the work was performed and the report was written, e.g., Jun 1997 - Jun 1998; 1-10 Jun 1996; May - Nov 1998; Nov 1998.

4. TITLE. Enter title and subtitle with volume number and part number, if applicable. On classified documents, enter the title classification in parentheses.

5a. CONTRACT NUMBER. Enter all contract numbers as they appear in the report, e.g. F33615-86-C-5169.

5b. GRANT NUMBER. Enter all grant numbers as they appear in the report, e.g. AFOSR-82-1234.

5c. PROGRAM ELEMENT NUMBER. Enter all program element numbers as they appear in the report, e.g. 61101A.

5d. PROJECT NUMBER. Enter all project numbers as they appear in the report, e.g. 1F665702D1257; ILIR.

5e. TASK NUMBER. Enter all task numbers as they appear in the report, e.g. 05; RF0330201; T4112.

5f. WORK UNIT NUMBER. Enter all work unit numbers as they appear in the report, e.g. 001; AFAPL30480105.

6. AUTHOR(S). Enter name(s) of person(s) responsible for writing the report, performing the research, or credited with the content of the report. The form of entry is the last name, first name, middle initial, and additional qualifiers separated by commas, e.g. Smith, Richard, J, Jr.

7. PERFORMING ORGANIZATION NAME(S) AND ADDRESS(ES). Self-explanatory.

8. PERFORMING ORGANIZATION REPORT NUMBER. Enter all unique alphanumeric report numbers assigned by the performing organization, e.g. BRL-1234; AFWL-TR-85-4017-Vol-21-PT-2.

9. SPONSORING/MONITORING AGENCY NAME(S) AND ADDRESS(ES). Enter the name and address of the organization(s) financially responsible for and monitoring the work.

10. SPONSOR/MONITOR'S ACRONYM(S). Enter, if available, e.g. BRL, ARDEC, NADC.

11. SPONSOR/MONITOR'S REPORT NUMBER(S). Enter report number as assigned by the sponsoring/ monitoring agency, if available, e.g. BRL-TR-829; -215.

12. DISTRIBUTION/AVAILABILITY STATEMENT. Use agency-mandated availability statements to indicate the public availability or distribution limitations of the report. If additional limitations/ restrictions or special markings are indicated, follow agency authorization procedures, e.g. RD/FRD, PROPIN, ITAR, etc. Include copyright information.

13. SUPPLEMENTARY NOTES. Enter information not included elsewhere such as: prepared in cooperation with; translation of; report supersedes; old edition number, etc.

14. ABSTRACT. A brief (approximately 200 words) factual summary of the most significant information.

15. SUBJECT TERMS. Key words or phrases identifying major concepts in the report.

16. SECURITY CLASSIFICATION. Enter security classification in accordance with security classification regulations, e.g. U, C, S, etc. If this form contains classified information, stamp classification level on the top and bottom of this page.

17. LIMITATION OF ABSTRACT. This block must be completed to assign a distribution limitation to the abstract. Enter UU (Unclassified Unlimited) or SAR (Same as Report). An entry in this block is necessary if the abstract is to be limited.

Final Technical Report

FA9550-10-1-0439

Prime Award Institution: University of Washington

Subaward Institution: University of Delaware

Title: Optoelectronic Device Integration in Silicon (OpSIS)

AFOSR POC:
Dr. Gernot Pomrenke, Program Officer
Air Force Office of Scientific Research
gernot.pomrenke@us.af.mil

Principal Investigator:
Dr. Michael Hochberg
Associate Professor
University of Washington (2010 – 2011)
Dr. David Castner (2012 – 2013)
Dr. Xiaodong Xu (2013 – 2015)

Subaward Principal Investigator:
Dr. Michael Hochberg
Associate Professor
University of Delaware (September 2012 – September 2014)

Dr. Mark Mirotznik (September 2014 – September 2015)
Professor of Electrical Engineering
University of Delaware
mirotzni@udel.edu

Table of Contents

I. Abstract

This report summarizes achievements in Professor Hochberg's research group at the University of Washington and University of Delaware in the development of fundamental design tools and methodologies for optoelectronic devices in silicon photonics, as well as in fundamental novel devices that were enabled by these new tools. This work has been supported by the AFOSR OpSIS award since 2010.

In the original proposal, we proposed to develop the fundamental tools and methodologies that will be required to successfully design complex electronic-photonic integrated devices in silicon. We worked with a number of foundry partners, including BAE Systems, IME, and Luxtera, to develop leading-edge devices, including best-in-class modulators, couplers and detectors, and we prototyped integrated high-complexity devices that showcase these new design and layout capabilities. In particular we focused on devices that closely coupled electronics with photonics for low-loss data transmission, in order to realize multiple order-of-magnitude gains in performance and SWaP metrics. The goals of the project were twofold: First, to develop methodologies for designing and validating electronic-photonic integrated devices in silicon, and second to demonstrate leading-edge performance for a variety of device categories, including some fundamentally new device types. We worked to develop a community of users for these processes, in order to enable the creation of a multi-project-wafer infrastructure for silicon photonics.

II. Summary of Results

The research goals began as a program centered on creating a shared platform for silicon photonics which would be accessible to a wide community. We sought to prove that such a community of users, sharing a single process, could in fact be developed. In this, OpSIS was a wild success. Across several development runs and 5 public MPW runs, OpSIS scaled to hundreds of active users. The model was a technical success, and produced a vibrant and much-imitated community.

Having observed the success and emerging economic impact of this model, several organizations around the world imitated it: PETRA in Japan is rumored to have been funded for ~$300M, IMEC in Belgium is spending tens of millions of dollars per year, IME is spending similar amounts in Singapore, and new efforts are booting up at CMC in Canada and in Korea. OpSIS tools are the best in the world, and represent the state of the art in photonic design automation and PDK depth.

OpSIS fulfilled its scientific mission, of proving that building these tools could be developed and used successfully by a wide swath of users. Unfortunately, the next step, which would have been to competitively fund an organization to transition these innovations into the commercial sphere, at a level commensurate with competing organizations around the world, proved to be elusive in the current funding climate.

Thus, Professor Hochberg has chosen to resign from UD and from NUS, in order to pursue a career in industry. OpSIS has delivered on everything that he promised, and has kick-started the creation of a new industry. A direct follow-on to OpSIS, the NMI in integrated photonics manufacturing, has been funded at the multi-hundred-million dollar level.

With Professor Hochberg's resignation from UD, and the shutdown of the OpSIS program, the new UD PI on this program is Professor Mirotznik. The program is now at an end, though new publications continue to emerge from labs such as Keren Bergman's, Dirk Englund's, and others around the world who have accessed the OpSIS chips.

Google Scholar indicates that 919 papers have been published including the words “OpSIS and Silicon”, as of the end of August 2015. AFOSR support has been acknowledged in all these publications and presentations.

III. The OpSIS Community

The OpSIS proposal outlined the developing of a community of users that utilize the processes developed through the OpSIS project including developing the methods to integrate electronics and optics together and demonstrate devices such as all-silicon EO modulators, low-loss junctions between waveguides and CMOS components.

External members of a silicon photonics “OpSIS Community” began working with the OpSIS group one year ahead of schedule and have far exceeded proposed numbers. Note; these numbers are research groups that utilize OpSIS technology for device design and do not include our long list of collaborators.

	Proposed	**Actual**
8/1/10 – 1/31/11	**0**	**0**
2/1/11 – 1/31/12	**0**	**0**
2/1/12 – 1/31/13	**0**	**25**
2/1/13 – 1/31/14	**10**	**28**
2/1/14 – 1/31/15	**20**	**60**

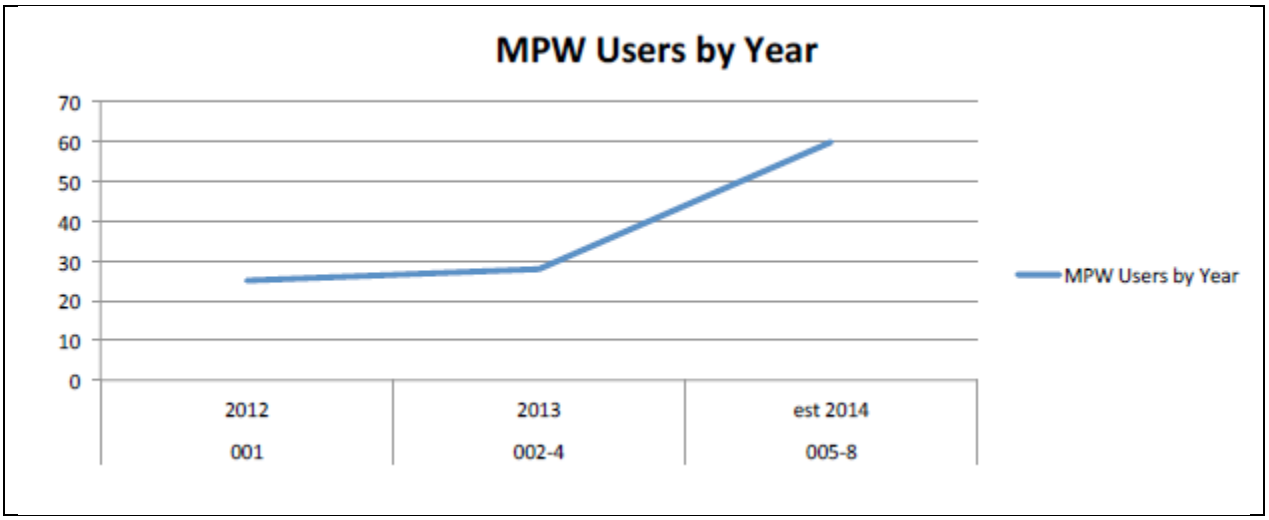

In the performance period the OpSIS grant has supported eleven graduate students, five staff and worked with eight affiliated faculty. In addition to students in the PIs group, OpSIS has supported the training of scientists in silicon photonics design methods. OpSIS has developed advanced photonic Process Design Kits at both IME and at BAE Systems and entered into a collaboration with the Institute for Microelectronics (IME) and National University of Singapore to obtain access to their PDK for device design. Sadly, the BAE Systems interaction came to an end shortly after the delivery to them of a working photonics process, due to the shutdown of their captive fabrication facility serving the DOD.

OpSIS collaborators and users include distinguished faculty from universities around the globe including the National University of Singapore (Singapore), McGill University (Canada), the University of Pavia (Italy), California Institute of Technology, MIT, Columbia University and many more. OpSIS work also

includes collaborations with the research divisions of corporations including Intel, Finisar, Chiral Photonics and others.

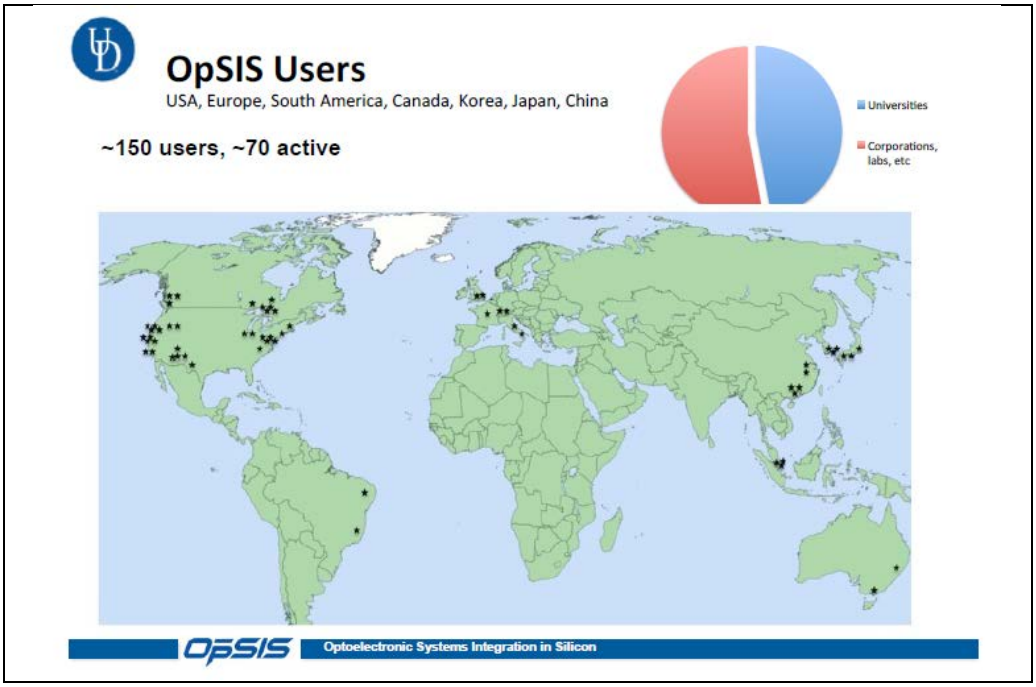

IV. Summary of Selected Publications Associated with OpSIS Support

The results of the research including scientific publications and patents are included in this report. AFOSR support has been acknowledged in these publications and presentations.

Published Papers Prior to 2014

Abdul-Majid, Sawsan, et al. "Photonic integrated interferometer based on silicon-on-insulator nano-scale MMI couplers." *Photonics Conference (IPC), 2013 IEEE*. IEEE, 2013.

Merget, Florian, et al. "Silicon photonics plasma-modulators with advanced transmission line design." Optics Express, Vol. 21, No. 17 (2013): 19593-19607. (2 citations)

Xiong, Yule, and W. Ye. "Silicon MMI-coupled slotted conventional and MZI racetrack microring resonators." Photonics Technology Letters, Vol. 25, No. 9 (2013): 1885-1888.

Sacher, Wesley, Tymon Barwicz, and Joyce K. Poon. "Silicon-on-Insulator Polarization Splitter-Rotator Based on TM0-TE1 Mode Conversion in a Bi-level Taper." CLEO: Science and Innovations. Optical Society of America (2013).

Simard, Alexandre D., Yves Painchaud, and Sophie LaRochelle. "Integrated Bragg gratings in spiral waveguides." Optics Express Vol. 21 No. 7 (2013): 8953-8963. (3 citations)

Zhu, Kehan, et al. "Design of a 10-Gb/s integrated limiting receiver for silicon photonics interconnects." Circuits and Systems (MWSCAS), 2013 IEEE 56th International Midwest Symposium on Circuits and

System. IEEE, 2013.

Runxiang Yu, Stanley Cheung, Yuliang Li, Katsunari Okamoto, Roberto Proietti, Yawei Yin, and S. J. B. Yoo, "A scalable silicon photonic chip-scale optical switch for high performance computing systems," Optics Express Vol. 21 No. 26, (2013): 32655-32667.

Mohammed Shafiqul Hai, Meer Nazmus Sakib, and Odile Liboiron-Ladouceur, "A 16 GHz silicon-based monolithic balanced photodetector with on-chip capacitors for 25 Gbaud front-end receivers," Optics Express Vol. 21, No. 26, (2013): 32680-32689.

Yule Xiong; Ye, W.N., "Slotted silicon microring resonators with multimode interferometer couplers," Group IV Photonics (GFP), 2013 IEEE 10th International Conference on Group IV Photonics (2013): 118 - 119, 28-30 August 2013.

Merget, F., et al. "Novel Transmission Lines for Si MZI Modulators." Group IV Photonics (GFP), 2013 IEEE 10th International Conference on Group IV Photonics (2013): 61 – 62, 28-30 August 2013.

K Zhu, S Balagopal, V Saxena, W Kuang . "Design of a 10-Gb/s integrated limiting receiver for silicon photonics interconnects" Circuits and Systems (MWSCAS), 2013 IEEE 56th International Midwest Symposium on Circuits and Systems (2013): 713 – 716, 4-7 August 2013.

Published Papers Associated with OpSIS Support in 2014 and 2015

Hochberg Group

Yi Zhang, Shuyu Yang, Hang Guan, Andy Eu-Jin Lim, Guo-Qiang Lo, Peter Magill, Tom Baehr-Jones, and Michael Hochberg, "Sagnac loop mirror and micro-ring based laser cavity for silicon-on-insulator," Opt. Express **22**, 17872-17879 (2014)

Y. Yang, C. Galland, Y. Liu, K. Tan, R. Ding, Q. Li, K. Bergman, T. Baehr-Jones, M. Hochberg. "Experimental demonstration of broadband Lorentz non-reciprocity in an integrable photonic architecture based on Mach-Zehnder modulators." Optics Express Vol. 22, No 14; 17409-17422 (2014).

Y. Liu, R. Ding, Y. Ma, Y. Yang, Z. Xuan, Q. Li, A. E.-J. Lim, P. G.-Q. Lo, K. Bergman, T. Baehr-Jones, M. Hochberg. "Silicon Mod-MUX-Ring transmitter with 4 channels at 40 Gb/s." Optics Express Vol. 22, No. 13; 16431-16438 (2014).

R. Ding, Y. Liu, Q. Li, Z. Xuan, Y. Ma, Y. Yang, A. E.-J. Lim, P. G.-Q. Lo, K. Bergman, T. Baehr-Jones, M. Hochberg. "A Compact Low-Power 320-Gb/s WDM Transmitter Based on Silicon Microrings." Photonics Journal Vol. 6, No. 3 (2014).

Y. Zhang, S. Yang, Y. Yang, M. Gould, N. Ophir, A. E.-J. Lim, P. G.-Q. Lo, P. Magill, K. Bergman, T. Baehr-Jones, M. Hochberg. "A high-responsivity photodetector absent metalgermanium direct contact." Optics Express, Vol. 22, No. 9; 11367-11375 (2014).

H. Guan, A. Novack, M. Streshinsky, R. Shi, Y. Liu, Q. Fang, A. E.-J. Lim, G.-Q. Lo, M. Hochberg, T. Baehr-Jones. "High-efficiency low-crosstalk 1310-nm polarization splitter and rotator built on a SOI platform." Photonics Technology Letters. Vol. PP, No. 99 (2014).

R. Ding, Y. Liu, Q. Li, Y. Ma, K. Padmaraju, A. E.-J. Lim, G.- Q. Lo, K. Bergman, T. Baehr-Jones, M. Hochberg. "Design and characterization of a 30-GHz bandwidth low-power silicon traveling-wave modulator." Optics Communications, Vol. 321; 124-133 (2014).

H. Guan, A. Novack, M. Streshinsky, R. Shi, Q. Fang, A. E.-J. Lim, P. G.-Q. Lo, T. Baehr-Jones, M. Hochberg. "CMOS-compatible highly efficient polarization splitter and rotator based on a double-etched directional coupler." Optics Express, Vol. 22, No. 3; 2489-2496 (2014).

S. Yang, Y. Zhang, D. Grund, G. Ejzak, Y. Liu, A. Novack, D. Prather, A. E.-J. Lim, P. G.-Q. Lo, T. Baehr-Jones, M. Hochberg. "A single adiabatic microring-based laser in 220 nm silicon-on-insulator." Optics Express Vol. 22. No. 1; 1173-1180 (2014).

M. Streshinsky, R. Shi, A. Novack, R. T. P. Cher, A. E.-J. Lim, P. G.-Q. Lo, T. Baehr-Jones, M. Hochberg. "A compact bi-wavelength polarization splitting grating coupler fabricated in a 220 nm SOI platform." Optics Express Vol. 21 No. 25; 31019-31028 (2013).

M. Streshinsky, R. Ding, Y. Liu, A. Novack, Y. Yang, Y. Ma, X. Tu, E. K. S. Chee, A. E.-J. Lim, P. G.-Q. Lo, T. Baehr-Jones, M. Hochberg. "Low power 50 Gb/s silicon traveling wave Mach-Zehnder Modulator near 1300 nm." Optics Express Vol. 21 No. 25; 30350-30357 (2013).

Y. Ma, Y. Zhang, S. Yang, A. Novack, R. Ding, A. E.-J. Lim, G.-Q. Lo, T. Baehr-Jones and M. Hochberg. "Ultralow loss single layer submicron waveguide crossing for SOI optical interconnect." Optics Express Vol. 21 No. 24; 29374-29382 (2013).

A. Novack, M. Gould, Y. Yang, Z. Xuan, M. Streshinsky, Y. Liu, G. Capellini, A. E.-J. Lim, G.-Q. Lo, T. Baehr-Jones and M. Hochberg. "Germanium photodetector with 60GHz bandwidth using inductive gain peaking." Optics Express Vol. 21 No. 23; 28387-28393 (2013).

Y. Liu, M. Hochberg, et. al. "Ultra-responsive Phase Shifters for depletion mode silicon modulators." IEEE/OSA Journal of Lightwave Technology Vol. 31 No. 23; 3787-3793 (2013).

M. Streshinsky, R. Ding, Y. Liu, A. Novack, C. Galland, A.E.-J Lim, P.Guo-Qiang Lo, T. Baehr-Jones and M. Hochberg. "The Road to Affordable, Large -Scale Silicon Photonics." Optics and Photonics News Vol. 24 No. 9; 32 – 39 (2013).

Example papers from OpSIS Users:

S. Bowers, B. Abiri, F. Aflatouni, and A. Hajimiri, "A Compact Optically Driven Travelling-Wave Radiating Source," in *Optical Fiber Communication Conference*, OSA Technical Digest (online) (Optical Society of America, 2014), paper Tu2A.3.

A. Malacarne, F. Gambini, S. Faralli, J. Klamkin, and L. Poti, "30-Gbps Silicon Microring Modulator for Short- and Medium-Reach Optical Interconnects," in *Optical Fiber Communication Conference*, OSA Technical Digest (online) (Optical Society of America, 2014), paper Th2A.4.

F. Gambini, G. Meloni, S. Faralli, G. Contestabile, L. Poti and J. Klamkin, "Ultra-Compact 56Gb/s QPSK and 80-Gb/s 16-QAM Silicon Coherent Receiver Free of Waveguide Crossings" (submitted to Group IV Photonics)

F. Gambini, S. Faralli, A. Malacarne, G. Meloni, G. Berrettini, G. Contestabile, L. Poti, J. Klamkin, "A Silicon Receiver for 100 Gb/s PDM-DQPSK Signals" 18th OptoElectronics and Communications Conference held jointly with 2013 International Conference on Photonics in Switching (OECC/PS)

Jonathan Klamkin, Fabrizio Gambini, Stefano Faralli, Antonio Malacarne, Gianluca Meloni, Gianluca Berrettini, Giampiero Contestabile, and Luca Potì, "A 100-Gb/s noncoherent silicon receiver for PDM-DBPSK/DQPSK signals," Opt. Express **22**, 2150-2158 (2014)

V. Technical Description of Selected Published Work Associated with OpSIS Support

1. Baehr-Jones, Tom; Ding, Ran; Ayazi, Ali; Pinguet, Thierry; Streshinsky, Matt; Harris, Nick; Li, Jing; He, Li; Gould, Mike and Zhang, Yi, "A 25 Gb/s silicon photonics platform," arXiv:1203.0767 (2012). (31 Google Scholar Citations)

Abstract: Silicon has attracted attention as an inexpensive and scalable material system for photonic-electronic, system-on-chip development. For this, a platform with both photodetectors and modulators working at high speeds, with excellent cross-wafer uniformity, is needed. We demonstrate an optical-lithography, wafer-scale photonics platform with 25 Gb/s operation. We also demonstrate modulation with an ultra-low drive voltage of 1 Vpp at 25 Gb/s. We demonstrate attractive cross-wafer uniformity, and provide detailed information about the device geometry. Our platform is available to the community as part of a photonics shuttle service.

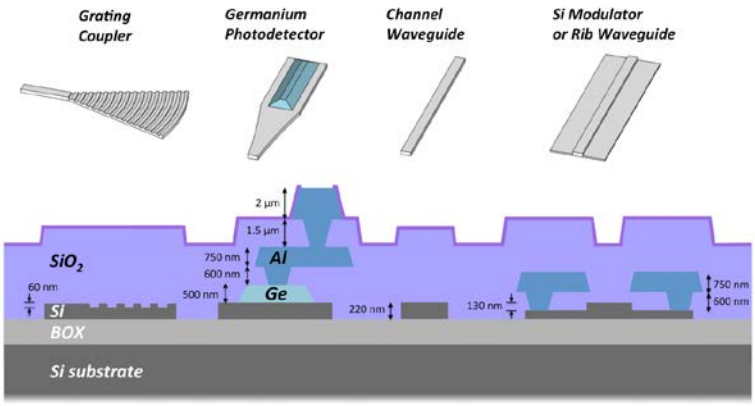

Fig. 1. Platform geometry. A diagram of the cross-sections of key devices is shown, as well as layer thicknesses. The platform features a 220 nm top silicon layer that has three possible etch depths, an epitaxially grown Ge layer, and two metal layers for electronic routing.

2. Gould, Michael; Baehr-Jones, Tom; Ding, Ran; and Hochberg, Michael, "Bandwidth enhancement of waveguide-coupled photodetectors with inductive gain peaking," Optics Express Vol.20, No. 7; 7101–7111 (2012). (10 Google Scholar Citations)

Abstract: Silicon has recently attracted a great deal of interest as an economical platform for integrated photonics systems. Integrated photodetectors are a key component of such systems, and CMOS compatible processes involving epitaxially grown germanium for photodetection have been demonstrated. Detector parasitic capacitance is a key limitation, which will likely worsen if techniques such as bump bonding are employed. Here we propose leveraging the complexity available in silicon photonics processes to compensate for this using a technique known as gain peaking. We predict that by simply including an inductor and capacitor in the photodetector circuit with the properly chosen values, detector bandwidths can be as much as doubled, with no undesired effects.

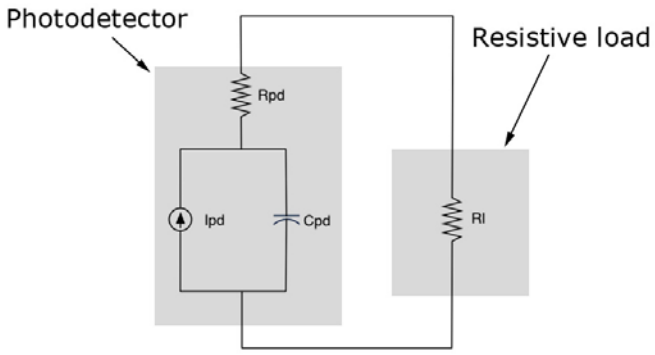

Fig. 1. Equivalent small-signal AC circuit for a photodetector and a simple resistive load. The parasitic capacitance and resistance of the detector is shown. The detector appears as a current source.

3. Ran Ding, Tom Baehr-Jones, Yang Liu, Ali Ayazi, Thierry Pinguet, Nick Harris, Matt Streshinsky, Poshen Lee, Yi Zhang, Andy Eu-Jin Lim, Tsung-Yang Liow, Selin Hwee-Gee Teo, Guo-Qiang Lo, and Michael Hochberg, "A 25 Gb/s 400 fJ/bit silicon traveling-wave modulator," Optical Interconnects Conference; 131-132 (2012). (2 Google Scholar Citations)

Abstract: We present a traveling-wave Mach-Zehnder modulator operates at 25 Gb/s with 1 Vpp. The 400 fJ/bit energy consumption is a 10X improvement over the best reported values in silicon Mach-Zehnders, becoming competitive with ring modulators.

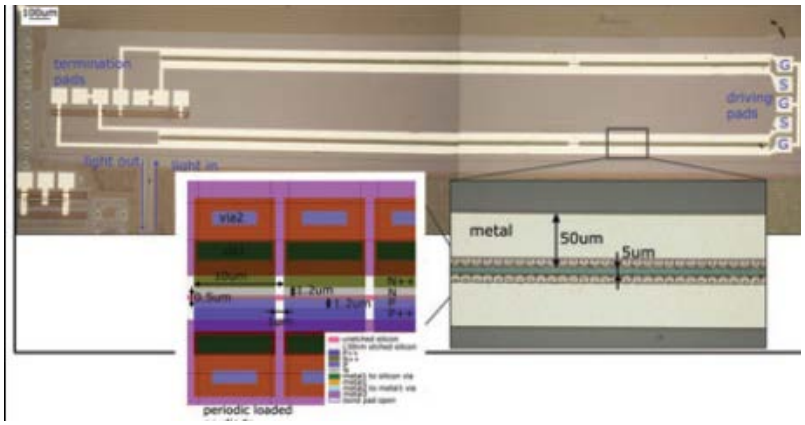

Figure 1 Device structure. Optical micrograph of the traveling-wave device, with the inset showing the detailed junction geometry and layout.

4. Baehr-Jones, Tom; Ding, Ran; Liu, Yang; Ayazi, Ali; Pinguet, Thierry; Harris, Nicholas C; Streshinsky, Matt; Lee, Poshen; Zhang, Yi; Lim, Andy Eu-Jin; "Ultralow drive voltage silicon traveling-wave modulator" Optics express Vo.20, No. 12; 12014-12020 (2012). (86 Google Scholar citations)

Abstract: There has been great interest in the silicon platform as a material system for integrated photonics. A key challenge is the development of a low-power, low drive voltage, broadband modulator. Drive voltages at or below 1 Vpp are desirable for compatibility with CMOS processes. Here we demonstrate a CMOS-compatible broadband traveling-wave modulator based on a reverse-biased pn junction. We demonstrate operation with a drive voltage of 0.63 Vpp at 20 Gb/s, a significant improvement in the state of the art, with an RF energy consumption of only 200 fJ/bit.

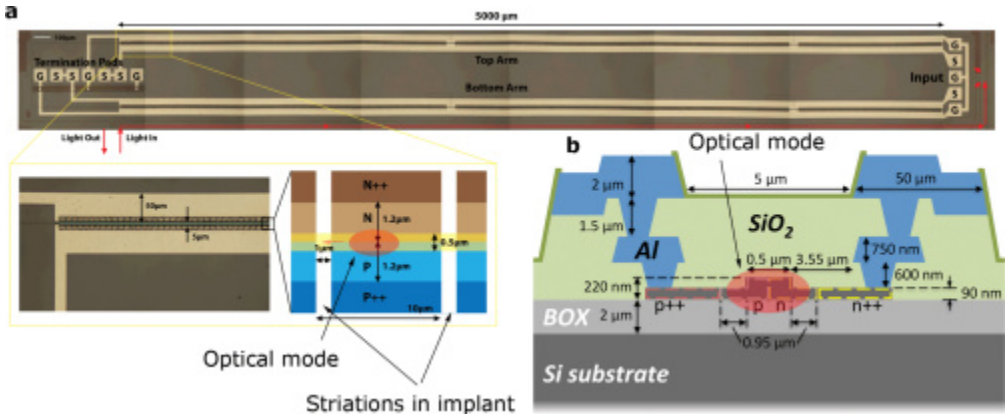

Fig. 1 Device structure and fabrication. (a) Optical micrograph of the traveling-wave device, with the inset showing the detailed junction geometry. Note that termination is achieved with a GSSGSSG configuration, providing a 25 Ω termination on each arm. The inset at highest magnification is a rendering of the layout file used in fabrication. (b) A cross-section of the fabricated device is shown, with the two metal layers indicated, as well as the rib waveguide structure and the lateral pn junction. The

current for the RF mode propagates largely in the thicker top metal layer due to striations in the pn junction and lower metal layer, lowering ohmic losses.

5. Ayazi, Ali; Baehr-Jones, Tom; Liu, Yang; Lim, Andy Eu-Jin; Hochberg, Michael; " Linearity of silicon ring modulators for analog optical links" Optics express Vol.20, No. 12; 13115-13122 (2012). (0 Google Scholar Citations)

Abstract: We study the nonlinear distortions of a silicon ring modulator based on the carrier depletion effect for analog links. Key sources of modulation nonlinearity are identified and modeled. We find that the most important source of nonlinearity is from the pn junction itself, as opposed to the nonlinear wavelength response of the ring modulator. Spurious free dynamic range for intermodulation distortion of as high as 84 dB.$Hz^{2/3}$ is obtained.

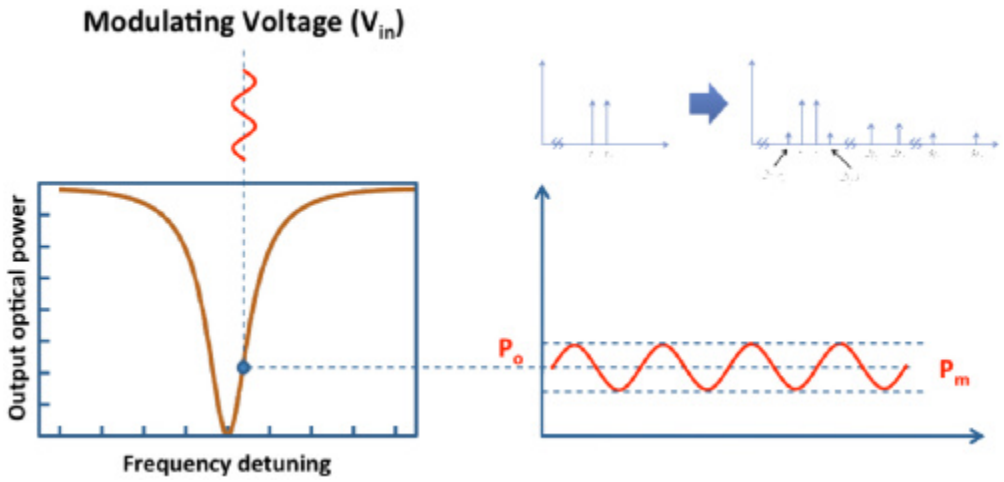

Fig. 1 Steady state transfer function of the silicon ring modulator.

6. Shi, Wei; Wang, Xu; Lin, Charlie; Yun, Han; Liu, Yang; Baehr-Jones, Tom; Hochberg, Michael; Jaeger, Nicolas AF; Chrostowski, Lukas; "Electrically tunable resonant filters in phase-shifted contra-directional couplers" IEEE Group IV Photonics Conference (San Diego, CA, USA 2012), paper WP2 (2012). (4 Google Scholar Citations)

Abstract: We demonstrate an electrically tunable resonant filter with FSR-free operation using a silicon photonic quarter-wavelength phase-shifted, grating-assisted contra-directional coupler. The spectrum shows a stop-band of 7nm, an extinction of 24dB, and a Q of 7,000.

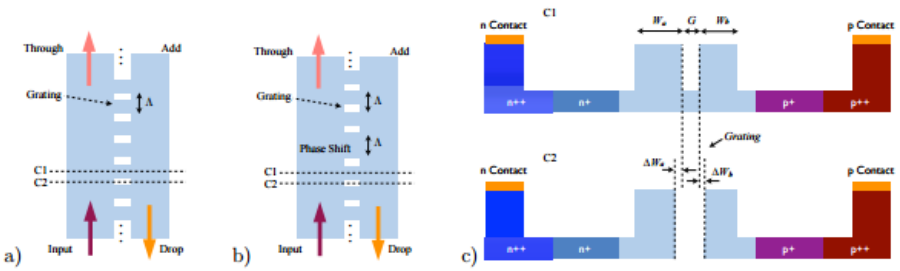

Fig. 1. a) Schematic top-view of a contra-directional coupler; b) Phase-shifted contra-directional coupler; c) Cross-sectional views of the contra-directional couplers at the positions (C1 and C2) indicated in (a) and (b).

7. Galland, Christophe; Novack, Ari; Liu, Yang; Ding, Ran; Gould, Michael; Baehr-Jones, Tom; Li, Qi; Yang, Yisu; Ma, Yangjin; Zhang, Yi; "Systems and devices in a 30 GHz Silicon-on-Insulator platform" ECOC Mo Vol. 3 (2013). (2 Google Scholar Citations)

Abstract: We present a 30 GHz silicon photonic platform that includes low-loss passive components, high-speed modulators and Ge-on-Si photodetectors. The platform is available to the community as part of the OpSIS-IME multi-project-wafer foundry service. We conclude with a proposal for a fully CMOS-compatible optical isolator based on multistage phase modulation.

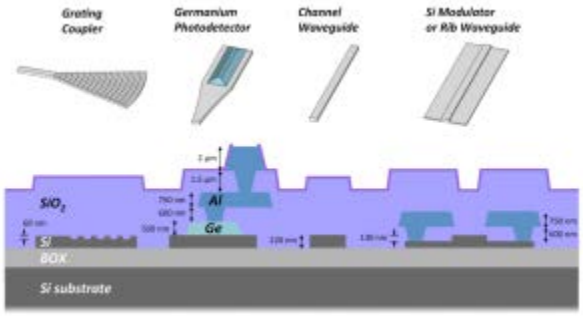

Fig. 1: Schematics of the layers cross-section

8. Zhang, Yi; Yang, Shuyu; Lim, Andy Eu-Jin; Lo, Guo-Qiang; Galland, Christophe; Baehr-Jones, Tom; Hochberg, Michael; "A compact and low loss Y-junction for submicron silicon waveguide" Optics express Vol. 21, No. 3; 1310-1316 (2013). (57 Google Scholar Citations)

Abstract: We designed a compact, low-loss and wavelength insensitive Y-junction for submicron silicon waveguide using finite difference time-domain (FDTD) simulation and particle swarm optimization (PSO), and fabricated the device in a 248 nm complementary metal-oxide-semiconductor (CMOS) compatible process. Measured average insertion loss is 0.28 ± 0.02 dB, uniform across an 8-inch wafer.

The device footprint is less than 1.2 μm x 2 μm, an order of magnitude smaller than typical multimode interferometers (MMIs) and directional couplers.

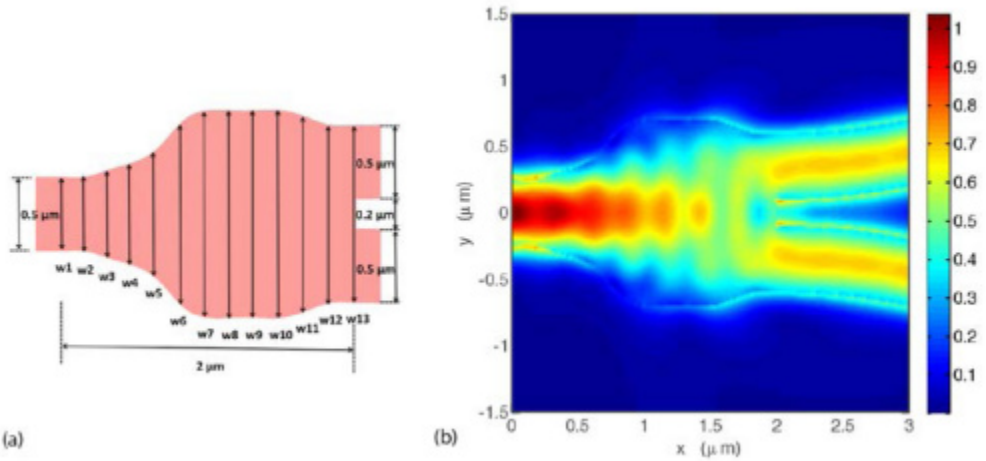

Fig. 1 *(a) Schematic of device layout. The taper geometry is defined by spline interpolation of w1 to w13. (b) Contour plot of simulated E-field distribution at 1550 nm wavelength.*

9. Shi, Wei; Wang, Xu; Lin, Charlie; Yun, Han; Liu, Yang; Baehr-Jones, Tom; Hochberg, Michael; Jaeger, Nicolas AF; Chrostowski, Lukas; "Silicon photonic grating-assisted, contra-directional couplers" Optics express Vol. 21, No. 3; 3633-3650 (2013). (21 Google Scholar Citations)

Abstract: We demonstrate, in both theory and experiment, 4-port, electrically tunable photonic filters using silicon contra-directional couplers (contra-DCs) with uniform and phase-shifted waveguide Bragg gratings. Numerical analysis, including both intra- and inter-waveguide couplings, is performed using coupled-mode theory and the transfer-matrix method. The contra-DC devices were fabricated by a CMOS-photonics manufacturing foundry and are electrically tunable using free-carrier injection. A 4-port, grating-based photonic resonator has been obtained using the phase-shifted contra-DC, showing a resonant peak with a 3-dB bandwidth of 0.2 nm and an extinction ratio of 24 dB. These contra-DC devices enable on-chip integration of Bragg-grating-defined functions without using circulators and have great potential for applications such as wavelength-division multiplexing networks and optical signal processing.

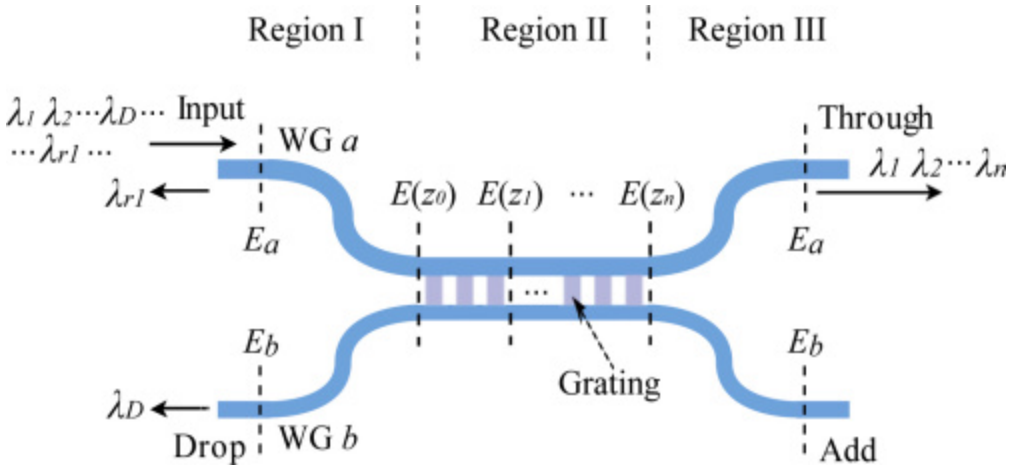

Fig. 1 Schematic drawing of a contra-DC-based add-drop filter. The field, E(z), in the coupler region, can be decomposed into the transverse modes, E_1 and E_2.

10. Streshinsky, Matthew; Ayazi, Ali; Xuan, Zhe; Lim, Andy Eu-Jin; Lo, Guo-Qiang; Baehr-Jones, Tom; Hochberg, Michael; "Highly linear silicon traveling wave Mach-Zehnder carrier depletion modulator based on differential drive" Optics express Vol. 21, No. 3; 3818-3825 (2013). (17 Google Scholar Citations)

Abstract: We present measurements of the nonlinear distortions of a traveling-wave silicon Mach-Zehnder modulator based on the carrier depletion effect. Spurious free dynamic range for second harmonic distortion of 82 dB·$Hz^{1/2}$ is seen, and 97 dB·$Hz^{2/3}$ is measured for intermodulation distortion. This measurement represents an improvement of 20 dB over the previous best result in silicon. We also show that the linearity of a silicon traveling wave Mach-Zehnder modulator can be improved by differentially driving it. These results suggest silicon may be a suitable platform for analog optical applications.

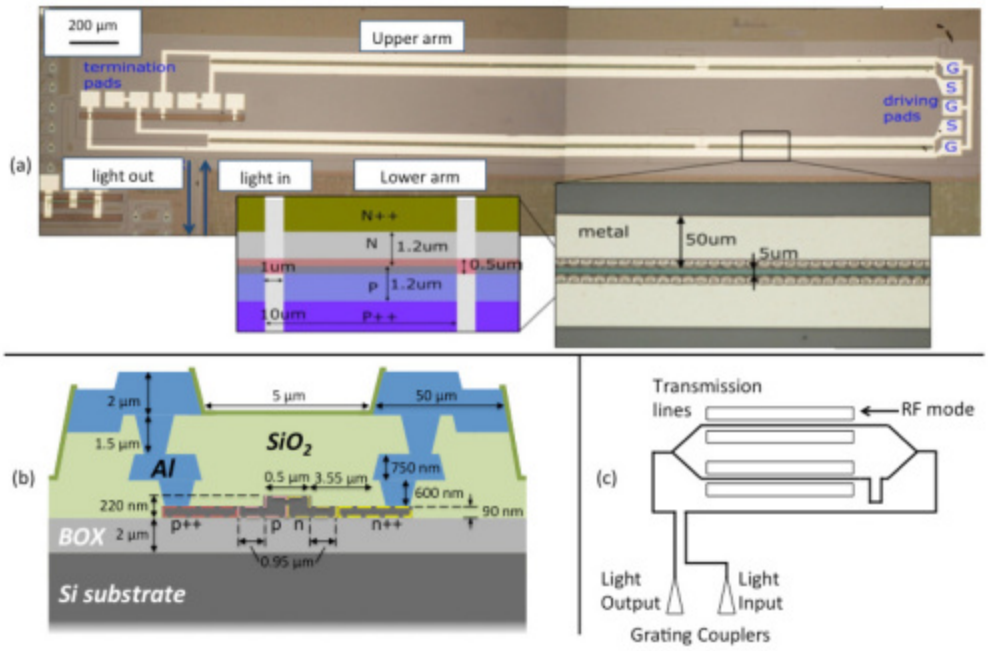

Fig. 1 *Device structure and fabrication. (a) Optical Micrograph of the traveling wave device, with the inset showing the detailed junction geometry. The inset at highest magnification is a rendering of the layout file used in fabrication. (b) A cross-section of the fabricated device is shown, with the two metal layers indicated, as well as the rib waveguide structure and the lateral pn junction. (c) Top-view schematic layout of the traveling wave device.*

11. Zhang, Yi; Yang, Shuyu; Lim, Andy Eu-Jin; Lo, G; Galland, Christophe; Baehr-Jones, Tom; Hochberg, Michael; "A CMOS-compatible, low-loss, and low-crosstalk silicon waveguide crossing" IEEE Photon. Technol. Lett Vol.25, No. 5; 422-425 (2013). (21 Google Scholar Citations)

Abstract: We demonstrated a waveguide crossing for submicron silicon waveguides with average insertion loss 0.18±0.03 dB and cross-talk -41±2 dB, uniform across an 8-inch wafer. The device was fabricated in a CMOS-compatible process using 248 nm lithography, with only one patterning step.

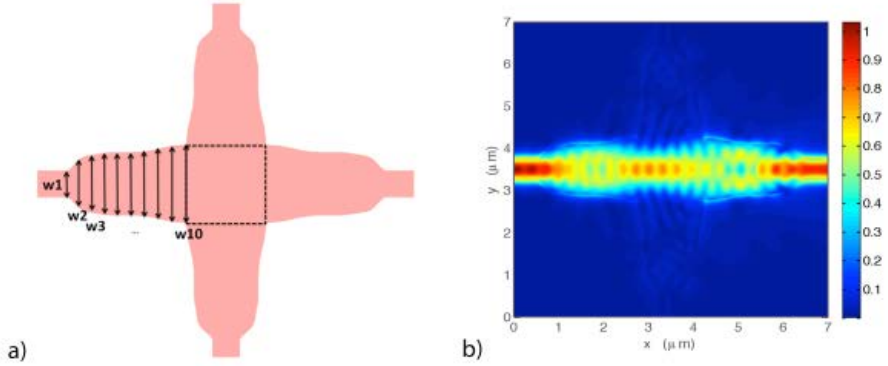

Fig. 1 Schematic layout of the waveguide crossing a) and contour plot of E-field distribution from FDTD simulation. The geometry of the taper connecting the input waveguide and intersection square is defined by spline interpolation of w1 to w10

12. Liu, Yang; Ding, Ran; Gould, Michael; Baehr-Jones, Tom; Yang, Yisu; Ma, Yangjin; Zhang, Yi; Lim, Andy Eu-Jin; Liow, Tsung-Yang; Teo, Selin Hwee-Gee; "30GHz silicon platform for photonics system" Optical Interconnects Conference; 27-28 (2013). (4 Google Scholar Citations)

Abstract: We present a silicon photonic platform offering low loss passive components, integrated highspeed silicon traveling wave MZ modulators (30GHz), ring modulators (45GHz) and inductance peaking Germanium photodetectors (58GHz). The bandwidth of the photonic devices is sufficient to support 50Gb/s bit rate. Our platform is available to the community as part of the OpSIS project.

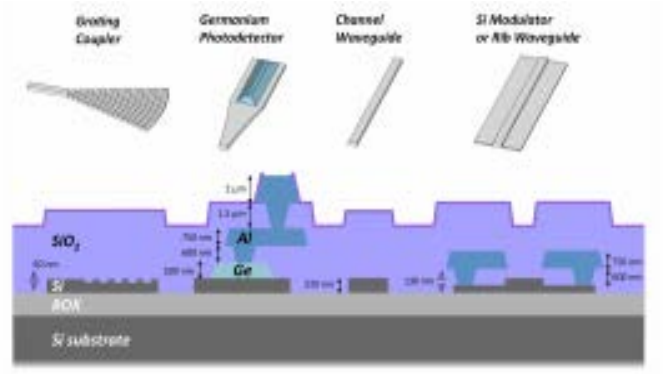

Fig 1. Illustration of the cross-section of opsis platform[6]

13. Novack, Ari; Liu, Yang; Ding, Ran; Gould, Michael; Baehr-Jones, Tom; Li, Qi; Yang, Yisu; Ma, Yangjin; Zhang, Yi; Padmaraju, Kishore; "A 30 GHz silicon photonic platform" SPIE Optics+ Optoelectronics 878107-87810 (2013). (25 Google Scholar Citations)

Abstract: Silicon photonics has emerged as a promising material system for the fabrication of photonic devices as well as electronic ones. The key advantage is that many electronic and photonic functions that up to now have only been available as discrete components can be integrated into a single package. We present a silicon photonic platform that includes low-loss passive components as well as high-speed modulators and photodetectors at or above 30 GHz. The platform is available to the community as part of the OpSIS-IME MPW service.

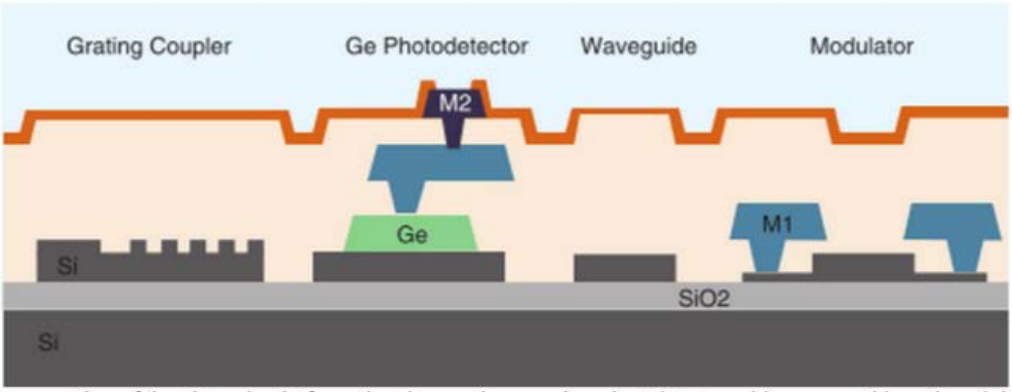

Figure 1. Cross section of the photonic platform showing grating coupler, photodetector, ridge waveguide and modulator

14. Galland, Christophe; Novack, Ari; Liu, Yang; Ding, Ran; Gould, Michael; Baehr-Jones, Tom; Li, Qi; Yang, Yisu; Ma, Yangjin; Zhang, Yi; "A CMOS-compatible silicon photonic platform for high-speed integrated opto-electronics" SPIE Microtechnologies 8767-G-87670G (2013). (8 Google Scholar Citations)

Abstract: We have developed a CMOS-compatible Silicon-on-Insulator photonic platform featuring active components such as pi-n and photoconductive (MIM) Ge-on-Si detectors, p-i-n ring and Mach-Zehnder modulators, and traveling-wavemodulators based on a p-n junction driven by an RF transmission line. We have characterized the yield and uniformity of the performance through automated cross-wafer testing, demonstrating that our process is reliable and scalable. The entire platform is capable of more than 40 GB/s data rate. Fabricated at the IME/A-STAR foundry in Singapore, it is available to the worldwide community through *OpSIS*, a successful multi-project wafer service based at the University of Delaware. After exposing the design, fabrication and performance of the most advanced platform components, we present our newest results obtained after the first public run. These include low loss passives (Y-junctions: 0.28 dB; waveguide crossings: 0.18 dB and cross-talk -41±2 dB; non-uniform grating couplers: 3.2±0.2 dB). All these components were tested across full 8" wafers and exhibited remarkable uniformity. The active devices were improved from the previous design kit to exhibit 3dB bandwidths ranging from 30 GHz (modulators) to 58 GHz (detectors). We also present new packaging services available to *OpSIS* users: vertical fiber coupling and edge coupling.

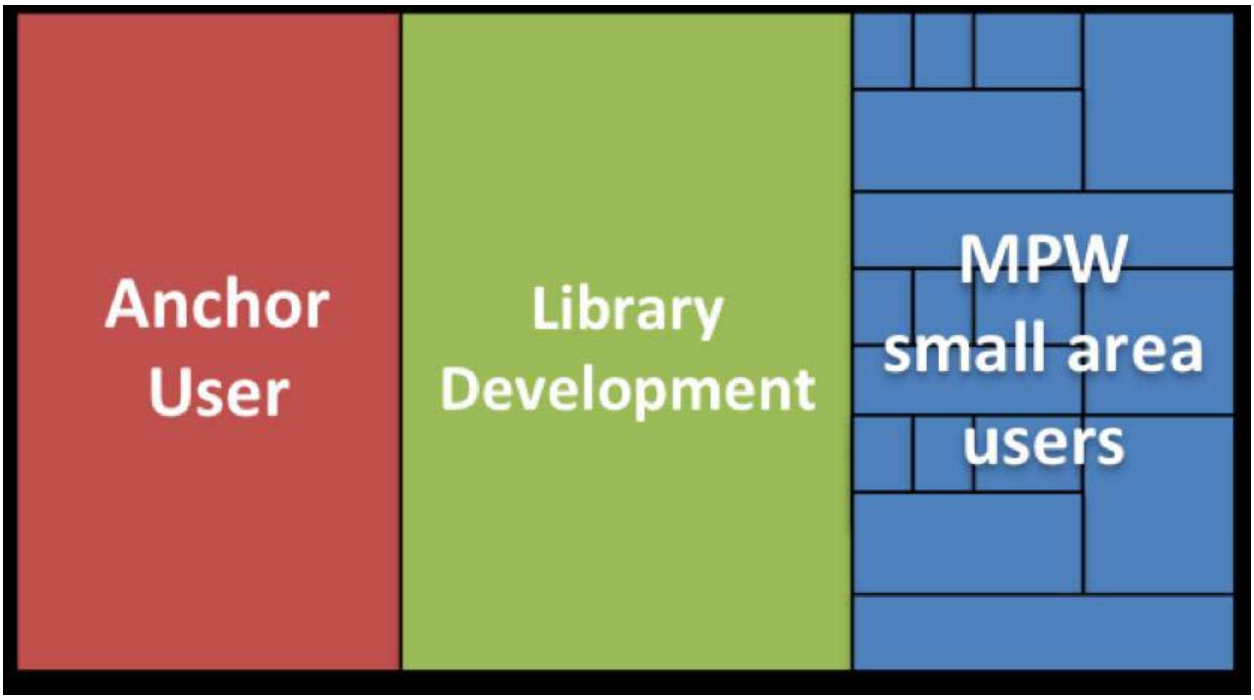

Fig. 1: Concept of Multi-Project-Wafer (MPW) service. Anchor users are typically companies buying large areas over several runs for long-term projects

15. Galland, Christophe; Ding, Ran; Harris, Nicholas C; Baehr-Jones, Tom; Hochberg, Michael; "Broadband on-chip optical non-reciprocity using phase modulators" Optics express Vol. 21, No. 12; 14500-14511 (2013). (5 Google Scholar Citations)

Abstract: Breaking the reciprocity of light propagation in a nanoscale photonic integrated circuit (PIC) is a topic of intense research, fostered by the promises of this technology in areas ranging from experimental research in classical and quantum optics to high-rate telecommunications and data interconnects. In particular, silicon PICs fabricated in processes compatible with the existing complementary metal-oxide-semiconductor (CMOS) infrastructure have attracted remarkable attention. However, a practical solution for integrating optical isolators and circulators within the current CMOS technology remains elusive. Here, we introduce a new nonreciprocal photonic circuit operating with standard single-mode waveguides or optical fibers. Our design exploits a time-dependent index modulation obtained with conventional phase modulators such as the one widely available in silicon photonics platforms. Because it is based on fully balanced interferometers and does not involve resonant structures, our scheme is also intrinsically broadband. Using realistic parameters we calculate an extinction ratio superior to 20dB and insertion loss below 3dB.

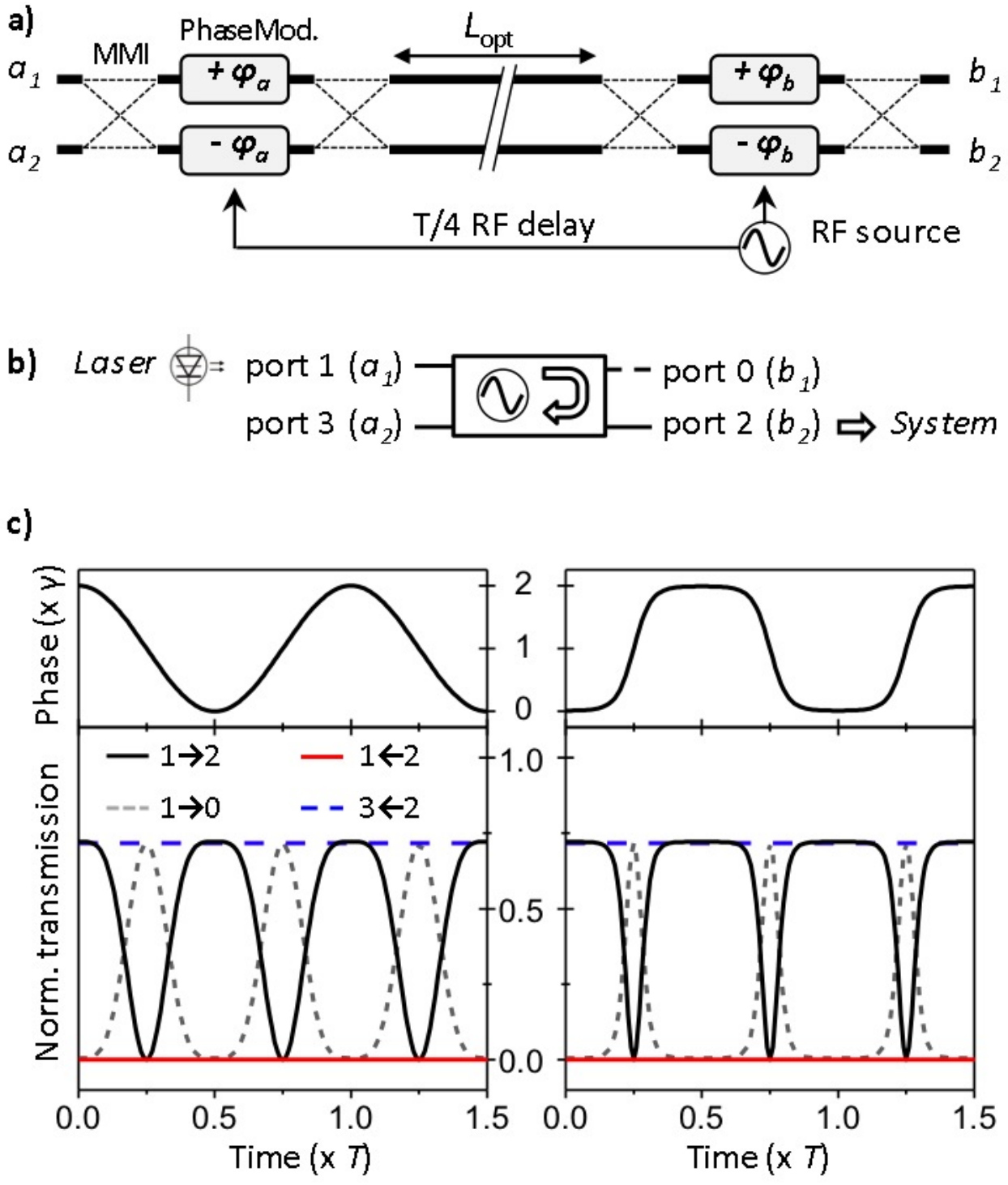

Fig. 1. (a) Schematic of the proposed design. MMI: multimode interferometer. The waveguide length of the optical delay is Lopt = T/4 c/ng. (b) Conceptualization of the device as a nonreciprocal modulator. (c) Computed behavior for a cosine (left panels) and a bandwidth-limited square wave (right panels) as modulator drive signals. The waveforms are shown in the upper panels. In the lower panels, we plot the transmission coefficients from port 1 to 2 (solid black line), 2 to 1 (solid red line), 1 to 0 (dashed grey line) and 2 to 3 (dashed blue line). We note that the device is symmetric under the simultaneous

permutation 1↔3 and 0↔2. For the simulations we used the following parameters: MMI loss = 0.1dB [21, 22]; waveguide loss = 0.3dB/cm [23]; total waveguide length = 8 mm; dynamic loss = 2dB / π phase shift (see section 5.2).

16. He, Li; Liu, Yang; Galland, Christophe; Lim, Andy Eu-Jin; Lo, Guo-Qiang; Baehr-Jones, Tom; Hochberg, Michael; "A high-efficiency nonuniform grating coupler realized with 248-nm optical lithography" Photonics Technology Letters, IEEE Vol.25, No. 14;1358-1361 (2013).

Abstract: We describe a high-efficiency grating coupler (GC) fabricated on a silicon-on-insulator wafer with 220 nm top silicon layer. One single 60 nm shallow etch is required to define the diffractive gratings with a minimum lithographic feature size of 180 nm, which is within the limitation of 248 nm deep ultraviolet lithography. The measured average insertion loss is 3.1 ± 0.2 dB ~1550 nm with a 1 dB bandwidth of 41 ± 4 nm for TE polarization, whereas the best device exhibits 2.7 dB loss. The measured GC backreflection loss is better than 17 dB across the wafer. Cross-wafer data shows good uniformity and tolerance to fabrication variations. This is the best result reported for the commonly used 220 nm thickness Si that uses only a shallow etch step.

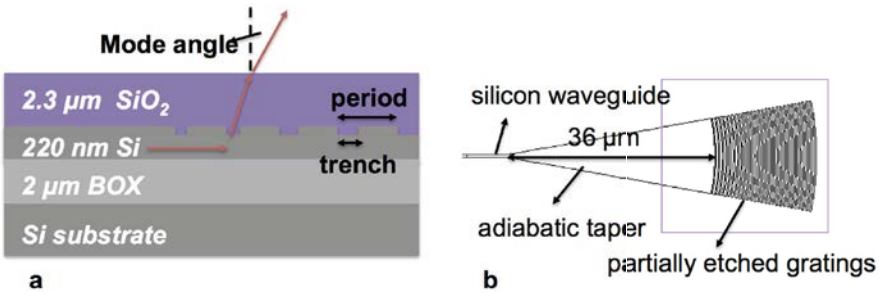

Fig. 1. Device geometry. (a) Cross-section view of the grating couplers. (b) Lateral layout of the grating couplers.

17. Streshinsky, M; Ding, R; Liu, Y; Novack, A; Galland, C; Lim, AE-J; Guo-Qiang Lo, P; Baehr-Jones, T; Hochberg, M; "The road to affordable, large-scale silicon photonics" Optics and Photonics News Vol.24, No. 9; 32-39 (2013).

Abstract: Large-scale optical systems in silicon can become a reality by building upon the existing infrastructure. Due to the shifting economics of silicon photonics, some cost-effective fabless silicon products may even emerge over the next several years.

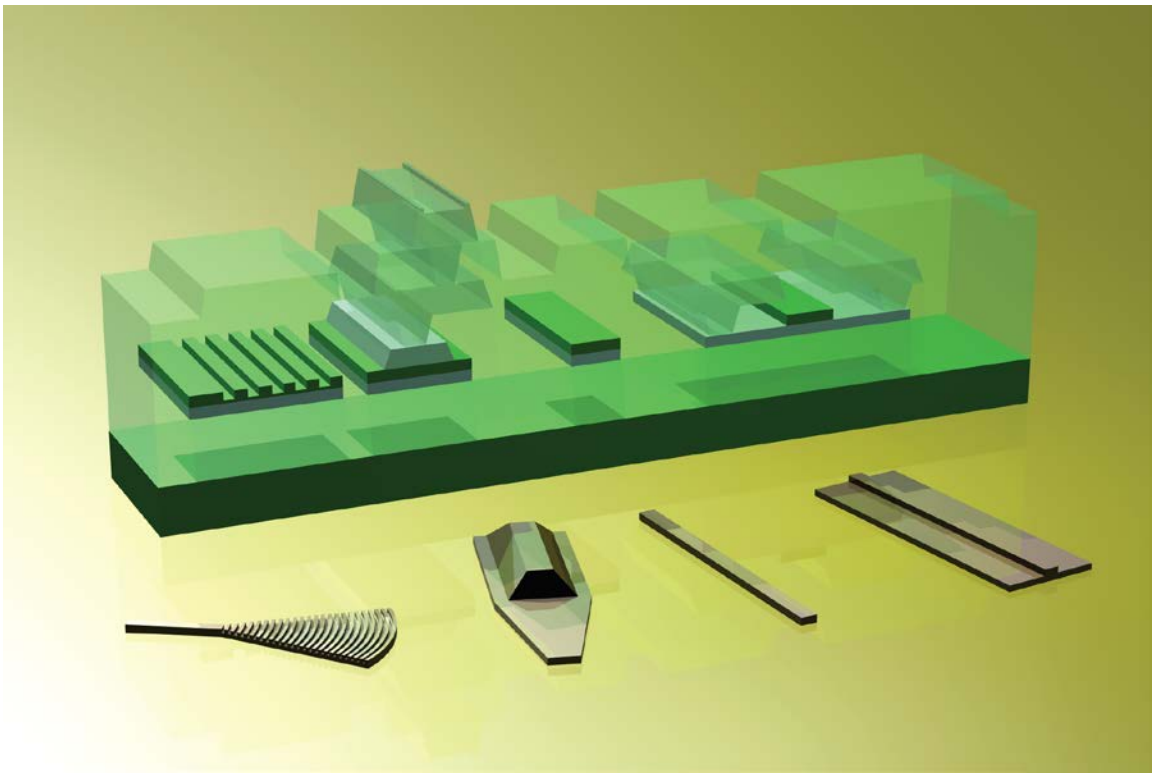

18. Novack, Ari; Gould, Mike; Yang, Yisu; Xuan, Zhe; Streshinsky, Matthew; Liu, Yang; Capellini, Giovanni; Lim, Andy Eu-Jin; Lo, Guo-Qiang; Baehr-Jones, Tom; "Germanium photodetector with 60 GHz bandwidth using inductive gain peaking" Optics express Vol.21, No. 23; 28387-28393 (2013). (23 Google Scholar Citations)

Abstract: Germanium-on-silicon photodetectors have been heavily investigated in recent years as a key component of CMOS-compatible integrated photonics platforms. It has previously been shown that detector bandwidths could theoretically be greatly increased with the incorporation of a carefully chosen inductor and capacitor in the photodetector circuit. Here, we show the experimental results of such a circuit that doubles the detector 3dB bandwidth to 60 GHz. These results suggest that gain peaking is a generally applicable tool for increasing detector bandwidth in practical photonics systems without requiring the difficult process of lowering detector capacitance.

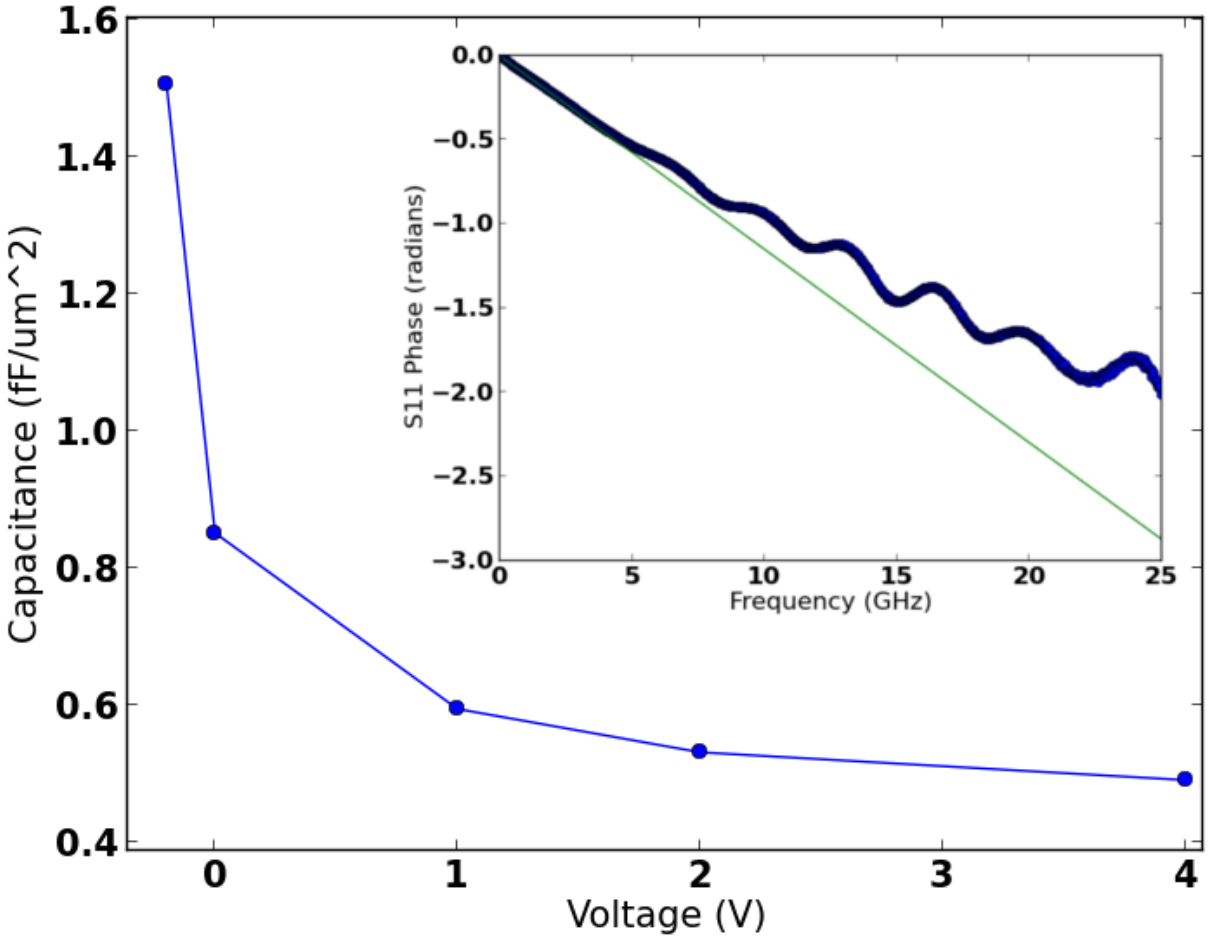

Fig. 1. Junction capacitance per unit area as a function of reverse bias voltage (positive voltage on graph is reverse bias). The curve was measured by determining the capacitance from the detector S11 parameter (as seen in inset) using a number of test structures of different areas. The junction capacitance

19. Ma, Yangjin; Zhang, Yi; Yang, Shuyu; Novack, Ari; Ding, Ran; Lim, Andy Eu-Jin; Lo, Guo-Qiang; Baehr-Jones, Tom; Hochberg, Michael; "Ultralow loss single layer submicron silicon waveguide crossing for SOI optical interconnect" Optics express Vol.21, No.24; 29374-29382 (2013).

Abstract: Germanium-on-silicon photodetectors have been heavily investigated in recent years as a key component of CMOS-compatible integrated photonics platforms. It has previously been shown that detector bandwidths could theoretically be greatly increased with the incorporation of a carefully chosen inductor and capacitor in the photodetector circuit. Here, we show the experimental results of such a circuit that doubles the detector 3dB bandwidth to 60 GHz. These results suggest that gain peaking is a generally applicable tool for increasing detector bandwidth in practical photonics systems without requiring the difficult process of lowering detector capacitance.

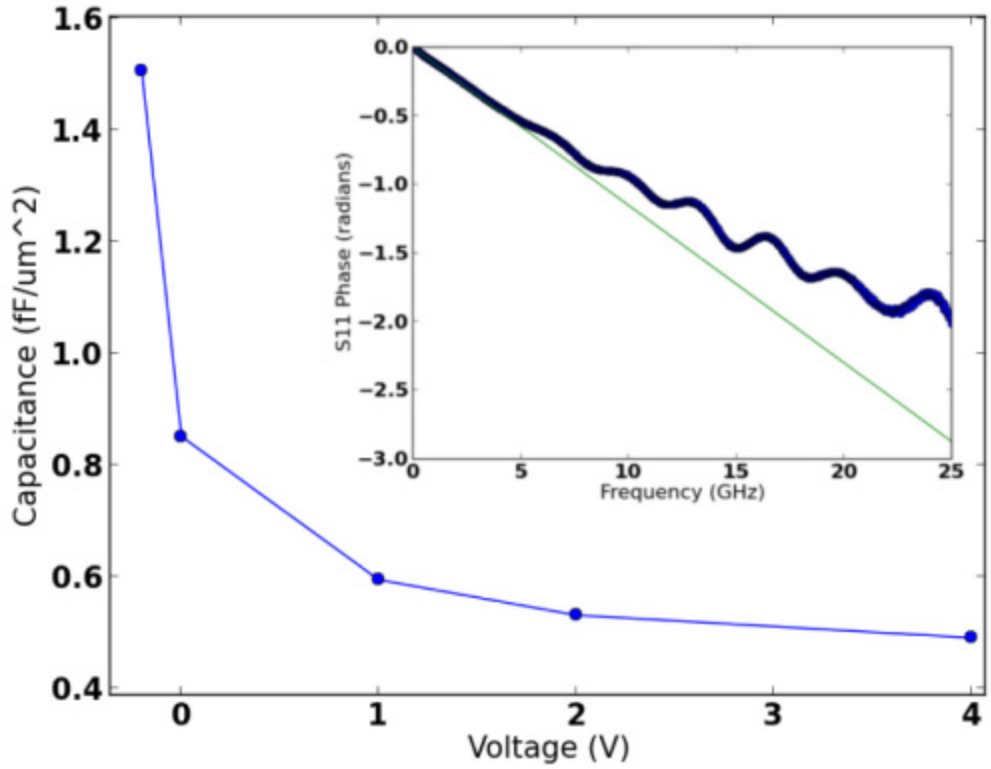

Fig. 1 *Junction capacitance per unit area as a function of reverse bias voltage (positive voltage on graph is reverse bias). The curve was measured by determining the capacitance from the detector S11 parameter (as seen in inset) using a number of test structures of different areas. The junction capacitance*

20. Streshinsky, Matthew; Ding, Ran; Liu, Yang; Novack, Ari; Yang, Yisu; Ma, Yangjin; Tu, Xiaoguang; Chee, Edward Koh Sing; Lim, Andy Eu-Jin; Lo, Patrick Guo-Qiang; "Low power 50 Gb/s silicon traveling wave Mach-Zehnder modulator near 1300 nm" Optics express Vol.21, No.25;30350-30357 (2013). (36 Google Scholar Citations)

Abstract: The wavelength band near 1300 nm is attractive for many telecommunications applications, yet there are few results in silicon that demonstrate high-speed modulation in this band. We present the first silicon modulator to operate at 50 Gbps near 1300 nm. We demonstrate an open eye at this speed using a differential 1.5 V_{pp} signal at 0 V reverse bias, achieving an energy efficiency of 450 fJ/bit.

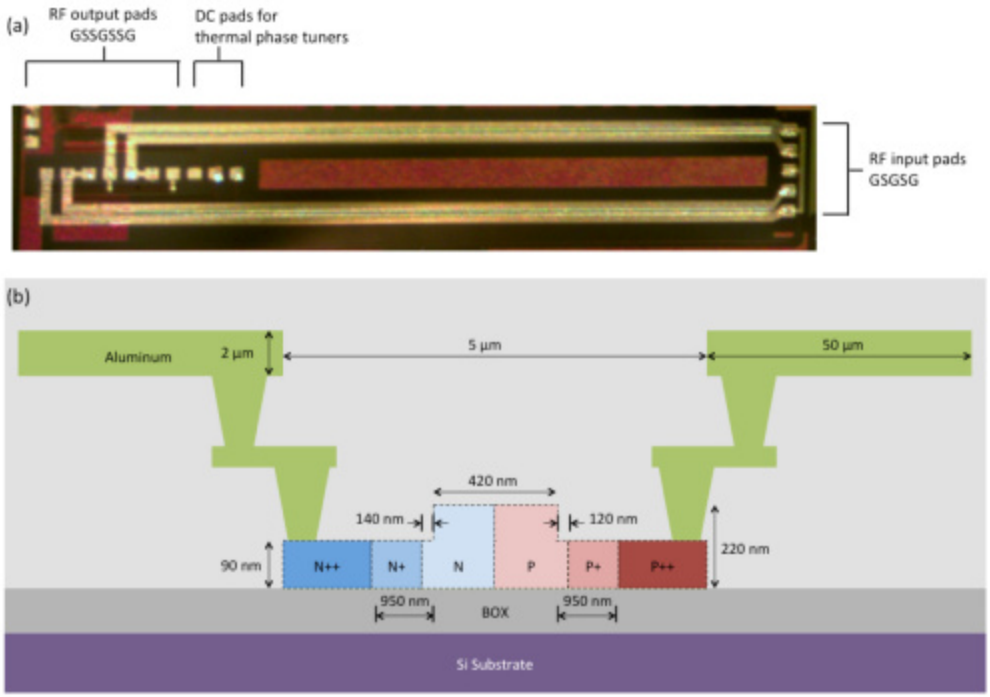

Fig. 1 *(a) Micrograph of the device. (b) Simplified cross sectional diagram of the phase shifter, not to scale.*

21. Liu, Yang; Ding, Ran; Li, Qi; Zhe, Xuan; Li, Yunchu; Yang, Yisu; Lim, Andy E; Lo, Patrick Guo-Qiang; Bergman, Keren; Baehr-Jones, Tom; "Ultra-compact 320 Gb/s and 160 Gb/s WDM transmitters based on silicon microrings" Optical Fiber Communication Conference; Th4G. 6 (2014). (13 Google Scholar Citations)

Abstract: We demonstrated 320Gb/s 8-channel and 160Gb/s 4-channel WDM transmitter using silicon microrings based on conventional common-bus architecture and a new "Mod-MUX" architecture respectively. We discuss and compare the two designs and highlight their complementary merits.

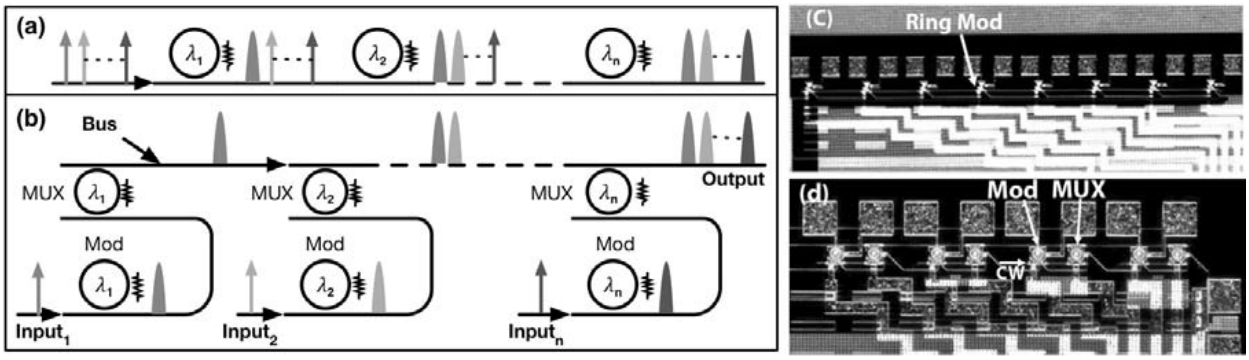

Fig.1 (a) schematic diagram of the common bus design, (b) schematic diagram of the Mod-MUX design, (c) photograph of fabricated 8 ring transmitter based on traditional common bus design; (d) photograph of the fabricated Mod-MUX design.

22. Li, Qi; Liu, Yang; Padmaraju, Kishore; Ding, Ran; Logan, Dylan F; Ackert, Jason J; Knights, Andrew P; Baehr-Jones, Tom; Hochberg, Michael; Bergman, Keren; "10-Gb/s BPSK link using silicon microring resonators for modulation and demodulation" Optical Fiber Communication Conference; Tu2E. 5, (2014). (1 Google Scholar Citation)

Abstract: We demonstrate the first binary-phase-shift-keying (BPSK) link based on silicon microring resonators, with an operational bit-rate at 10 Gb/s. Bit-error-rate measurements and eye diagrams are used to compare the link's performance with conventional BPSK modulation and demodulation techniques.

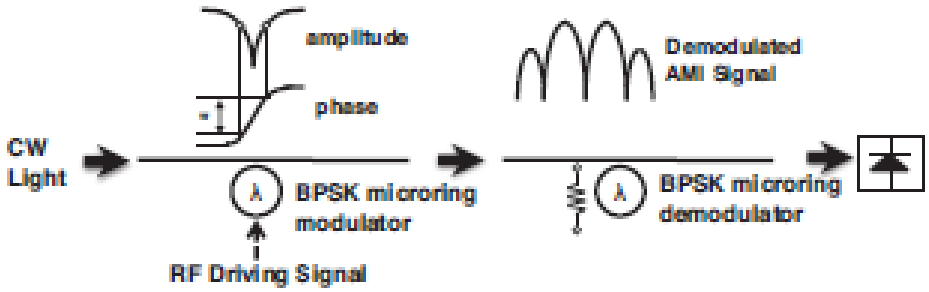

Fig. 1. Microring based BPSK link.

23. Ma, Yangjin; Xuan, Zhe; Liu, Yang; Ding, Ran; Li, Yunchu; Lim, AE; Lo, G; Baehr-Jones, Tom; Hochberg, Michael; "Silicon Microring Based Modulator and Filter for High Speed Transmitters at 1310 nm" IEEE Opt. Interconnect Conf. MC6 ; 23-24 (2014). (1 Google Scholar Citation)

Abstract: We present silicon microring based high--speed modulator and highly tunable filter working near 1310 nm with CMOS compatible process. Our design shows great potential in building ultra--compact silicon photonic WDM transmitters for O--band telecommunications.

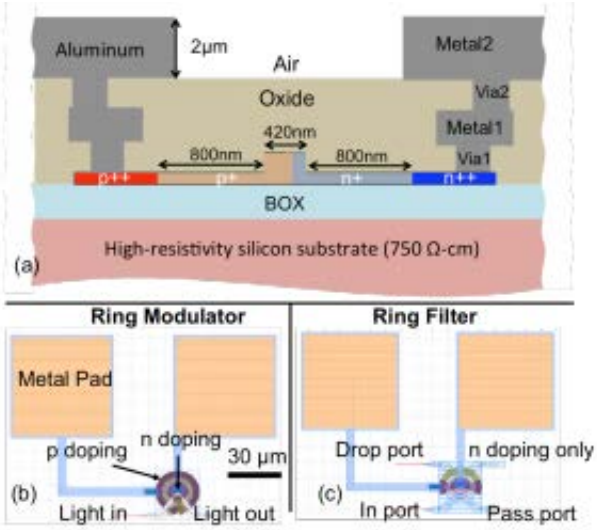

Fig. 1 (a) Schematic cross sectional diagram of ring modulator, not to scale. (b) Micrograph of ring modulator.

24. Liu, Yang; Ding, Ran; Li, Qi; Ma, Yangjin; Yang, Yisu; Lim, Andy Eu-Jin; Lo, Guo-Qiang; Bergman, Keren; Baehr-Jones, Tom; Hochberg, Michael; "40-Gb/s Silicon Modulators for Mid-Reach Applications at 1550 nm" Optical Interconnects Conference, 2014 IEEE ; 19-20 (2014). (0 Google Scholar Citations)

Abstract: We characterize fiber transmissions of silicon Mach-Zehnder and ring modulators at 1550 nm and show that 2-km reach in standard SMF is achieved with minimal power penalty at 40 Gb/s

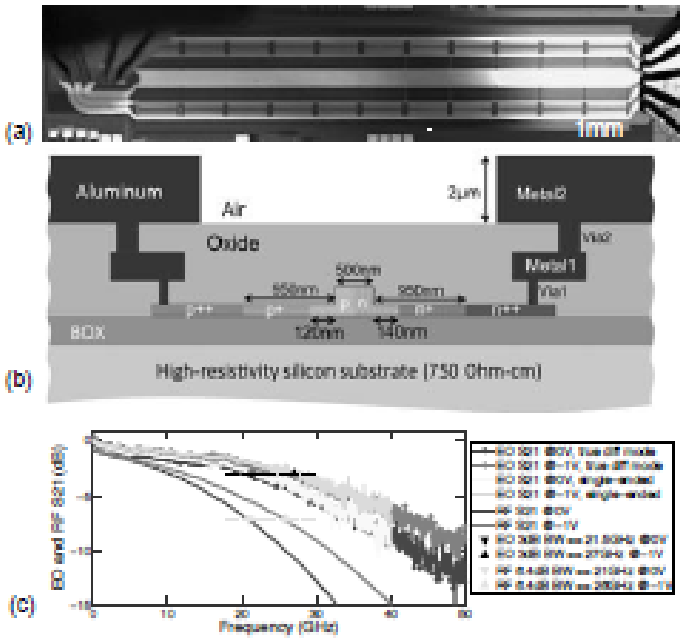

Figure 1. (a) Fabricated TWMZ under probed testing: GSGSG probe on the right is for driving, and GSGSG probe on the left is for providing 50 Ohm termination to each device arm (b) simplified cross sectional diagram of the phase shifter, not to scale (c) EO and RF S21 at 0 V and -1 V bias.

25. Zhang, Yi; Yang, Shuyu; Yang, Yisu; Gould, Michael; Ophir, Noam; Lim, Andy Eu-Jin; Lo, Guo-Qiang; Magill, Peter; Bergman, Keren; Baehr-Jones, Tom; "A high-responsivity photodetector absent metal-germanium direct contact" Vol.22, No.9; 11367-11375 (2013). (9 Google Scholar Citations)

Abstract: We report a Ge-on-Si photodetector without doped Ge or Gemetal contacts. Despite the simplified fabrication process, the device shows a responsivity of 1.14 A/W at− 4 V reverse bias and 1.44 A/W at− 12V, at 1550 nm wavelength. Dark current is less than 1μA under both bias conditions. We also demonstrate open eye diagrams at 40Gb/s.

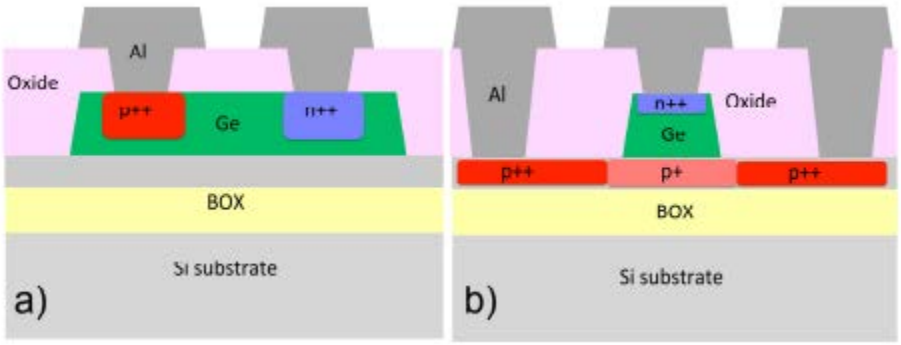

Fig. 1. Lateral and vertical p-i-n Ge-on-Si photodetectors.

26. Streshinsky, Matthew; Shi, Ruizhi; Novack, Ari; Cher, Roger Tern Poh; Lim, Andy Eu-Jin; Lo, Patrick Guo-Qiang; Baehr-Jones, Tom; Hochberg, Michael; "A compact bi-wavelength polarization splitting grating coupler fabricated in a 220 nm SOI platform" Optics express Vol.21, No.3; 3109-31028 (2013). (5 Google Scholar Citations)

Abstract: We experimentally demonstrate a polarization splitting grating coupler that is operational near 1310 nm and 1550 nm in a silicon-on-insulator platform, using the same fiber angle for both wavelength bands. At 1550 nm, the device has an insertion loss of 7.1 dB and a 1.5-dB transmission window of 35 nm. At 1310 nm, the insertion loss and 1.5-dB transmission window are 8.2 dB and 18 nm, respectively. Polarization isolation at 1550 nm is 24 dB. This is the first experimental demonstration of a bi-wavelength polarization-splitting grating coupler.

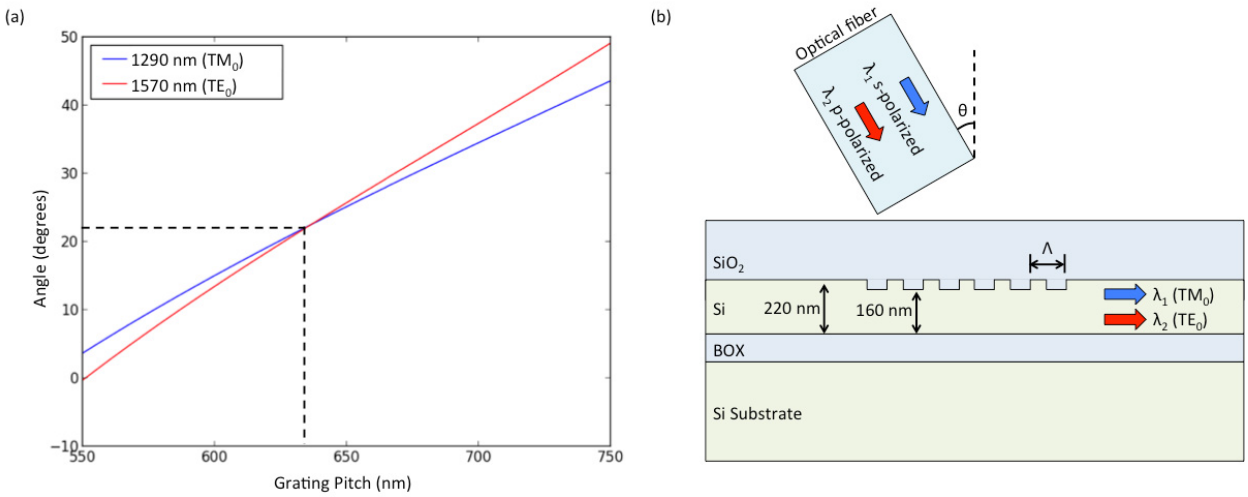

Fig. 1. (a) Phase matching condition for the TM0 mode at 1290 nm and TE0 mode at 1570 nm. The optimum grating pitch and fiber angle is 636 nm and 22.5°, respectively. (b) Schematic illustration of a 1-D device (not to scale).

27. Ding, Ran; Liu, Yang; Li, Qi; Xuan, Zhe; Ma, Yangjin; Yang, Yisu; Lim, Andy Eu-Jin; Lo, Guo-Qiang; Bergman, Keren; Baehr-Jones, Tom; "A compact low-power 320-Gb/s WDM transmitter based on silicon microrings" Photonics Journal, IEEE Vol.6, No.3; 8-Jan (2014). (3 Google Scholar Citations)

Abstract: We demonstrate a compact and low-power wavelength-division multiplexing transmitter near a 1550-nm wavelength using silicon microrings. The transmitter is implemented on a silicon-on-insulator photonics platform with a compact footprint of 0.5 mm^2. The transmitter incorporates 8 wavelength channels with 200-GHz spacing. Each channel achieved error-free operation at 40 Gb/s, resulting in an aggregated data transmission capability of 320 Gb/s. To our knowledge, this is the highest aggregated data rate demonstrated in silicon wavelength-division multiplexing transmitters. Owing to the small device capacitance and the efficient pn-junction modulator design, the transmitter achieves low energy-per-bit values of 36 fJ/bit under 2.4 Vpp drive and 144 fJ/bit under 4.8 Vpp drive. Comparisons are made to a commercial lithium niobate modulator in terms of bit-error-rate versus optical signal-to-noise ratio.

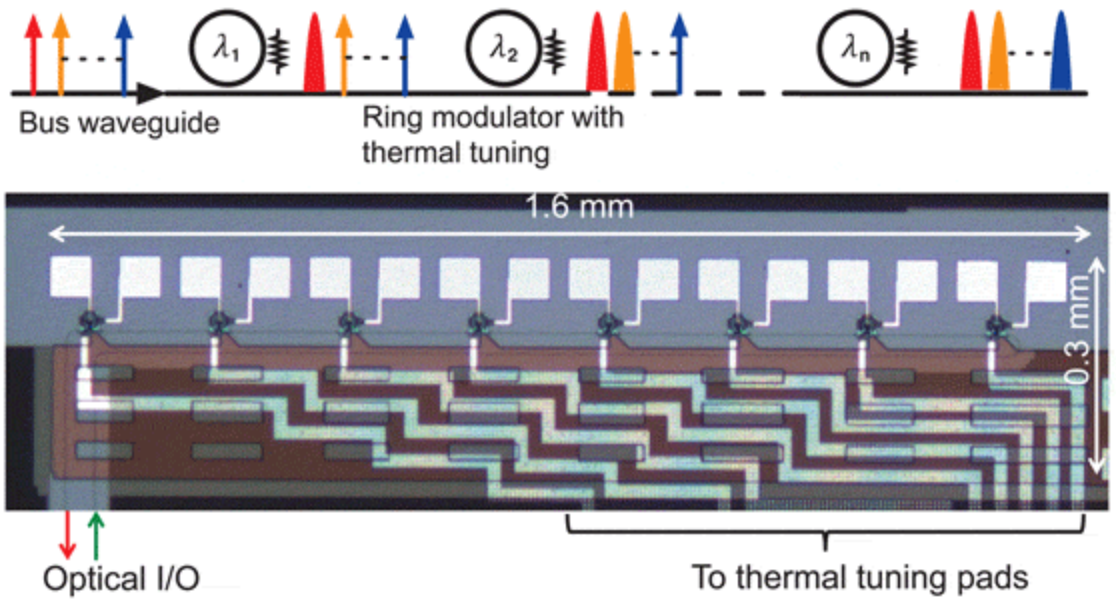

Fig. 1 WDM ring transmitter. (a) Architecture diagram. (b) Chip photo.

28. Ding, Ran; Liu, Yang; Li, Qi; Yang, Yisu; Ma, Yangjin; Padmaraju, Kishore; Lim, Andy Eu-Jin; Lo, Guo-Qiang; Bergman, Keren; Baehr-Jones, Tom; "Design and characterization of a 30-GHz bandwidth low-power silicon traveling-wave modulator" Optics Communication Vol.321, 124-133 (2014). (3 Google Scholar Citations)

Abstract: We present the design and characterization of a silicon PN junction traveling-wave Mach–Zehnder modulator near 1550 nm wavelength. The device shows 30 GHz bandwidth at 1 V reverse bias, with a 2.7 V-cm $V_\pi L_\pi$ and accordingly a 9-V small-signalV_π. The insertion loss of the phase shifter is 3.6 dB±0.4 dB. The device performance metrics in combination show significant improvement compared to the state-of-the-art in the sense that lower phase shifter loss and higher bandwidth are achieved for the sameV_π or vice versa. We demonstrated low modulation power of 640-fJ/bit at 40 Gb/s with a 1.6-V_{pp} differential-drive and 0-V DC bias, raising the prospect of direct compatibility with CMOS drive-voltages. Critical design tradeoffs are analyzed and design models are validated with measurement results. We proposed a new figure-of-merit (FOM)$V_\pi L_\pi R_{pn} C^2_{pn}$ as the junction design merit for high-speed traveling-wave modulators, and utilized 6 implants to achieve an optimal FOM with lower insertion loss. Several key RF design issues are addressed for the first time using simulation and measurement results. In particular, we discussed bandwidth extension using mismatched termination and closely matched experimental results. A bandwidth-limiting RF multi-mode behavior is noted, which also exists in other results in the literature; we suggested a widely applicable design remedy.

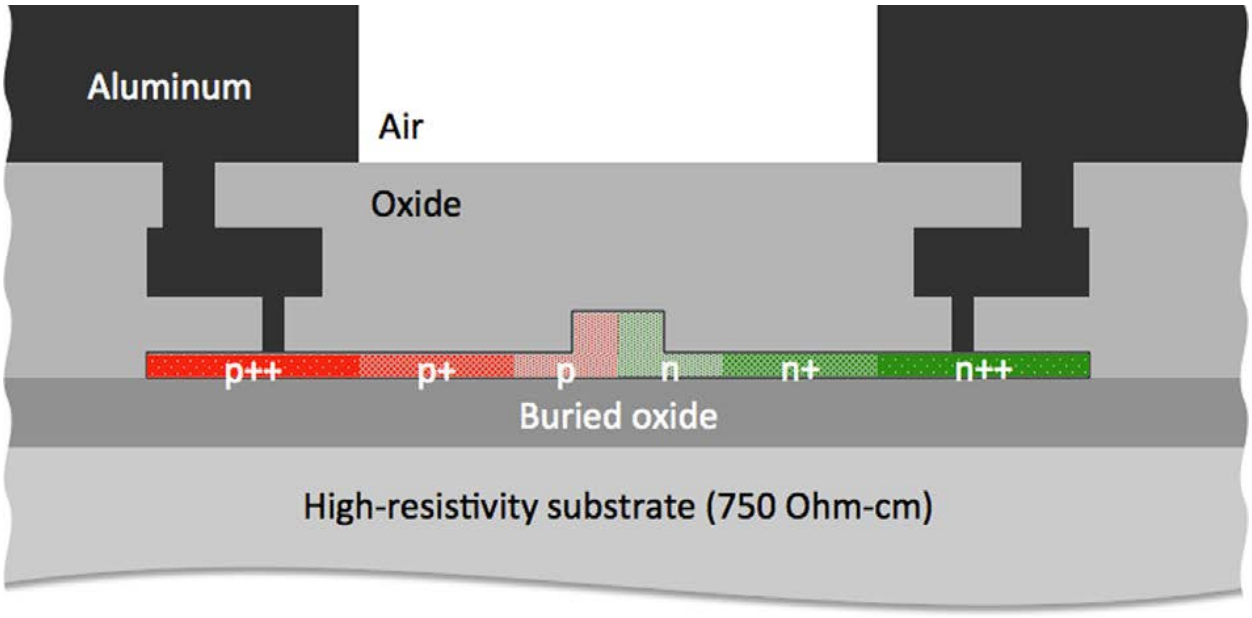

Fig. 1. Simplified device cross-section, not to scale.

29. Ding, Ran; Liu, Yang; Ma, Yangjin; Yang, Yisu; Li, Qi; Lim, Andy Eu-Jin; Lo, Guo-Qiang; Bergman, Keren; Baehr-Jones, Tom; Hochberg, Michael; "High-speed silicon modulator with slow-wave electrodes and fully independent differential drive" Journal of Lightwave Technology Vol.32, No.12; 2240-2247 (2014). (10 Google Scholar Citations)

Abstract: We demonstrate a fully independent differentialdrive capable of traveling-wave modulator in silicon using slowwave transmission line electrode. The reported 3.5-mm device achieves a bandwidth of 27 GHz at −1 V bias with 7.8-V small signal $V\pi$ and 50-Ω impedance. Raising the impedance to this extent

requires effectively expanding the RF mode size and radically changes the RF phase velocity, but we show that this can be done with minimal crosstalk effects between the two arms and overall velocity mismatch, and thus, with a high EO bandwidth achieved.40-Gb/s operation is demonstrated with 1.6-Vpp differential-drive, and performance comparisons to Lithium Niobate modulators are made.

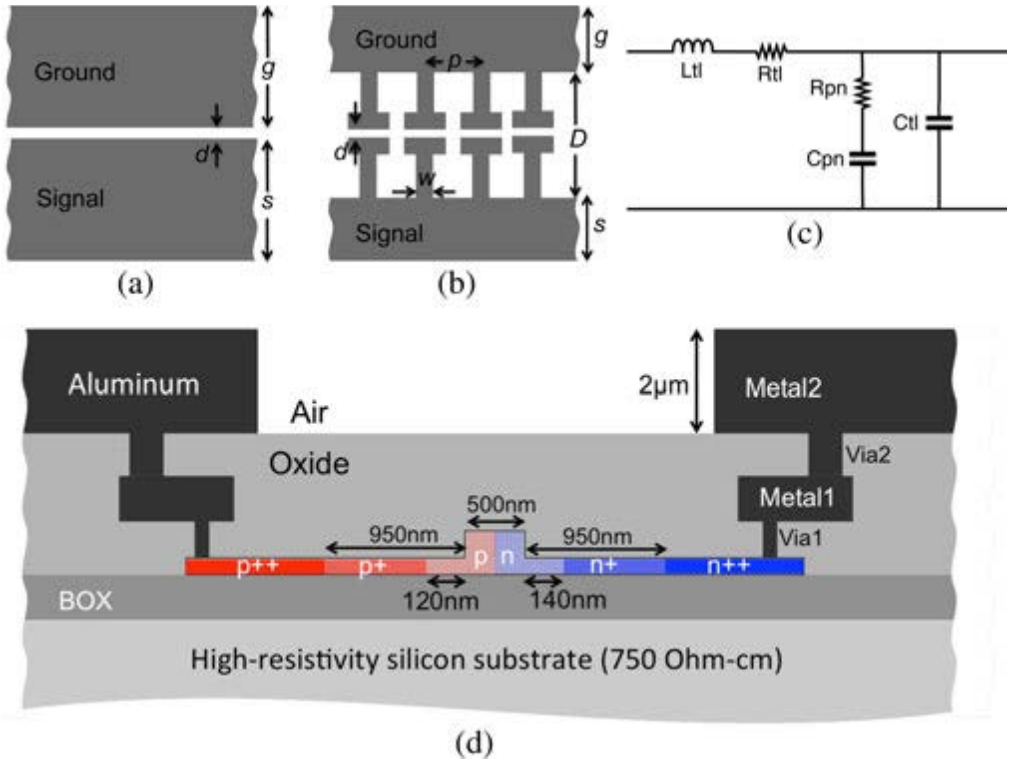

Fig. 1. (a) Coplanar strip transmission line. (b) Slow-wave transmission line. (c) Simplified equivalent circuit model of p-n junction loaded transmission line electrode. (d) Simplified cross sectional diagram of the phase shifter, not to scale.

30. Yang, Shuyu; Zhang, Yi; Grund, David W; Ejzak, Garret A; Liu, Yang; Novack, Ari; Prather, Dennis; Lim, Andy Eu-Jin; Lo, Guo-Qiang; Baehr-Jones, Tom; "A single adiabatic microring-based laser in 220 nm silicon-on-insulator" Optics Express Vol.22, No.1; 1172-1180 (2014) (30 Google Scholar Citations)

Abstract: We demonstrate a laser for the silicon photonics platform by hybrid integration with a III/V reflective semiconductor optical amplifier coupled to a 220 nm silicon-on-insulator half-cavity. We utilize a novel ultra-thin silicon edge coupler. A single adiabatic microring based inline reflector is used to select a lasing mode, as compared to the multiple rings and Bragg gratings used in many previous results. Despite the simplified design, the laser was measured to have on-chip 9.8mW power, less than 220KHz linewidth, over 45dB side mode suppression ratio, less than −135dB/Hz relative intensity noise, and 2.7% wall plug efficiency.

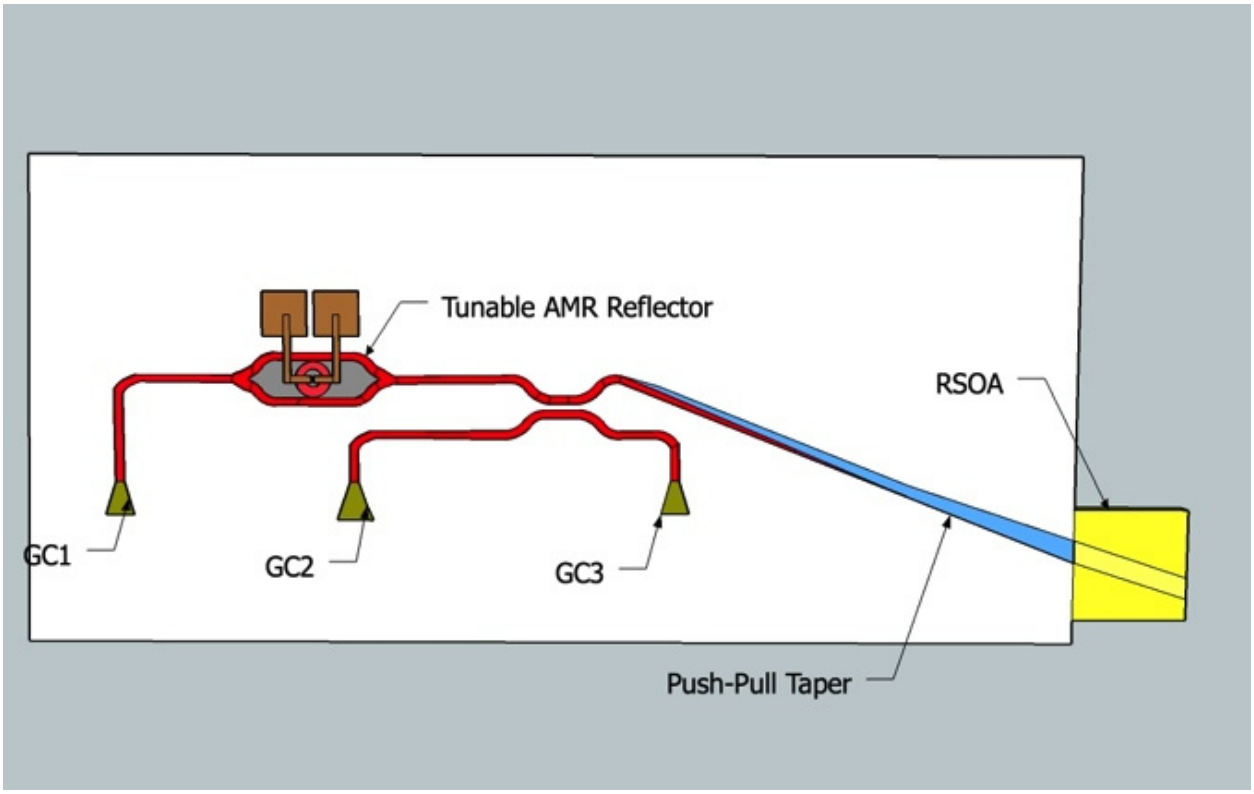

Fig. 1. Isometric diagram of the layout of the laser system. The InP based RSOA is shownbonded to the SOI chip, which includes a tunable AMR reflector to close the laser cavity.

31. Ma, Yangjin; Magill, Peter; Baehr-Jones, Tom; Hochberg, Michael; "Design and optimization of a novel silicon-on-insulator wavelength diplexer" Optics Express Vol.22, No.18; 21521-21528 (2014). (1 Google Scholar Citation)

Abstract: We propose a novel silicon-on-insulator (SOI) wavelength diplexer design based on an adiabatic bent taper and an unconventional multimode waveguide. The geometry of the device is optimized using particle swarm optimization (PSO). The device has an ultra-short length of 15 μm. Simulated insertion loss at peak wavelength is less than 0.25 dB with 1-dB bandwidth around 100 nm for both O band and C band. The device is fabrication tolerant as demonstrated by simulated yield estimates. The reported design targets 1310 and 1550 nm as peak wavelengths; the design methodology is easily applicable to other wavelengths of interest.

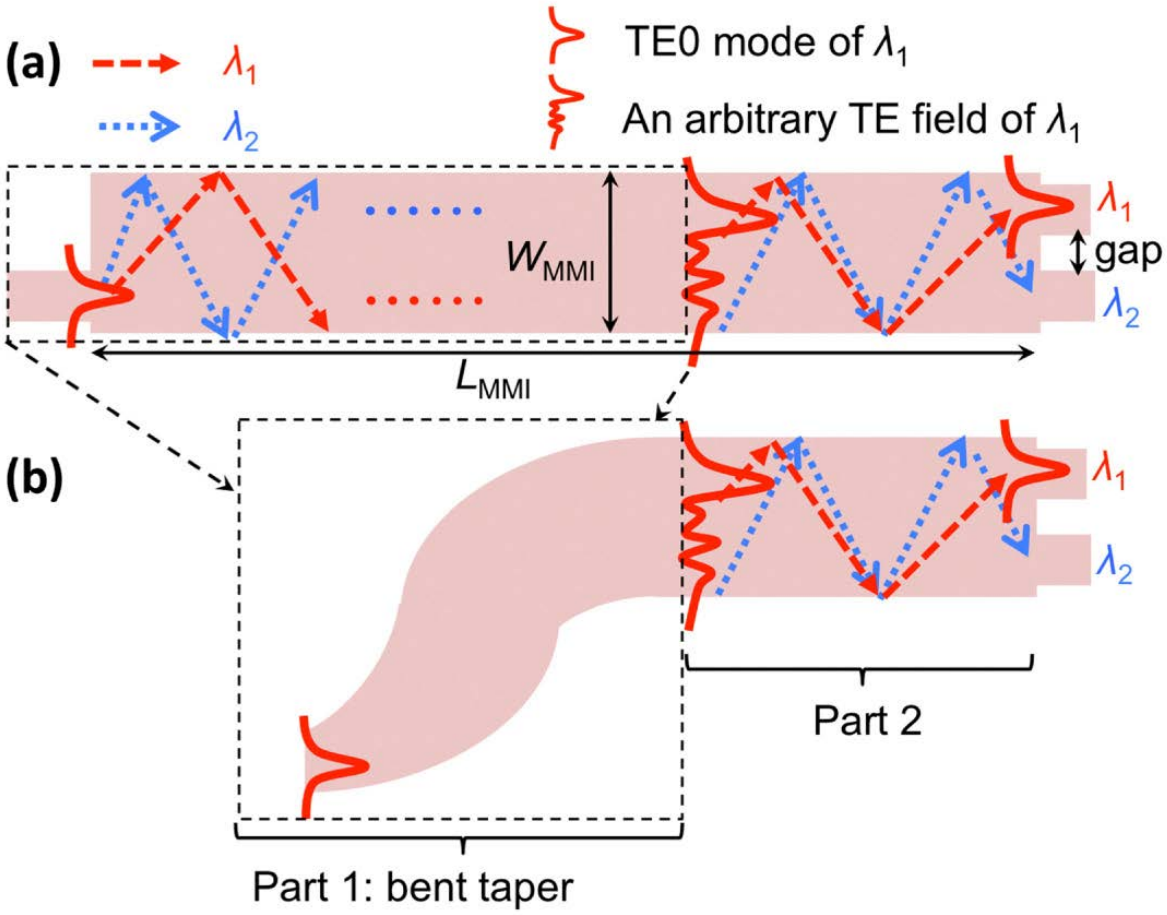

Fig. 1. (a) Schematic of a conventional MMI-based diplexer. (b) Schematic of a novel MMIbaseddiplexer using a combined bent taper and multimode waveguide.

32. Guan, Hang; Novack, Ari; Streshinsky, Matthew; Shi, Ruizhi; Fang, Qing; Lim, Andy Eu-Jin; Lo, Guo-Qiang; Baehr-Jones, Tom; Hochberg, Michael; "CMOS-compatible highly efficient polarization splitter and rotator based on a double-etched directional coupler" Optics Express Vol.22, No.2; 2489-2496 (2104). (14 Google Scholar Citations)

Abstract: We present a highly efficient polarization splitter and rotator (PSR), fabricated using 248 nm deep ultraviolet lithography on a silicon-on-insulator substrate. The PSR is based on a double-etched directional coupler with a length of 27 μm. The fabricated PSR yields a TM-to-TE conversion loss better than 0.5 dB and TE insertion loss better than 0.3 dB, with an ultra-low crosstalk (−20 dB) in the wavelength regime 1540-1570 nm.

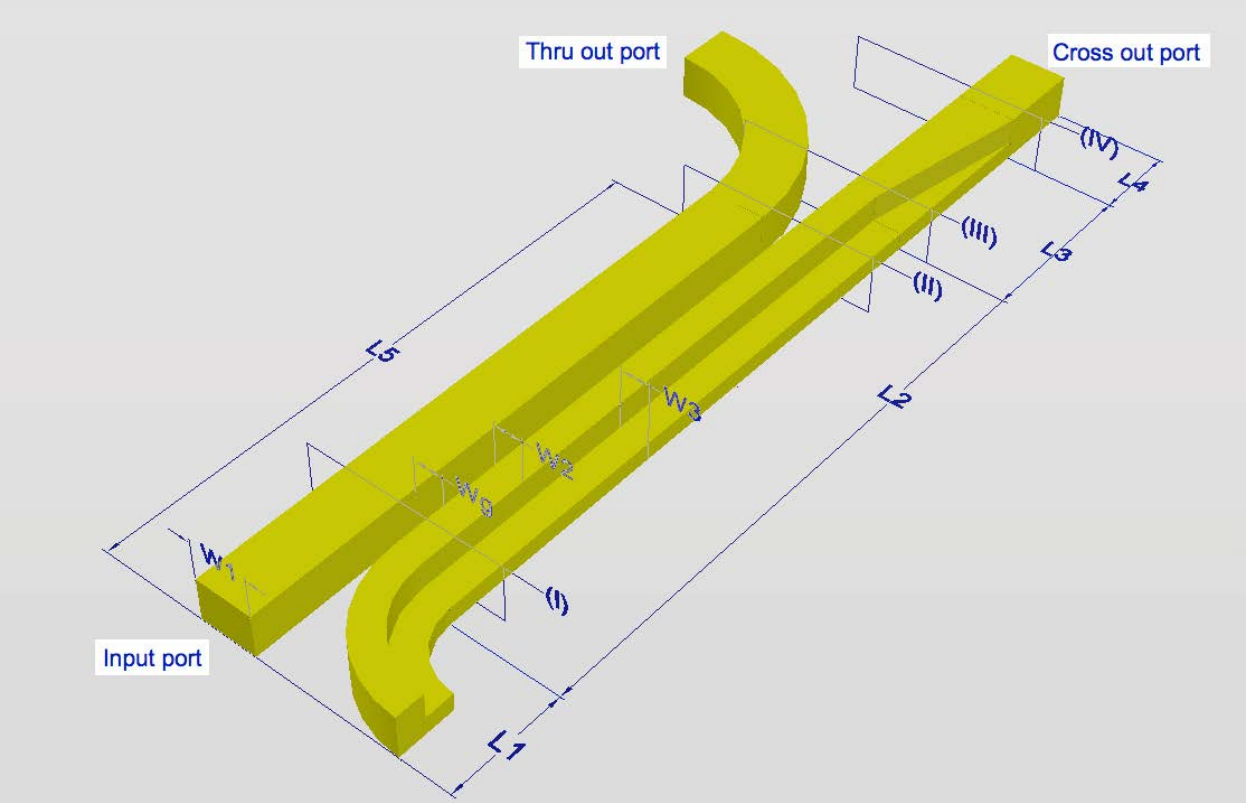

Fig. 1. Schematic structure of the proposed PSR with significant geometric parameters noted

33. Yang, Shuyu; Zhang, Yi; Li, Qi; Zhu, Xiaoliang; Bergman, Keren; Magill, Peter; Baehr-Jones, Thomas; Hochberg, Michael; "Quantum dot semiconductor optical amplifier/silicon external cavity laser for O-band high-speed optical communications" Optics Express Vol.54, No. 2; 026102-126102 (2015).

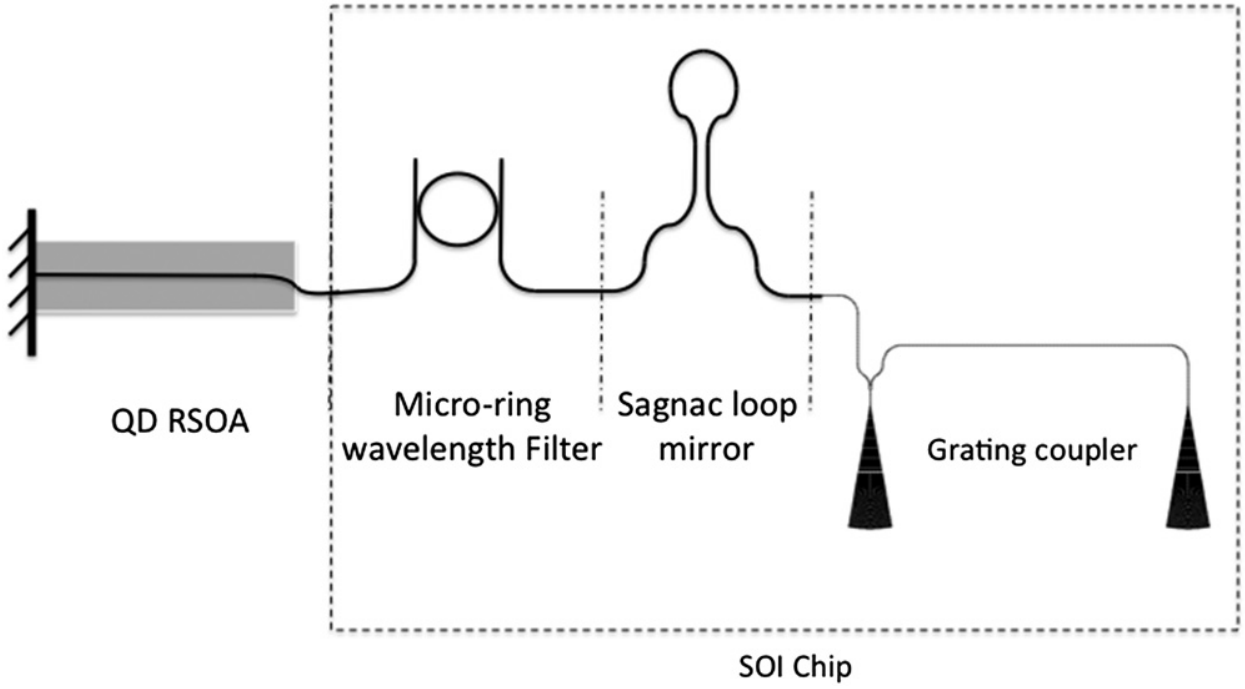

Fig. 1 *Diagram of the hybrid external cavity laser. A quantum dot semiconductor optical amplifier is butt coupled to a silicon-on-insulator chip. The half-cavity on silicon consists of a Sagnac loop mirror and a microring wavelength filter. Grating couplers used for device characterization are also shown.*

34. Calhoun, David; Li, Qi; Browning, Colm; Abrams, Nathan C; Liu, Yang; Ding, Ran; Barry, Liam P; Baehr-Jones, Thomas W; Hochberg, Michael; Bergman, Keren; "Programmable Wavelength Locking and Routing in a Silicon-Photonic Interconnection Network Implementation" Optical Fiber Communication Conference TuH. 3 (2015) (4 Google Scholar Citations)

Abstract: A programmable control system for wavelength locking WDM channels on microring arrays is used to demonstrate arbitrary demultiplexing and selection of fast switchable wavelengths. Successful data measurements verify the functionality within an interconnection network implementation.

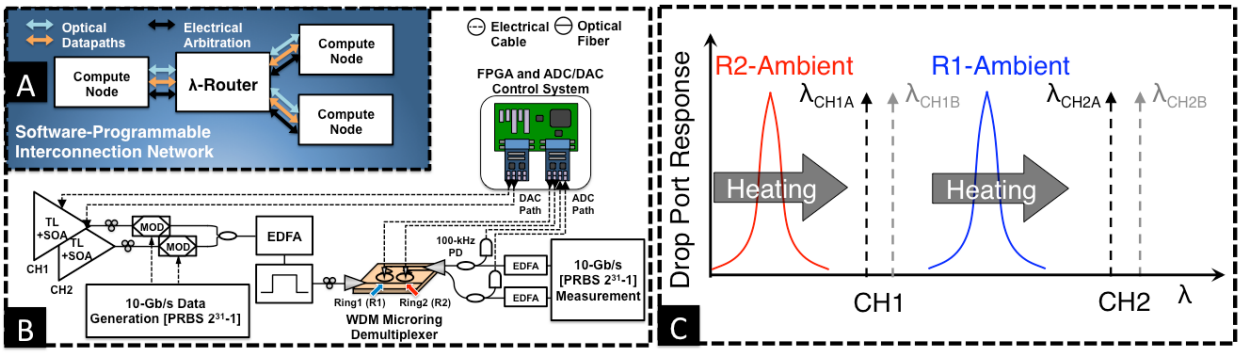

Figure 1: (A) System setup showing wavelength-routed datapaths and electrical arbitration; (B) experimental setup; (C) experimental scheme for tuning and locking cascaded microrings (R1 & R2) to specified wavelengths of interest.

35. Yang, Shuyu; Zhu, Xiaoliang; Zhang, Yi; Li, Ying; Jones, Tom Baehr; Hochberg, Michael; Bergman, Keren; "Thermal stabilization of a microring resonator using bandgap temperature sensor" Optical Interconnects Conference (OI), 2015 IEEE No. 44-45, (2105)

Abstract: We demonstrate a thermal stabilization method for microring modulator by measuring the absolute temperature of the ring and surrounding areas using two pairs of matched p-n junctions. Stabilization is accomplished without needing optical power.

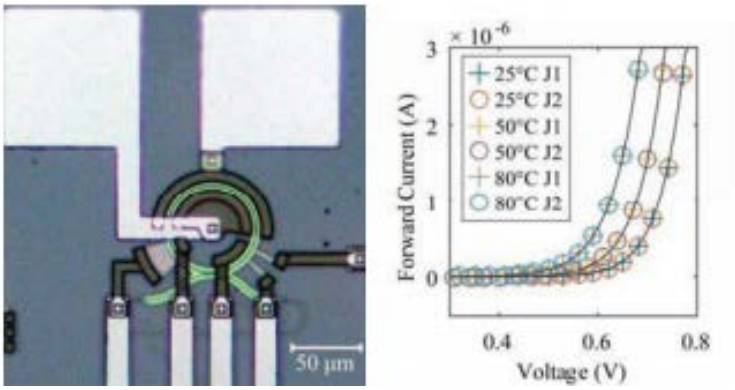

Fig. 1 (a) Fabricated microring modulator viewed through a microscope. The matched p-n junctions used for temperature sensing are on the lower right quadrant of the device, while the integrated heater is in the lower left. The high-speed modulation junction covers the top semicircle. (b) IV curves of the two junctions under different temperatures. The junctions match perfectly.

36. Harris, Nicholas C; Ma, Yangjin; Mower, Jacob; Baehr-Jones, Tom; Englund, Dirk; Hochberg, Michael; Galland, Christophe; "Efficient, compact and low loss thermo-optic phase shifter in silicon" Optics Express Vol.22, No.9; 10487-16438 (2014). (9 Google Scholar Citations)

Abstract: We design a resistive heater optimized for efficient and low-loss optical phase modulation in a silicon-on-insulator (SOI) waveguide and characterize the fabricated devices. Modulation is achieved by flowing current perpendicular to a new ridge waveguide geometry. The resistance profile is engineered using different dopant concentrations to obtain localized heat generation and maximize the overlap between the optical mode and the high temperature regions of the structure, while simultaneously minimizing optical loss due to free-carrier absorption. A 61.6 μm long phase shifter was fabricated in a CMOS process with oxide cladding and two metal layers. The device features a phase-shifting efficiency of 24.77 ± 0.43 mW/π and a −3 dB modulation bandwidth of 130.0 ± 5.59 kHz; the insertion loss measured for 21 devices across an 8-inch wafer was only 0.23 ± 0.13 dB. Considering the prospect of densely integrated photonic circuits, we also quantify the separation necessary to isolate thermo-optic devices in the standard 220 nm SOI platform.

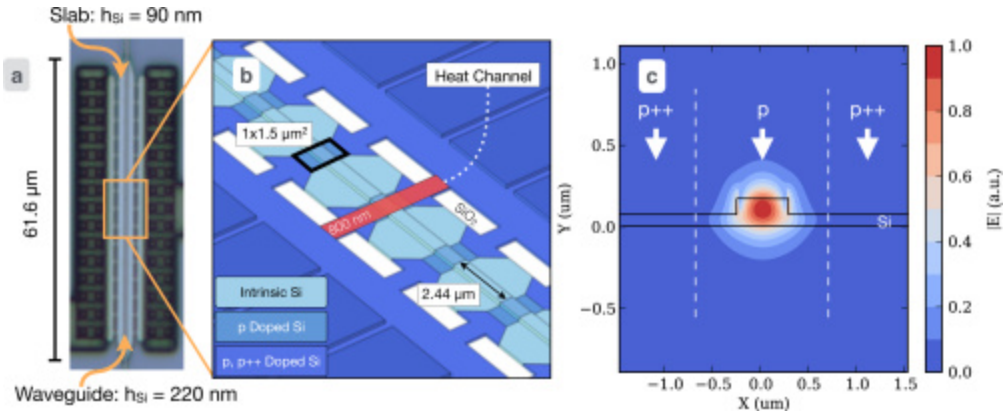

Fig. 1 *(a) Optical micrograph of the structure with the vias connecting the lowest metal layer and the doped silicon clearly visible.* h_{Si} *denotes silicon layer thickness. (b) Perspective view of the phase shifter with annotations for relevant dimensions. (c) Doping profile along the cross section marked red in (b), overlapped with the simulated amplitude of the horizontal component of the electric field.*

37. Liu, Yang; Ding, Ran; Ma, Yangjin; Yang, Yisu; Xuan, Zhe; Li, Qi; Lim, Andy Eu-Jin; Lo, Guo-Qiang; Bergman, Keren; Baehr-Jones, Tom; "Silicon Mod-MUX-Ring transmitter with 4 channels at 40 Gb/s" Optics Express Vol. 22, No. 13; 16431-16438, 2014. (6 Google Scholar Citations)

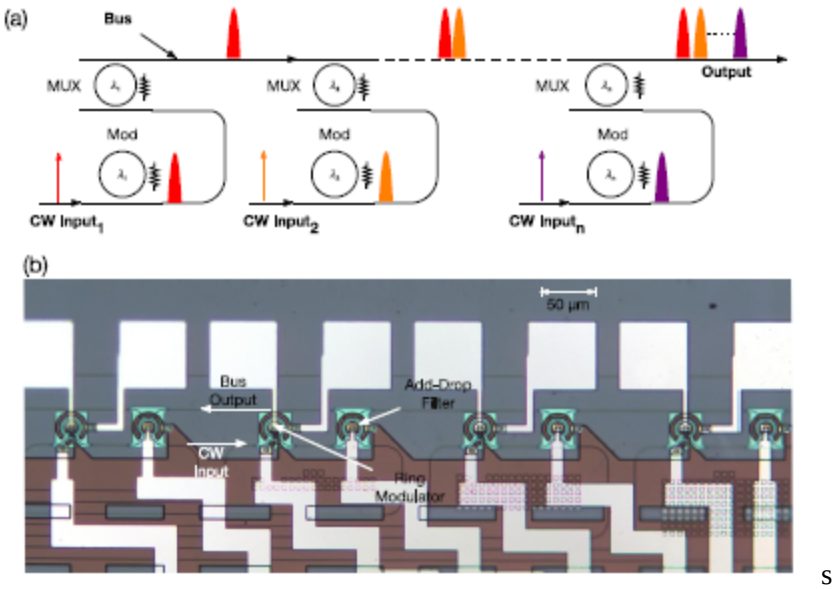

s

Fig. 1. (a) Sketch of Mod-MUX-Ring architecture. Individual single wavelength lasers are first modulated by ring modulators and then multiplexed on to a bus waveguide via ring add/drop filters. (b) Photograph of fabricated 4-channel Mod-MUX-Ring transmitter.

38. Yang, Yisu; Galland, Christophe; Lui, Yang; Tan, Kang; Ding, Ran; Li, Qi; Bergman, Keren; Baehr-Jones, Tom; Hochberg, Michael; "Experimental demonstration of broadband Lorentz non-reciprocity in an integrable photonic architecture based on Mach-Zehnder modulators" Optics Express Vol.22, No.13; 17409-17422 (2014). 3 Google Scholar Citations

Abstract: We propose for the first time the Mod-MUX-Ring architecture for microring based WDM transmitter. A prototype Mod-MUX-Ring transmitter with 4 channels and 400 GHz channel spacing is demonstrated and fully characterized at 40 Gb/s channel rate. Under 2.7 V driving voltage, error-free (BER < 10^{-12}) operation is achieved on all channels, with 3 dB extinction ratio. Performance comparisons to Lithium Niobate modulators are made.

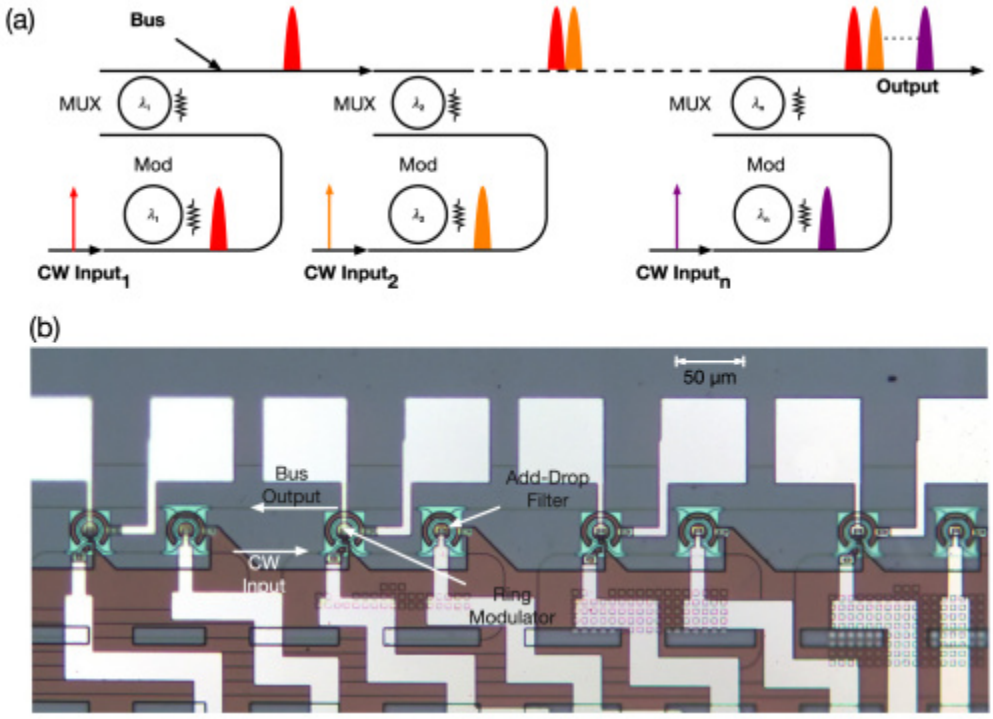

Fig. 1 *(a) Sketch of Mod-MUX-Ring architecture. Individual single wavelength lasers are first modulated by ring modulators and then multiplexed on to a bus waveguide via ring add/drop filters. (b) Photograph of fabricated 4-channel Mod-MUX-Ring transmitter.*

39. Chen, Christine P; Zhu, Xiaoliang; Liu, Yang; Li, Qi; Chan, Johnnie; Baehr-Jones, Tom; Hochberg, Michael; Bergman, Keren; "Performing Intelligent Power Distribution in a 4× 4 Silicon Photonic Switch Fabric" Optical Interconnects Conference (OI), 2015 IEEE; 50-51 (2015).

Abstract: A dynamically-programmable optical-power distribution scheme is proposed for increased reliability and energy efficiency in systems. Precise power allocation and intelligent switch control with 40 Gb/s error-free operation is realized on the 4× 4 multi-stage switch fabric.

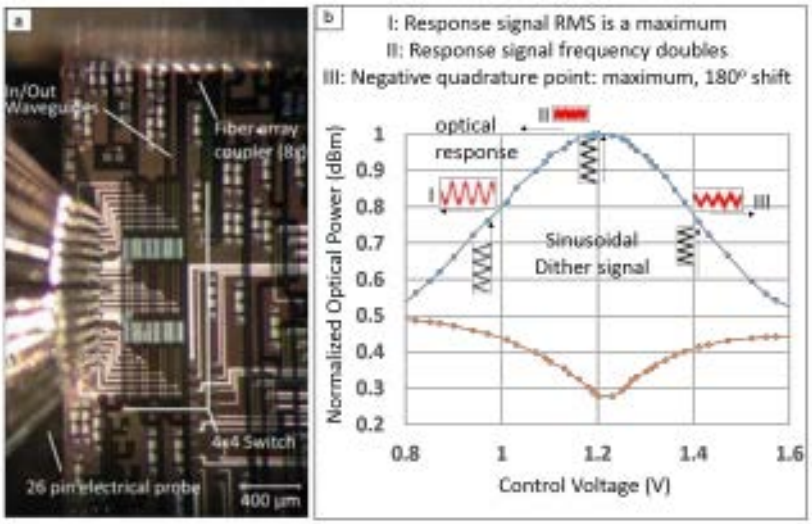

Fig. 1. (a) Microscope image of 4×4 (center) switch fabric and (b) dithering technique on 2 × 2 element, which makes up 4 × 4 topology, with scope screenshots overlay on switch characteristics of output 1 (blue) and 2 (orange)

40. Harris, Nicholas C; Steinbrecher, Gregory R; Mower, Jacob; Lahini, Yoav; Prabhu, Mihika; Baehr-Jones, Tom; Hochberg, Michael; Lloyd, Seth; Englund, Dirk; "Bosonic transport simulations in a large-scale programmable nanophotonic processor" arXiv preprint arXiv:1507.03406 (2015) (2 Google Scholar Citations)

Abstract: Environmental noise and disorder play a critical role in quantum particle and wave transport in complex media, including solid-state and biological systems. Recent work has predicted that coupling between noisy environments and disordered systems, in which coherent transport has been arrested due to localization effects, could actually enhance transport. Photonic integrated circuits are promising platforms for studying such effects, with a central goal being the development of large systems providing low-loss, high-fidelity control over all parameters of the transport problem. Here, we fully map out the role of static and dynamic disorder in quantum transport using a low-loss, phase-stable, nanophotonic processor consisting of a mesh of 56 generalized beamsplitters programmable on microsecond timescales. Over 85,600 transport experiments, we observe several distinct transport regimes, including environment-enhanced transport in strong, statically disordered systems. Low loss and programmability make this nanophotonic processor a promising platform for many-boson quantum simulation experiments.

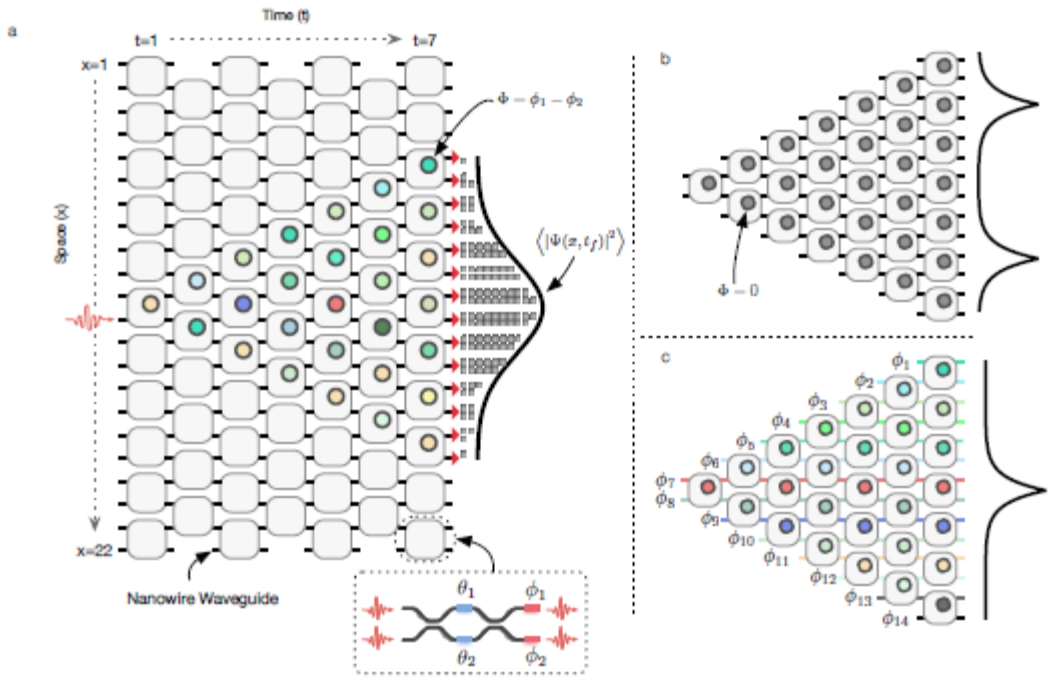

FIG. 1. Conceptual representation of quantum transport experiments. Schematic of programmable nanophotonic processor. Horizontal lines represent nanowire waveguides; boxes represent 4-port reconfigurable beamsplitter ((see lower inset of (a); thermal phase modulators control the splitting ratio via _1,2 and the phase shift between steps via _1,2)). Time is defined from left to right; space is defined from top to bottom. Colored regions represent output differential phase setting _. (a) Output phases are randomized, resulting in incoherent, diffusive transport shown conceptually with a Galton's board representation at the last time step. (b) Ballistic propagation configuration. The quantum walker is most likely found along the outer modes of the PNP in the absence of phase disorder. (c) Anderson localization configuration. The quantum walker is mainly confined to the central modes in the presence of strong static phase disorder (the phase setting on a given waveguide mode is constant in time and denoted by i).

41. Xuan, Zhe; Ma, Yangjin; Liu, Yang; Ding, Ran; Li, Yunchu; Ophir, Noam; Lim, Andy Eu-Jin; Lo, Guo-Qiang; Magill, Peter; Bergman, Keren; "Silicon microring modulator for 40 Gb/s NRZ-OOK metro networks in O-band" Vol.22, No. 2; 28284-28291 (2014) (2 Google Scholar Citations)

Abstract: A microring-based silicon modulator operating at 40 Gb/s near 1310 nm is demonstrated for the first time to our knowledge. NRZ-OOK signals at 40 Gb/s with 6.2 dB extinction ratio are observed by applying a 4.8 Vpp driving voltage and biasing the modulator at 7 dB insertion loss point. The energy efficiency is 115 fJ/bit. The transmission performance of 40 Gb/s NRZ-OOK through 40 km of standard single mode fiber without dispersion compensation is also investigated. We show that the link suffers negligible dispersion penalty. This makes the modulator a potential candidate for metro network applications.

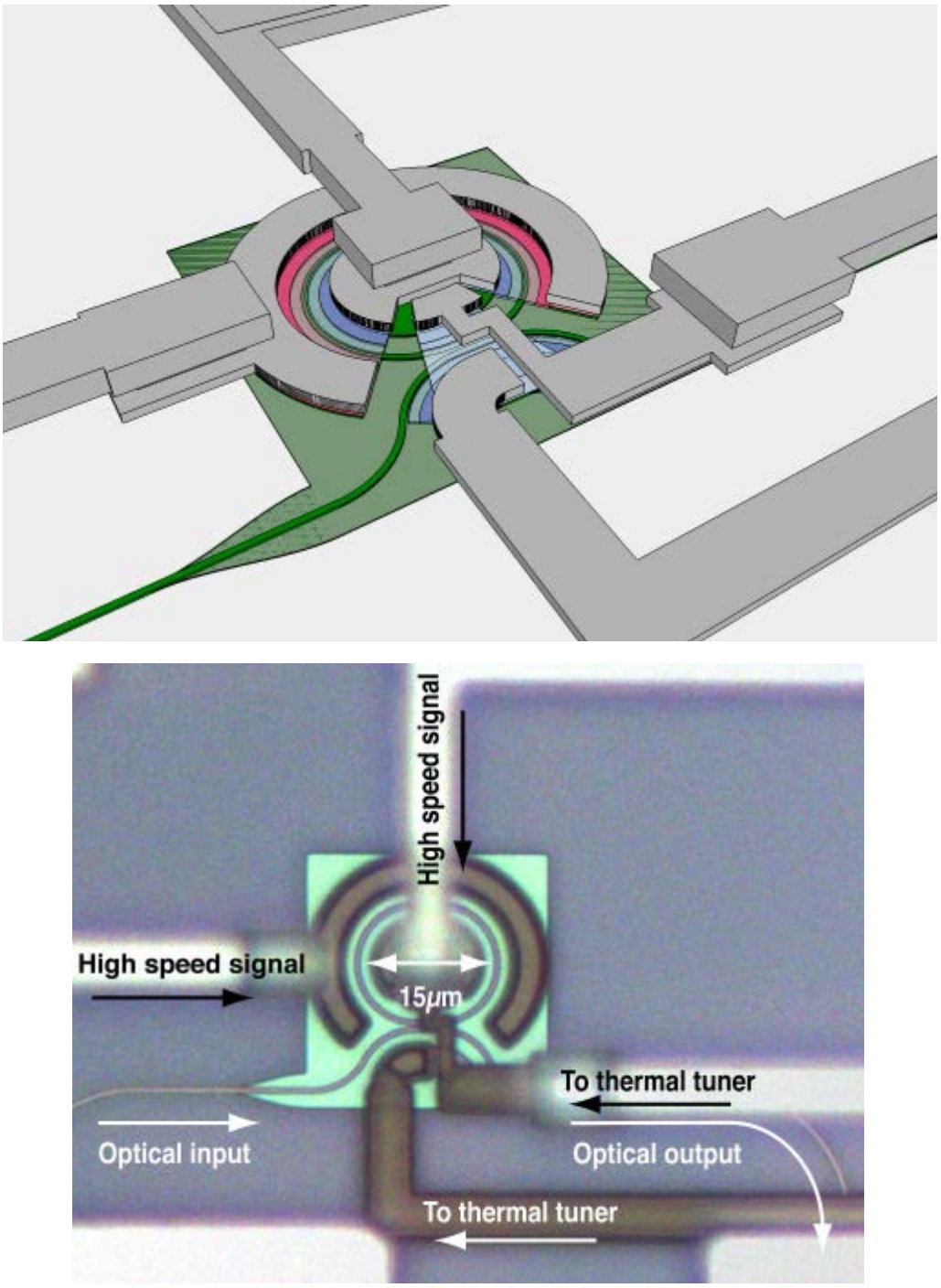

Fig. 1. (a) Layout of the modulator. Light green stands for the 90nm thick Si, dark green for the waveguide, and gray for the back-end metallization. Red stands for p doping, and blue for n doping. Deeper the color, heavier the dose. (b) Chip photograph of the fabricated device. Each electrical trace is connected to a 60μm × 60μm pad (not depicted in the picture).

42. Zhang, Yi; Yang, Shuyu; Zhu, Xiaoliang; Li, Qi; Guan, Hang; Magill, Peter; Bergman, Keren; Baehr-Jones, Thomas; Hochberg, Michael; "Quantum dot SOA/silicon external cavity multi-wavelength laser" Optics express Vol.23, No,25; 4666-4671 (2015). (1 Google Scholar Citation)

Abstract: We report a hybrid integrated external cavity, multi-wavelength laser for high-capacity data transmission operating near 1310 nm. This is the first demonstration of a single cavity multi-wavelength laser in silicon to our knowledge. The device consists of a quantum dot reflective semiconductor optical amplifier and a silicon-on-insulator chip with a Sagnac loop mirror and microring wavelength filter. We show four major lasing peaks from a single cavity with less than 3 dB power non-uniformity and demonstrate error-free 4 × 10 Gb/s data transmission.

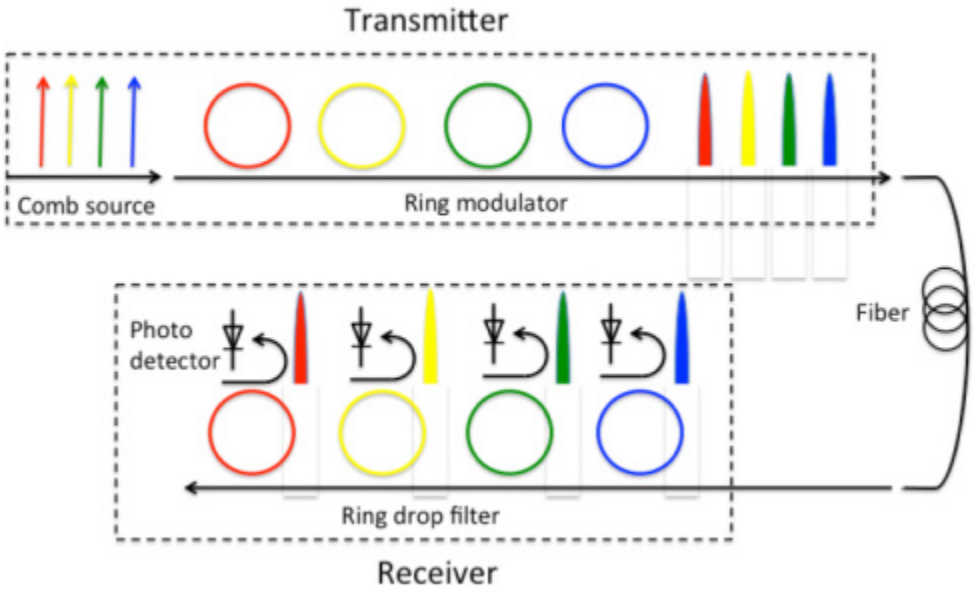

Fig. 1 *Schematic of a microring based WDM data transmission system.*

43. Yang, Shuyu; Zhang, Yi; Baehr-Jones, Tom; Hochberg, Michael; "High efficiency germanium-assisted grating coupler" Optics Express Vol.22, No.25; 30607-30612 (2014) (2 Google Scholar Citations)

Abstract: We propose a fiber to submicron silicon waveguide vertical coupler utilizing germanium-on-silicon gratings. The germanium is epitaxially grown on silicon in the same step for building photodetectors. Coupling efficiency based on FDTD simulation is 76% at 1.55 μm and the optical 1dB bandwidth is 40 nm.

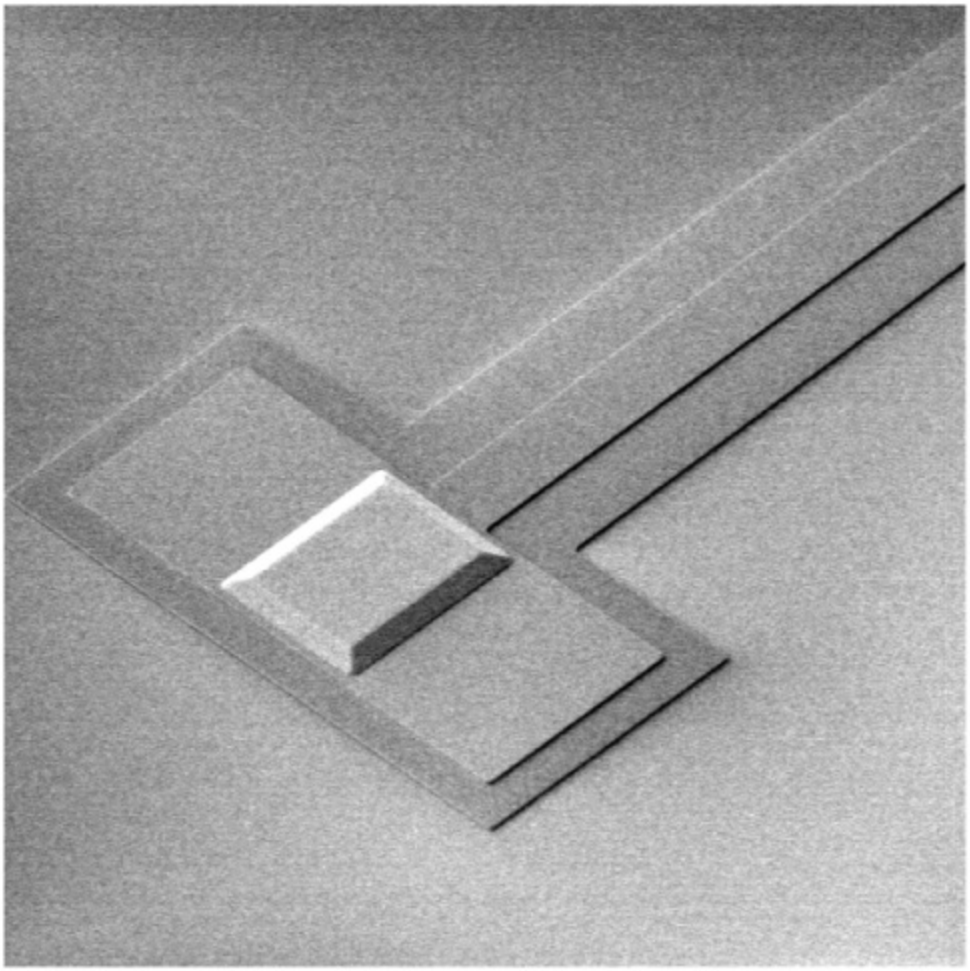

Fig. 1 *SEM image of Epi-Ge on an SOI wafer. Ge trapezoid base size is 8 µm x 11 µm. Unetched Si (220 nm thick) under Ge and partially etched Si (90 nm thick) surrounding unetched Si is also visible.*

44. Yang, Yisu; Ma, Yangjin; Guan, Hang; Liu, Yang; Danziger, Steven; Ocheltree, Stewart; Bergman, Keren; Baehr-Jones, Tom; Hochberg, Michael; "Phase coherence length in silicon photonic platform" Optics Express Vol.23, No.13; 16890-16902 (2015)

Abstract: We report for the first time two typical phase coherence lengths in highly confined silicon waveguides fabricated in a standard CMOS foundry's multi-project-wafer shuttle run in the 220nm silicon-on-insulator wafer with 248nm lithography. By measuring the random phase fluctuations of 800 on-chip silicon Mach-Zehnder interferometers across the wafer, we extracted, with statistical significance, the coherence lengths to be 4.17 ± 0.42 mm and 1.61 ± 0.12 mm for single mode strip waveguide and rib waveguide, respectively. We present a new experimental method to quantify the phase coherence length. The theory model is verified by both our and others' experiments. Coherence length is expected to become one key parameter of the fabrication non-uniformity to guide the design of silicon photonics.

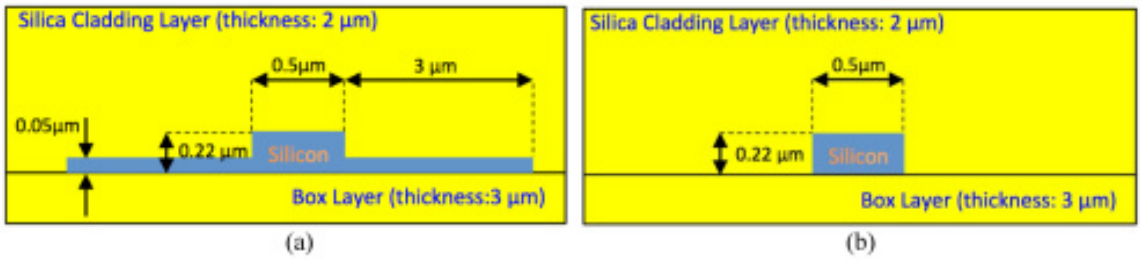

Fig. 1 *Cross-sections of two kinds of waveguides used to build MZIs: (a) the rib waveguide, (b) the strip waveguide*.

45. Zhang, Yi; Yang, Shuyu; Guan, Hang; Lim, Andy Eu-Jin; Lo, Guo-Qiang; Magill, Peter; Baehr-Jones, Tom; Hochberg, Michael; "Sagnac loop mirror and micro-ring based laser cavity for silicon-on-insulator" Optics Express Vol.22, No.15; 17872-17879 (2015). (4 Google Scholar Citations)

Abstract: An integrated laser is a key component in silicon based photonic integrated circuits. Beyond incorporating the gain medium, on-chip cavity design is critical to device performance and yield. Typical recent results involve cavities utilizing distributed Bragg gratings that require ultra-fine feature sizes. We propose to build laser cavity on silicon using a Sagnac loop mirror and a micro-ring wavelength filter for the first time. The Sagnac loop mirror provides broadband reflection, which is simple to fabricate, has an accurately-controlled reflectivity, and negligible excess loss. Single-mode operation is achieved with the intra-cavity micro-ring filter and, using a 248 nm stepper, the laser wavelength can be lithographically controlled within a standard deviation of 3.6 nm. We demonstrate a proof-of-concept device lasing at 1551.7 nm, with 44 dB SMSR, 1.2 MHz linewidth and 4.8 mW on-chip output power.

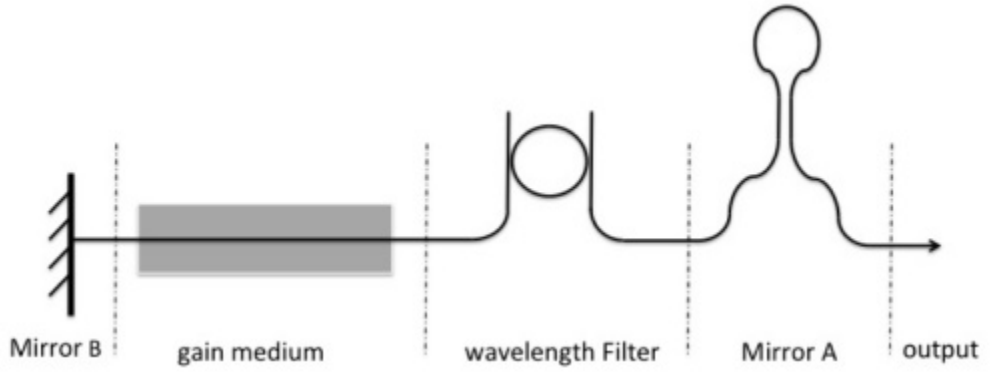

Fig. 1 *Diagram of Sagnac loop mirror based laser cavity.*

46. Ma, Yangjin; Liu, Yang; Guan, Hang; Gazman, Alexander; Li, Qi; Ding, Ran; Li, Yunchu; Bergman, Keren; Baehr-Jones, Tom; Hochberg, Michael; "Symmetrical polarization splitter/rotator design and application in a polarization insensitive WDM receiver" Vol.23, No.12; 16052-16062 (2015)

Abstract: In integrated photonics, the design goal of a polarization splitter/rotator (PSR) has been separating the TE0 and TM0 modes in a waveguide. This is a natural choice. But in theory, a PSR only needs to project the incoming State Of Polarization (SOP) orthogonally to its output ports, using any orthogonal mode basis set in the fiber. In this article, we introduce a novel PSR design that alternatively takes the linear combination of TE0 and TM0 (TE0 +/− TM0) as orthogonal bases. By contrast, existing approaches exclusively use TE0 and TM0 as their basis set. The design is based on two symmetric and robust structures: a bi-layer taper and a Y-junction, and involves no bends. To prove the concept, we incorporated it into a four-channel polarization insensitive wavelength division multiplexing (PI-WDM) receiver fabricated in a standard CMOS Si photonics process. 40 Gb/s data rate and 0.7 +/− 0.2 dB polarization dependent loss (PDL) is demonstrated on each channel. Lastly, we propose an improved PSR design with 12 μm device length, < 0.1 dB PDL, < 0.4 dB insertion loss and < 0.05 dB wavelength dependence across C-band for both polarizations. Overall, our PSR design concept is simple, easy to realize and presents a new perspective for future PSR designs.

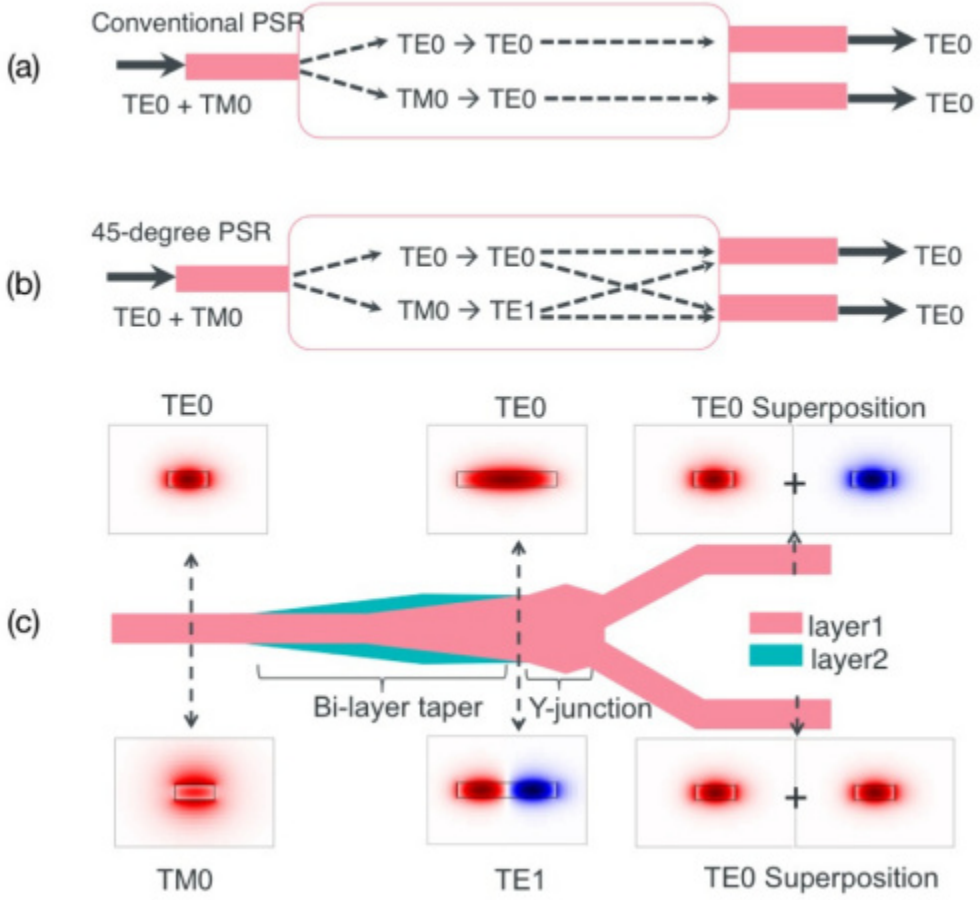

Fig. 1 *(a) Principle of a conventional PSR. (b) Principle of a 45-degree PSR. (c) Schematics of the 45-degree PSR and the evolution of its mode profile.*

47. He, Li; He, Yanling; Pomerene, Andrew; Hill, Craig; Ocheltree, Stewart; Baehr-Jones, Tom; Hochberg, Michael; "Ultrathin silicon-on-insulator grating couplers" Vol.24, No.24; 2247-2249 (2012)

Abstract: We demonstrate a novel grating coupler fabricated on a silicon-on-insulator (SOI) wafer operating at 1550 nm, based on an ultrathin 50-nm silicon geometry. The devices are fabricated in a CMOS-compatible process with a single etch step. A low insertion loss of –3.7 dB is achieved. We also calculate the backreflection loss to be –14 dB. The devices are likely to be useful in terms of light coupling between optical fibers and ultrathin silicon waveguides.

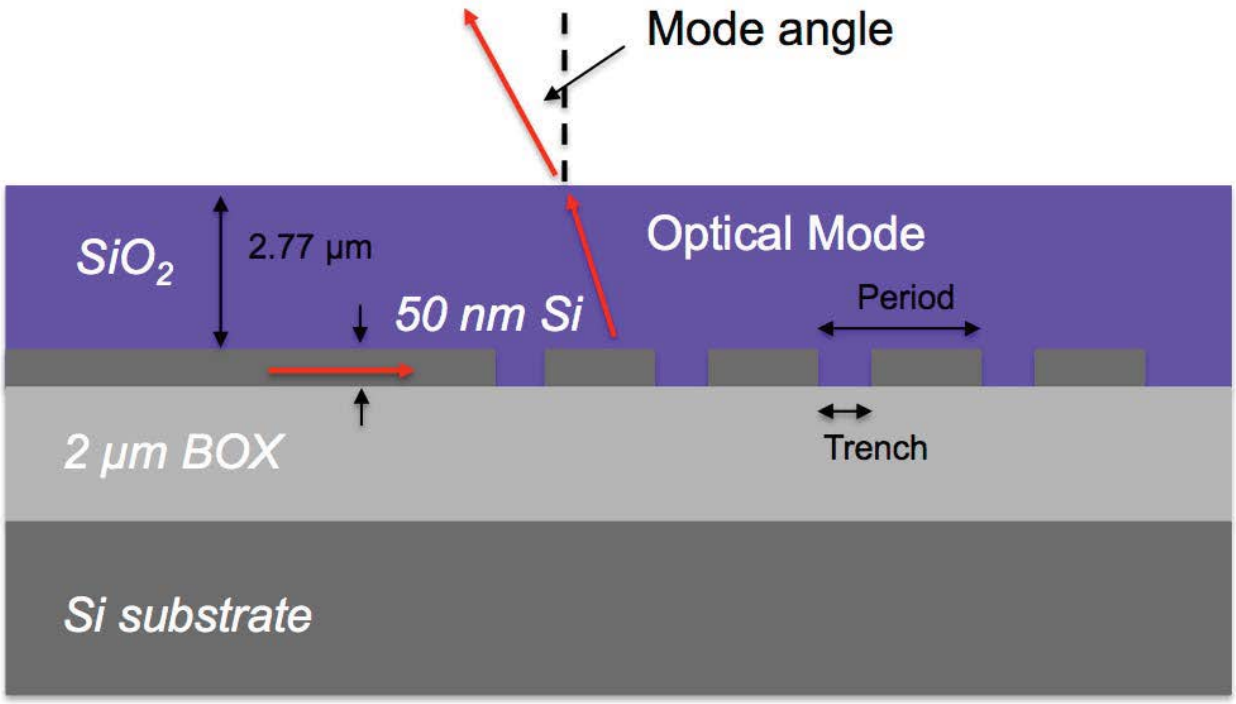

Fig. 1. Cross-sectional view of the thin grating coupler.

48. Harris, Nicholas C; Baehr-Jones, Tom; Lim, Andy Eu-Jin; Liow, TY; Lo, GQ; Hochberg, Michael; "Noise characterization of a waveguide-coupled MSM photodetector exceeding unity quantum efficiency" Journal of Lightwave Technology Vol. 31, No. 1;23-27 (2013)

Abstract: In the field of silicon photonics, it has only recently become possible to build complex systems. As system power constraints and complexity increase, design margins will decrease—making understanding device noise performance and device- specific noise origins increasingly necessary. We demonstrate a waveguide-coupled germanium metal–semiconductor–metalphotodetector exhibiting photoconductive gain with a responsivity of 1.76 A/W at 5 V bias and fF capacitance. Our measurements indicate that a significant portion of the dark current is not associated with the generation of shot noise. The noise elbow at 5 V bias is measured to be approximately 150 MHz and the high-frequency detector noise reaches the Johnson noise floor.

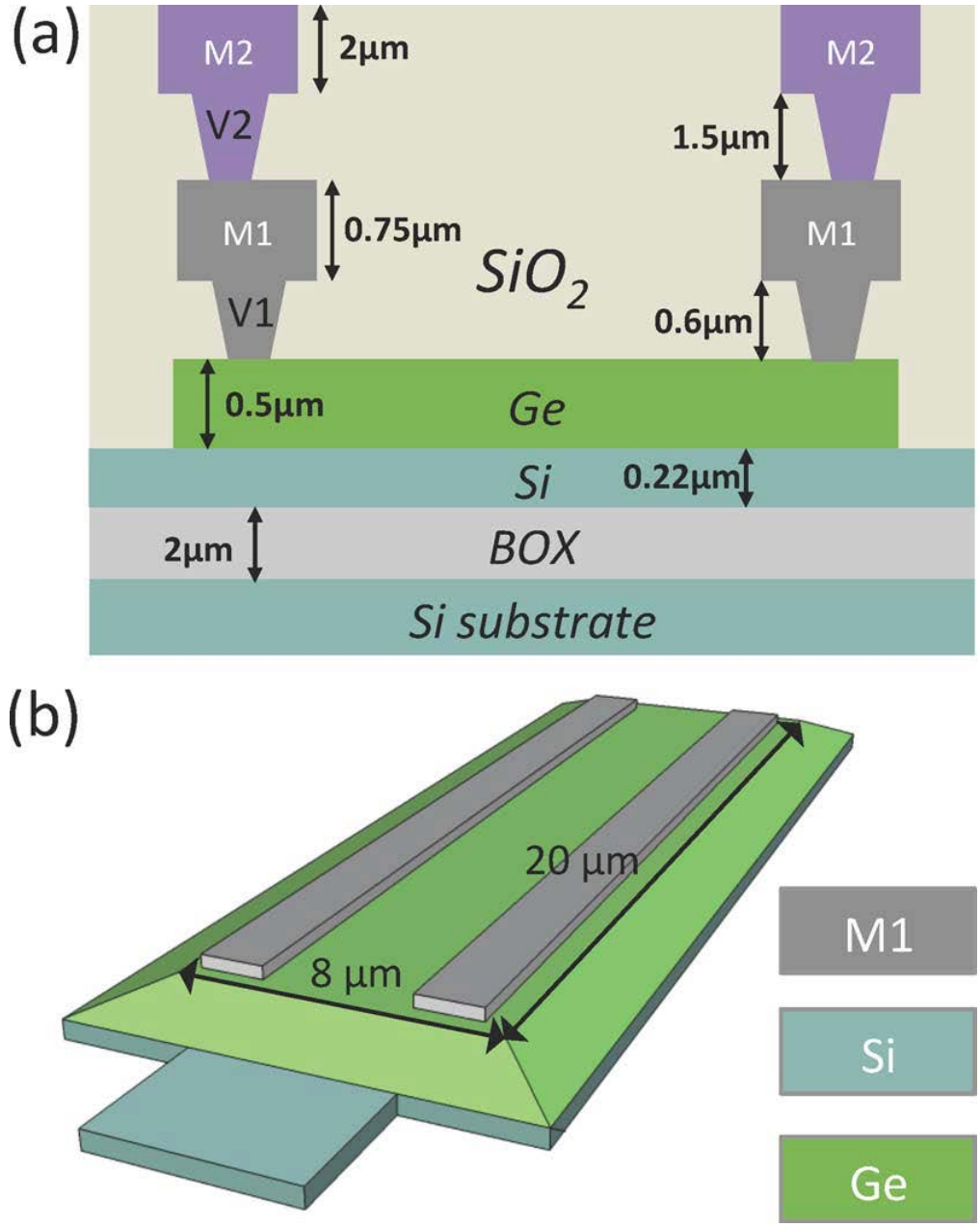

Fig. 1. MSM photodetector fabrication specifications. (a) Cross-sectional view of process stack for detector. (b) Schematic view of germanium detector.

49. Hochberg, Michael; Harris, Nicholas C; Ding, Ran; Zhang, Yi; Novack, Ari; Xuan, Zhe; Baehr-Jones, Tom; "Silicon photonics: the next fabless semiconductor industry" Solid-State Circuits Magazine, IEEE Vol. 5, No. 1 48-58 (2013)

Abstract: N/A

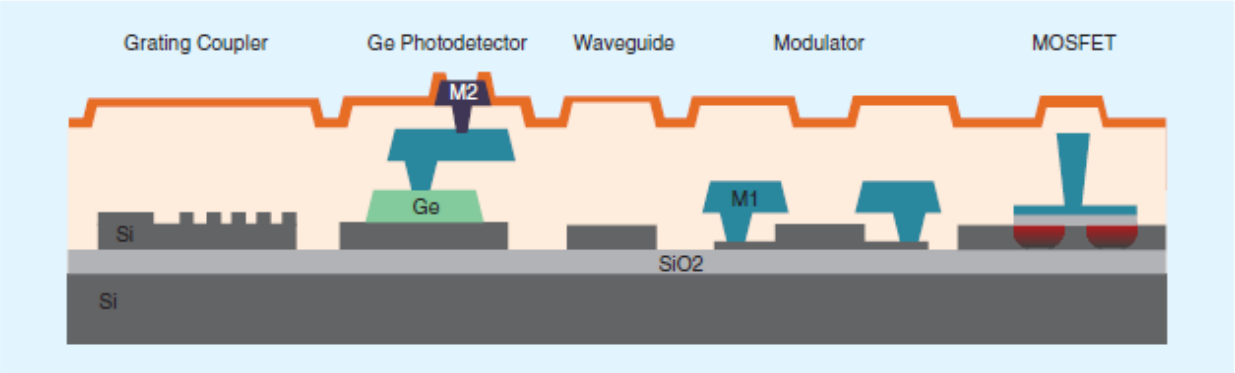

FIGURE 1: Typical process stack representing a silicon photonics platform with grating couplers, germanium photodetectors, waveguides, modulators, and MOSFET s on a silicon-on-insulator (SOI) wafer.

50. Liu, Yang; Dunham, Scott; Baehr-Jones, Tom; Lim, Andy Eu-Jin; Lo, Guo-Qiang; Hochberg, Michael; "Ultra-responsive phase shifters for depletion mode silicon modulators" Lightwave Technology, Journal of Vol.31, No. 23; 3787-3793 (2013)

Abstract: We propose a novel phase shifter design for carrier depletion based silicon modulators, based on an experimentally validated model.We note that the heretofore neglected effect of incomplete ionization will have a significant impact on ultra-responsive phase shifters.We predict a low $V\pi L$ product of 0.31 V.cm associated with a low propagation loss of 20 dB/cm. This would enable significantly smallerMach–Zehnder modulators to be constructed that nonetheless would have low drive voltages, with substantial decreases in insertion loss. The proposed fabrication process is of minimal complexity; in particular, no high-resolution lithographic step is required.

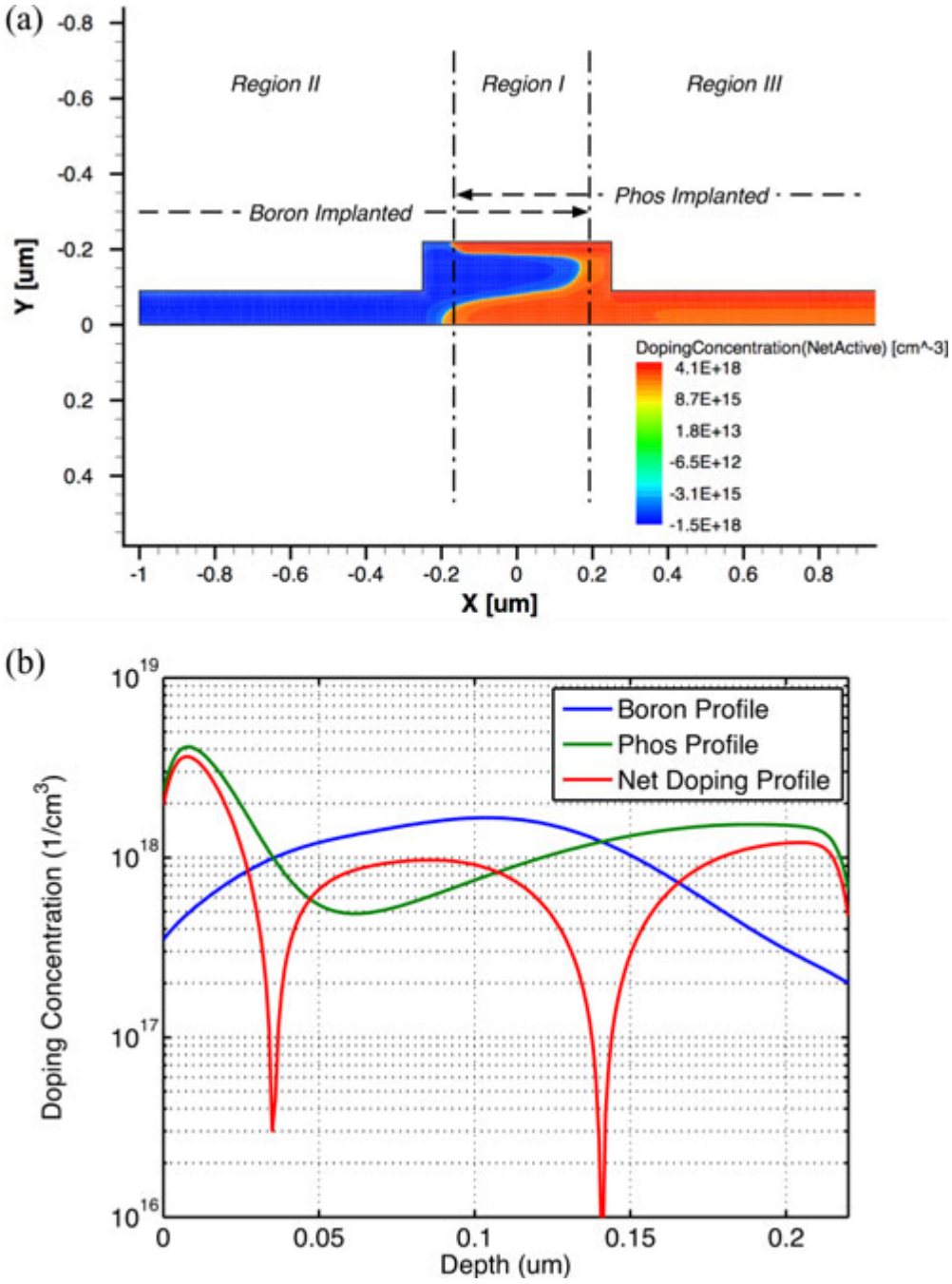

Fig. 1. (a) Simulated dopants distribution on the cross section of the phase shifter, following the implantation and annealing conditions listed in Table I. (b) Depth profile of phosphorus and boron.

51. Ding, Ran; Ma, Yangjin; Liu, Yang; Yang, Yisu; Lim, Andy Eu-Jin; Lo, Patrick Guo-Qiang; Baehr-Jones, Tom; Hochberg, Michael; "High-speed silicon modulators with slow-wave electrodes" Optical Fiber Communications Conference and Exhibition (OFC) ; 3-Jan (2014)

Abstract: We demonstrate a high-speed dual-drive silicon traveling-wave modulator with slowwave periodically phase-matched transmission-line electrodes and discuss the design aspects of such an approach. Our design also ensures true single-RF-mode operation independent of signaling schemes.

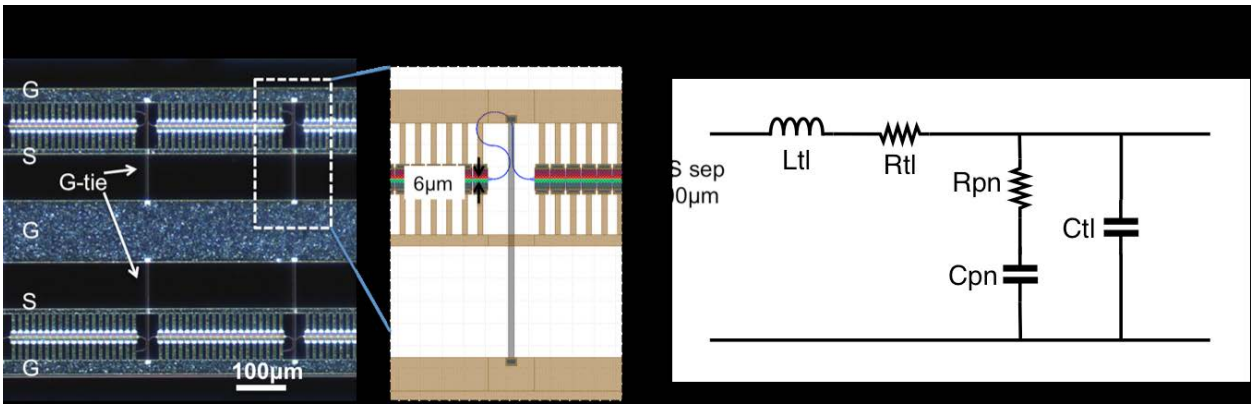

Fig. 1. (a) Microphotograph of a section of the device, mainly top metal is visible. Inset: details near a ground-plane lateral connection (G-tie) and the optical delay loop for re-aligning optical and RF phase (b) schematic of the simplified equivalent circuit of the PN junction loaded transmission line

52. Streshinsky, Matthew; Ding, Ran; Novack, Ari; Liu, Yang; Tu, Xiaoguang; Lim, Andy Eu-Jin; Chen, Edward Koh Sing; Lo, Patrick Guo-Qiang; Baehr-Jones, Tom; Hochberg, Michael; "50 Gb/s silicon traveling wave Mach-Zehnder modulator near 1300 nm" Optical Fiber Communications Conference and Exhibition (OFC); 3-Jan (2014).

Abstract: A silicon traveling-wave Mach-Zehnder modulator near 1300 nm is demonstrated to operate at 50 Gb/s with a differential 2 Vpp signal at 0 V reverse bias, achieving a 800 fJ/bit power consumption.

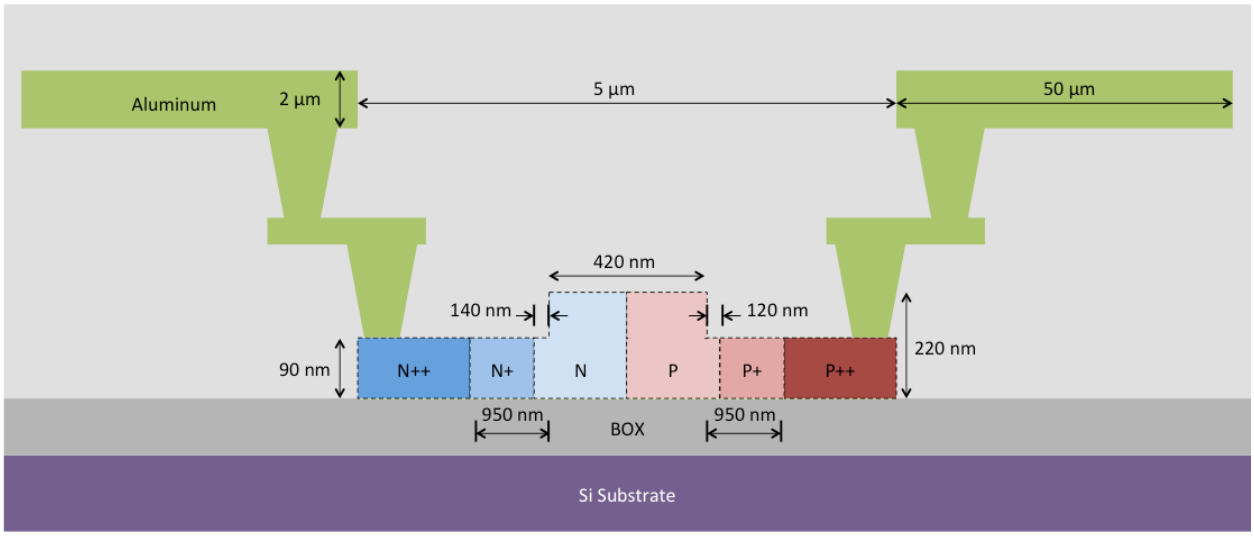

Fig. 1. Simplified cross sectional diagram of the phase shifter, not to scale.

53. Zhang, Yi; Yang, Shuyu; Lim, Andy Eu-Jin; Lo, Guo-Qiang; Baehr-Jones, Tom; Hochberg, Michael; "Sagnac loop mirror based laser cavity for silicon-on-insulator" Optical Interconnects Conference, 2014 IEEE; 77-78 (2014).

Abstract: We propose to build laser cavities on submicron silicon photonics platforms using Sagnac loop mirrors, which is easy to fabricate, has accurately controlled reflectivity, and negligible excess loss. A proof-of-concept device is demonstrated.

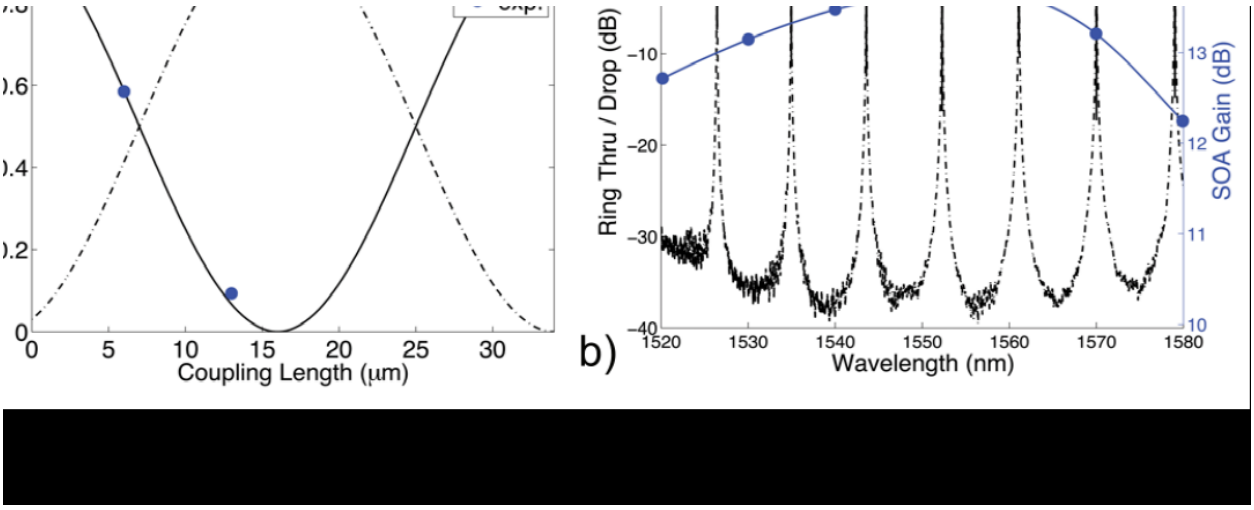

Fig. 3 a) Calculated and measured transmittance and reflectivity of Sagnac loop mirror as a function of DC coupling length; b) Ring filter drop (solid) and through (dashed) spectrum, and SOA gain spectrum at 150 mA (blue). The expected lasing wavelength (1552.3 nm) is labeled by a red pentagram. The ring FSR is 8.7 nm, and FWHM 0.075 nm, corresponding to Q of 20 000.

54. Shi, Ruizhi; Guan, Hang; Novack, Ari; Streshinsky, Matthew; Lim, Andy Eu-Jin; Lo, Guo-Qiang; Baehr-Jones, Tom; Hochberg, Michael; "High-efficiency grating couplers near 1310 nm fabricated by 248-nm DUV lithography" Photonics Technology Letters, IEEE Vol.26 No. 15;1569-1572 (2014).

Abstract: We demonstrate a highly efficient grating coupler with center wavelength near 1310 nm fabricated on a siliconon- insulator (SoI) wafer by 248-nm deep ultraviolet lithography. One of the lowest reported losses of 2 dB is achieved using feature sizes of 200 nm and without other process enhancements, such as polysilicon. The higher efficiency is obtained through improved mode-matching based on a novel genetic algorithm, which utilizes two different etch depths. The 3-dB bandwidth is 50 nm, and the back-reflection to the waveguide is better than 20 dB. The result shows low-loss coupling between waveguides and single-mode fibers for 1310~nm applications suitable for mass production on the commonly used 220-nm SoI platform.

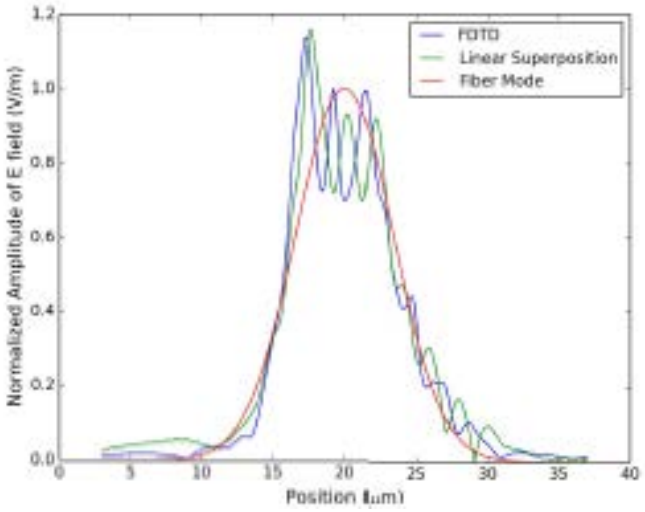

Fig. 2. Mode profile estimated by linear superposition of scattered fields and simulated in FDTD.

55. Ding, Ran; Xuan, Zhe; Baehr-Jones, Tom; Hochberg, Michael; "A 40-GHz bandwidth transimpedance amplifier with adjustable gain-peaking in 65-nm CMOS" Circuits and Systems (MWSCAS), 2014 IEEE 57th International Midwest Symposium; 965-968

Abstract: We present the design and characterization of a broadband, low-noise transimpedance amplifier (TIA) with adjustable gain-peaking, implemented in 65-nm CMOS. The TIA exhibits 40-GHz bandwidth, 20-dB gain and consumes 107 mW power. An additional continuously-tunable 12-dB gain-peaking near 40 GHz is available through a simple yet effective tuning mechanism, consuming only 14% more power. The adjustable gain-peaking functionality incorporated in the TIA can potentially reduce power consumption and complexity of an optical receiver and is highly desirable for adaptively-equalized receiver architectures. 50 Gb/s operation is demonstrated electrically as well as in an optical testbed. A low input-referred noise current of 2.5 uArms is achieved, suggesting an average optical power sensitivity of -14.6 dBm with a 0.5 A/W PD.

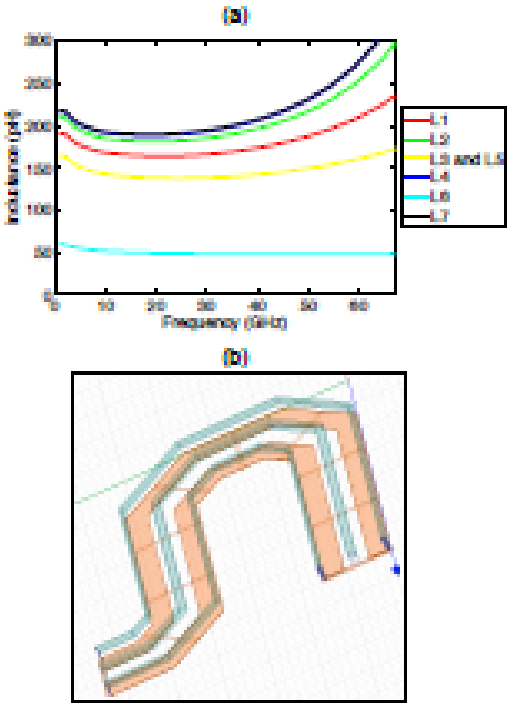

Fig. 3. Inductor modeling (a) simulated inductance (b) 3-D rendering of one of the shielded-microstrip-transmission-line inductors (L7) used in the circuit

56. Li, Hao; Xuan, Zhe; Titriku, Alex; Li, Cheng; Yu, Kunzhi; Wang, Binhao; Shafik, Ayman; Qi, Nan; Liu, Yang; Ding, Ran; "A 25Gb/s 4.4 V-swing AC-coupled Si-photonic microring transmitter with 2-tap asymmetric FFE and dynamic thermal tuning in 65nm CMOS" Solid-State Circuits Conference-(ISSCC), 2015 IEEE International , 3-Jan (2015).

Abstract: N/A

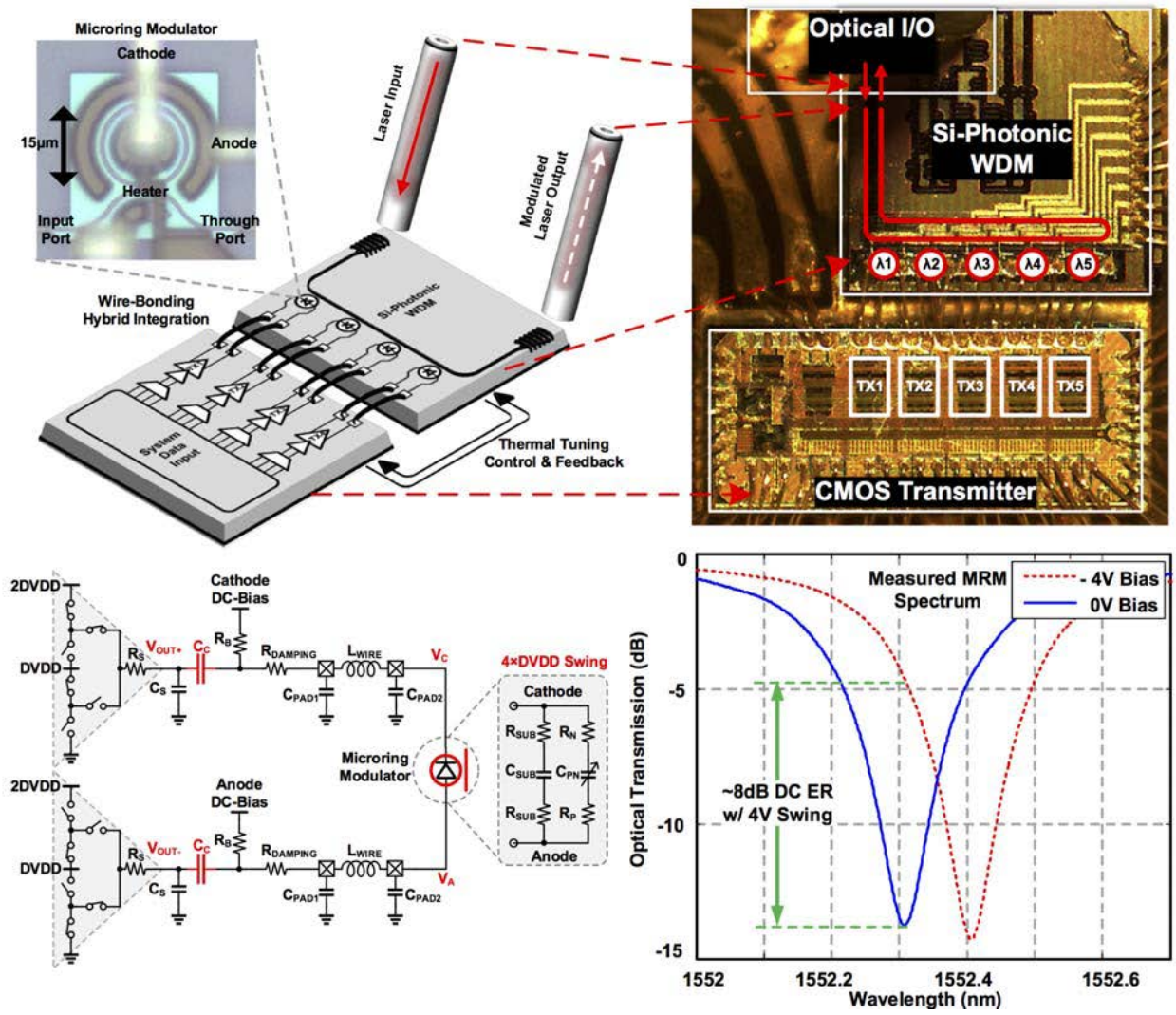

Figure 22.6.1: Hybrid integrated WDM transmitter concept and AC-coupled differential MRM modulation with 4×DVDD swing.

57. Li, Qi; Nikolova, Dessislava; Calhoun, David; Liu, Yang; Ding, Ran; Baehr-Jones, Tom; Hochberg, Michael; Bergman, Keren; "Single Microring-Based 2× 2 Silicon Photonic Crossbar Switches" (2015)

Abstract: Realizing small-footprint and energy-efficient optical switching fabrics is of crucial importance to solve the data movement challenges faced by optical interconnection networks. This letter demonstrates silicon photonic 2 × 2 full crossbar switching functionality based on a single microring. The ultracompact device is shown to successfully switch data channels from two input ports simultaneously. Data channels in both the multiple and the same wavelength switching experiments are measured to be error-free. Simulation shows that by optimizing some of the microring parameters crosstalk could be reduced. This letter confirms the applicability of a single microring as a 2 × 2 switch element for on-chip optical interconnects.

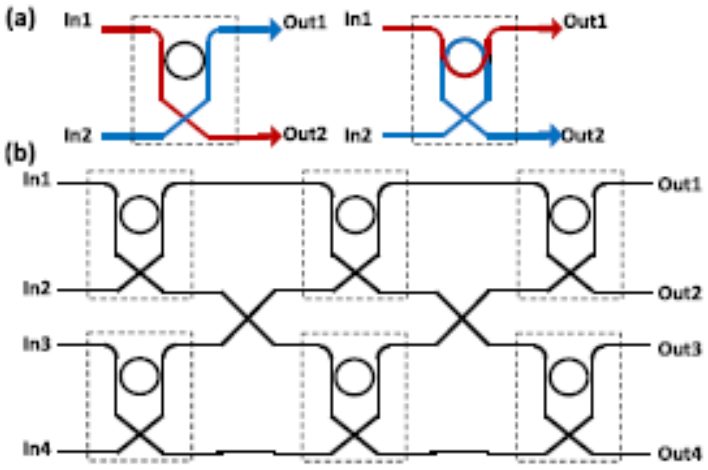

Fig. 1. (a) 2 × 2 switching element using single microring in two different states. (b) 4-by-4 multistage switch with Benes topology utilizing only 6 microrings.

58. Novack, Ari; Streshinsky, Matt; Ding, Ran; Liu, Yang; Lim, Andy Eu-Jin; Lo, Guo-Qiang; Baehr-Jones, Tom; Hochberg, Michael; "Progress in silicon platforms for integrated optics" Nanophotonics 5-April; 205-214 (2014).

Abstract: Rapid progress has been made in recent years repurposing CMOS fabrication tools to build complex photonic circuits. As the field of silicon photonics becomes more mature, foundry processes will be an essential piece of the ecosystem for eliminating process risk and allowing the community to focus on adding value through clever design. Multi-project wafer runs are a useful tool to promote further development by providing inexpensive, low-risk prototyping opportunities to academic and commercial researchers. Compared to dedicated silicon manufacturing runs, multi-project-wafer runs offer cost reductions of 100 × or more. Through OpSIS, we have begun to offer validated device libraries that allow designers to focus on building systems rather than modifying device geometries. The EDA tools that will enable rapid design of such complex systems are under intense development. Progress is also being made in developing practical optical and electronic packaging solutions for the photonic chips, in ways that eliminate or sharply reduce development costs for the user community. This paper will provide a review of the recent developments in silicon photonic foundry offerings with a focus on OpSIS, a multiproject-wafer foundry service offering a silicon photonics platform, including a variety of passive components as well as high-speed modulators and photodetectors, through the Institute of Microelectronics in Singapore.

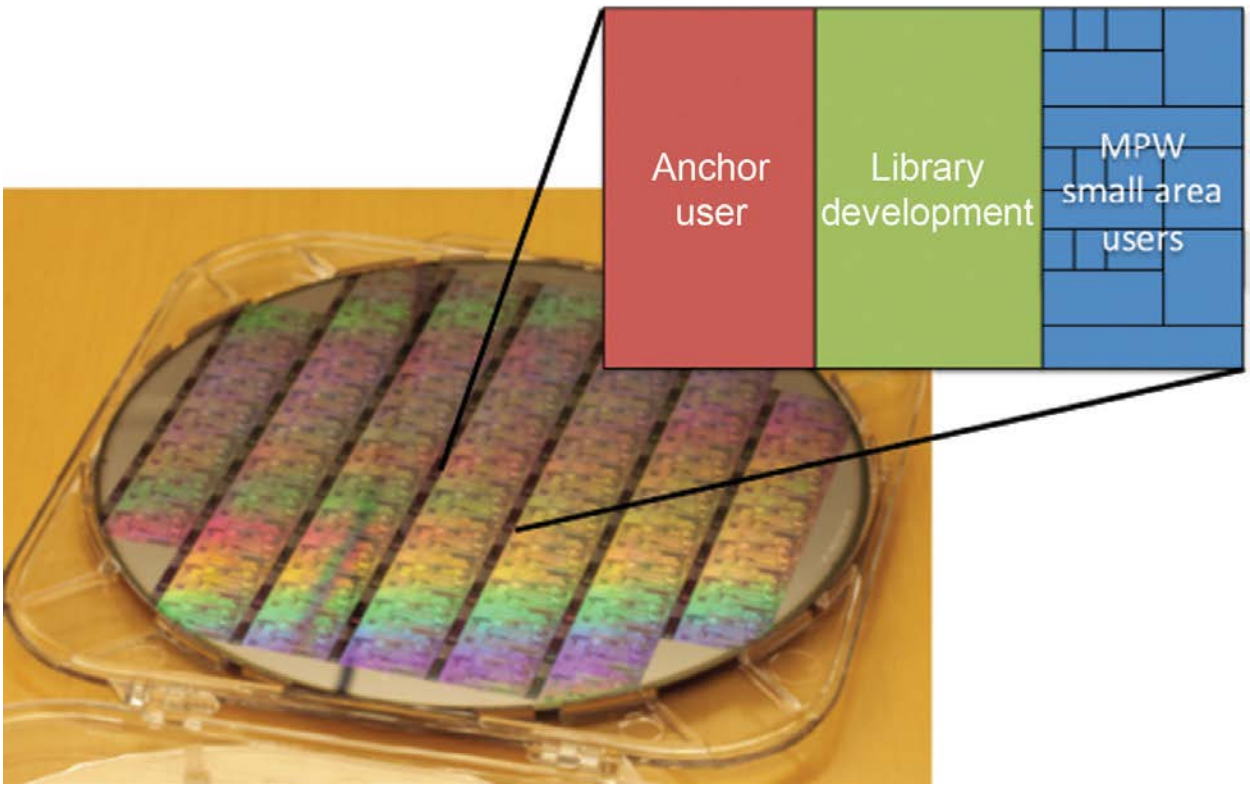

Figure 1 Photograph of an 8" wafer fabricated by the OpSIS_IME MPW service with an inset showing how the die are is divided amongst users.

59. Zhang, Yi; Baehr-Jones, Tom; Ding, Ran; Pinguet, Thierry; Xuan, Zhe; Hochberg, Michael; "Silicon multi-project wafer platforms for optoelectronic system integration" The 9th International Conference on Group IV Photonics (GFP) (2012)

Abstract: We report on several multi-project wafer (MPW) platforms for optoelectronic systems, which support monolithic integration of modulators and detectors at 25 Gb/s or higher. We also describe the Luxtera platform, which includes CMOS integration.

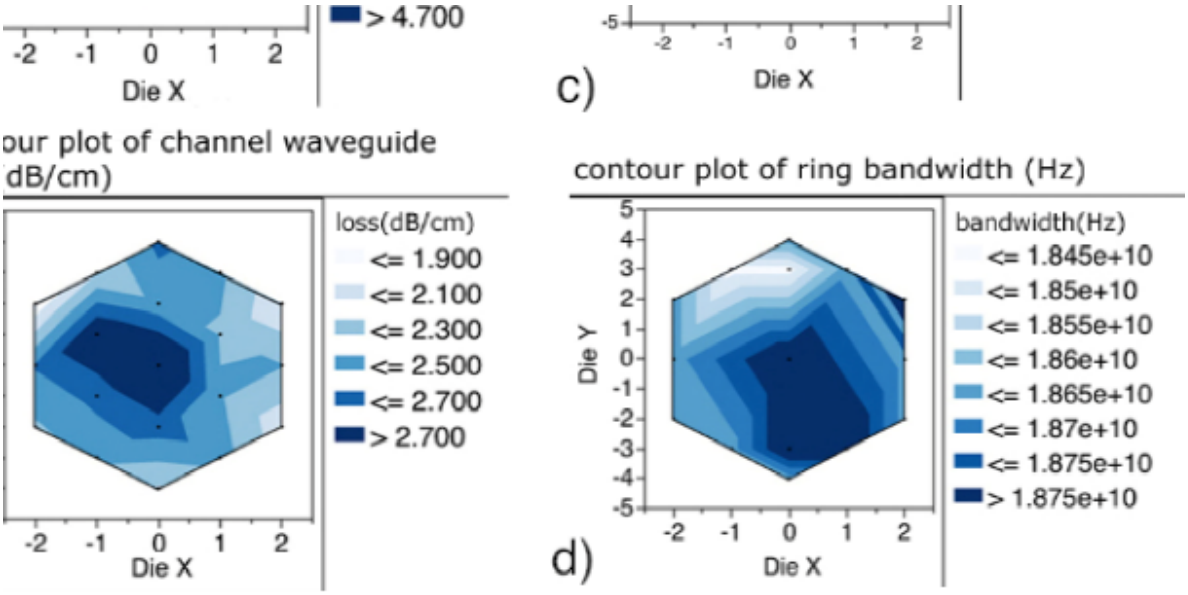

Figure 2. Cross-wafer data of a) grating coupler insertion loss, b) chanel waveguide propagation loss c) ring modulator tunability and d) ring modulator bandwidth.

60. Zhang, Yi, et al. "A compact and low-loss silicon waveguide crossing for O-band optical interconnect." *SPIE OPTO*. International Society for Optics and Photonics, 2014. (2 Google Scholar Citations)

Abstract: Silicon photonics has attracted extensive attention in recent years as a promising solution for next generation high-speed, low energy consumption, and low cost data transmission systems. Although a few experiments indicated board-level and long haul communication capability, major and near-future application of silicon photonics is commonly seen as Ethernet at 100Gb/s and beyond, such as interconnects in data centers, where O-Band (near 1310 nm wavelength) has been standardized for its low fiber dispersion. However, almost all silicon photonics devices demonstrated up to date operate at C-Band (1530 nm to 1560 nm), the fiber loss and erbium amplification window, probably due to the wider availability of lasers and testing apparatus at this wavelength. Typical C-Band devices cannot operate at O-Band, thus the whole device library needs to be redesigned and recalibrated for O-Band applications. In this paper, we present an ultra compact, low loss, and low crosstalk waveguide crossing operating at O-Band. It is designed using the finite difference time domain method coupled with a particle swarm optimization. Device footprint is only 6 μm × 6 μm. The measured insertion loss is 0.19±0.02 dB across an 8-inch wafer. Cross talk is lower than -35 dB. We also report a second waveguide crossing with a 9 μm × 9 μm footprint with 0.017±0.005 dB insertion loss. Finally we summarize the performance of our overall O-Band device library, including low-loss waveguides, high-speed modulators, and photodetectors.

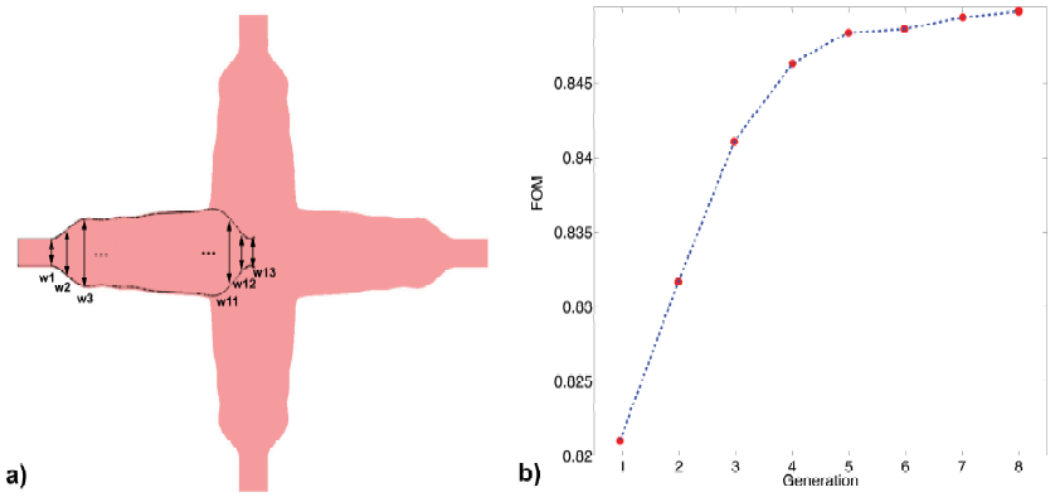

Fig. 1 a) Schematic device layout. The waveguide crossing consists of four identical tapers defined by w1 to w13; b) Evolution of FOM in the first 8 generations.

61. Hochberg, Michael, Thierry J. Pinguet, and Tom Baehr-Jones. "Future Requirements of Modeling Software for Integrated Optical Communication Systems." *Integrated Photonics Research, Silicon and Nanophotonics*. Optical Society of America, 2012.

Abstract: As silicon photonics processes mature and become available to an ever growing user base, the infrastructure needed to support large scale design needs to follow suit. We discuss here future requirements for modeling of integrated optical communication systems.

"Ideal" Model Features	Description	Examples
Multi-wavelength support	Simulator can run and output results over a range of wavelengths	
Polarization support	Simulator can run and output results for TE and/or TM modes and supports polarization conversion	
Dispersion	Every device's model has performance modeled depending on wavelength	Waveguide effective index dispersion Directional coupler splitting ratio vs. wavelength
Multi-directional propagation	Reflection at interfaces/ports and ability to model backward propagation, etc...	Inline grating
Environmental modeling	Performance changes as a function of T	Grating coupler peak wavelength drift w/temperature
Electro-optic effects	Models must represent effect of bias/currents on optical performance, and vice-versa	pn junction modulator photodiode
Nonlinear effects	Performance dependence on input power Frequency mixing (through various nonlinear effects, Xi2, Xi3, etc...)	Photodetector saturation with input power Raman amplification/lasing
DC and transient simulations supported	DC simulation for establishing operating points, etc... Transient for time-domain simulations Models must support phase and group velocity modeling and time delays	
Monte-Carlo/corners support	Simulator must be able to run MC or corner simulations and models must include device matching	Performance variability of devices placed next to each other vs. far away Need definition of corners
Co-simulation with electronics	Simulator must be able to co-simulate with existing Design Kits for electronics processes	Ability to simulate a TIA with a photodetector, or a modulator with a modulator drive
Restrictions	**Description**	**Examples**
Integrated photonics only	Devices have "ports" that connect to either waveguides on the chip or external optical elements like optical fiber or lasers Implies coupling from/to a primary mode in waveguides - coupling to another mode, for instance in multimode waveguides is considered loss	A single polarization grating coupler would have 1 in-plane port connecting to a waveguide and 1 out-of-plane port for a PM-fiber Optical ports can support one or two polarizations

Table 1: Basic requirements and constraints of future optical modeling

62. Baehr-Jones, Tom, et al. "Shared shuttles for integrated silicon optoelectronics." *SPIE MOEMS-MEMS*. International Society for Optics and Photonics, 2012. (3 Google Scholar Citations)

Abstract: Shared shuttle runs are an important factor of the microelectronics business ecosystem, allowing fabless semiconductor companies to access advanced processes and supporting the development of new tools and processes. We report on the creation and progress of a shared shuttle program for access to advanced silicon photonics optoelectronic platforms that we expect will create a similar environment for the field of integrated photonics.

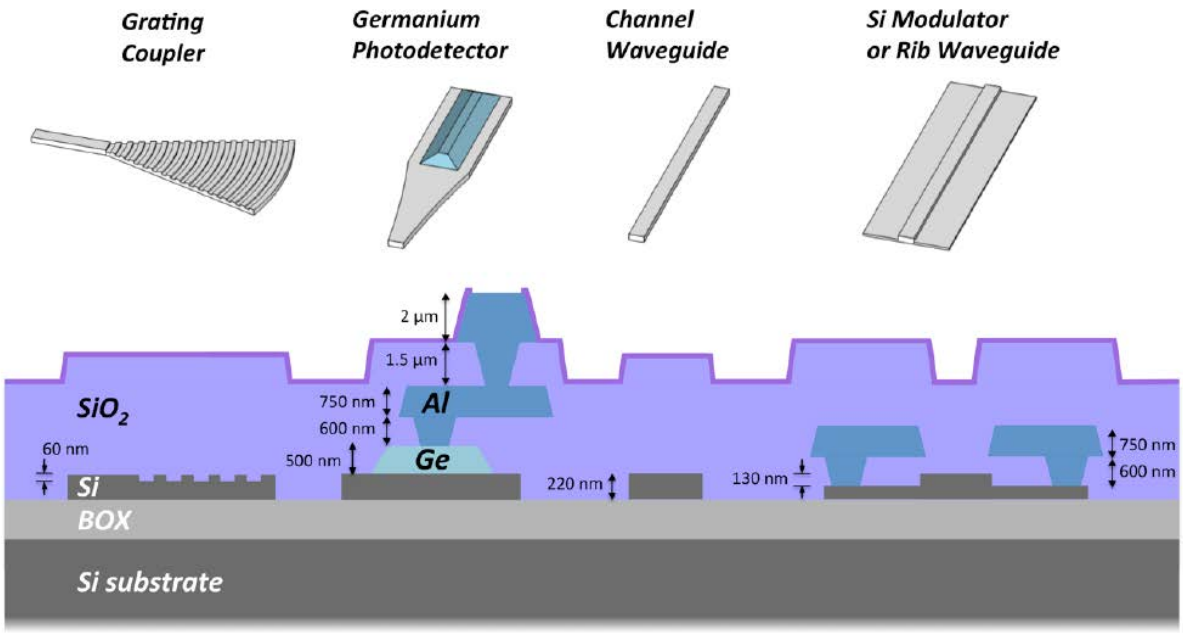

Figure 1. IME platform cross-section with example devices available in the design library

63. Hochberg, Michael, et al. "The Role of a Fabless Silicon Photonics Industry in the Era of Quantum Engineering." *Latin America Optics and Photonics Conference*. Optical Society of America, 2012.

Abstract: OpSIS is a foundry service for silicon photonics offering open processes and low access costs. We present the success of our project in conventional applications and how it can enable breakthroughs in applied quantum optics.

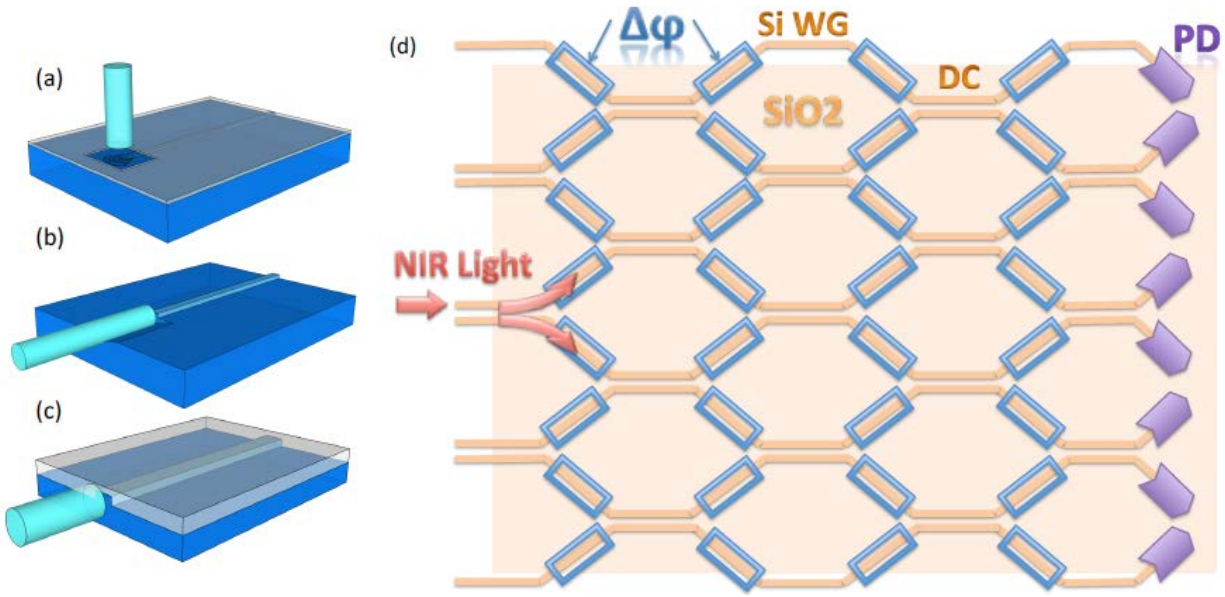

Fig. 1: (a-c) Three configurations to couple light between fiber and on-chip waveguide: (a) Top coupling through a grating coupler; (b) self-aligned V-groove coupling; (c) edge-coupling. (d) Schematic of the proposed photonic integrated circuit for large-scale, dynamically reconfigurable quantum walk. NIR: near infrared; $\Delta\phi$: phase shifter; WG: waveguide; DC: directional coupler; PD: Germanium photodetector. Electrical contacts are not shown.

64. Guan, Hang, Yangjin Ma, Ruizhi Shi, Ari Novack, Jingcheng Tao, Qing Fang, Andy Eu-Jin Lim, Guo-Qiang Lo, Tom Baehr-Jones, and Michael Hochberg. "Ultracompact silicon-on-insulator polarization rotator for polarization-diversified circuits." *Optics letters* 39, no. 16 (2014): 4703-4706. (7 Google Scholar Citations)

Abstract: We present an ultracompact (15.3 μmlong) and high-efficiency silicon-on-insulator polarization rotator designed for polarization-diversified circuits. The rotator is comprised of a bilevel-tapered TM0-to-TE1 mode converter and a novel bent-tapered TE1-to-TE0 mode converter. The rotator has a simulated polarization conversion loss lower than 0.2 dB and a polarization-extinction ratio larger than 25 dB over a wavelength range of 80 nm around 1550 nm. The rotator has a SiO2 top-cladding and can be fabricated in a CMOS-compatible process.

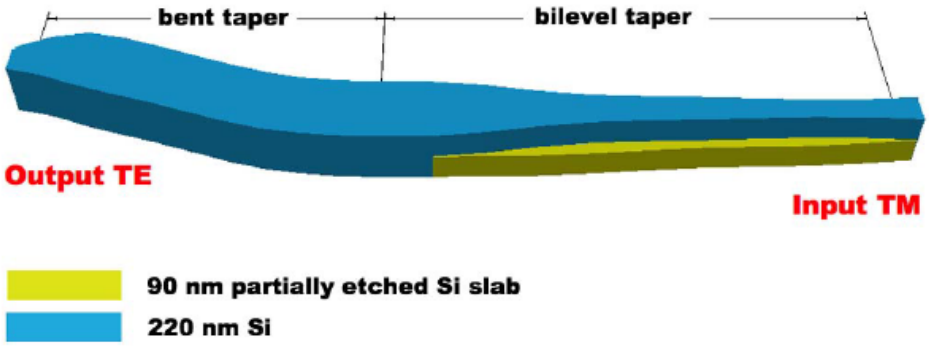

Fig. 1. Schematic of the PR, consisting of a bilevel taper and a bent taper. The PR is surrounded by a symmetric SiO2 cladding (a buried oxide bottom-cladding and a SiO2 top-cladding).

65. Gould, Michael, Andrew Pomerene, Craig Hill, Stewart Ocheltree, Yi Zhang, Tom Baehr-Jones, and Michael Hochberg. "Ultra-thin silicon-on-insulator strip waveguides and mode couplers." *Applied Physics Letters* 101, no. 22 (2012): 221106. (3 Google Scholar Citations)

Abstract: We demonstrate an ultra-thin silicon waveguide for wavelengths around 1.55 lm, and mode converters designed for transitions to and from standard 500 nm_220 nm strip waveguides. The devices were fabricated in a CMOS-compatible process requiring two photolithography and etch steps. The ultrathin waveguides exhibited losses of 2.0160.231 dB/cm, exhibited bend radii as small as 30 lm with losses of 0.0560.005 dB per bend, and exhibited coupling losses of 0.6660.014 dB to standard strip waveguides

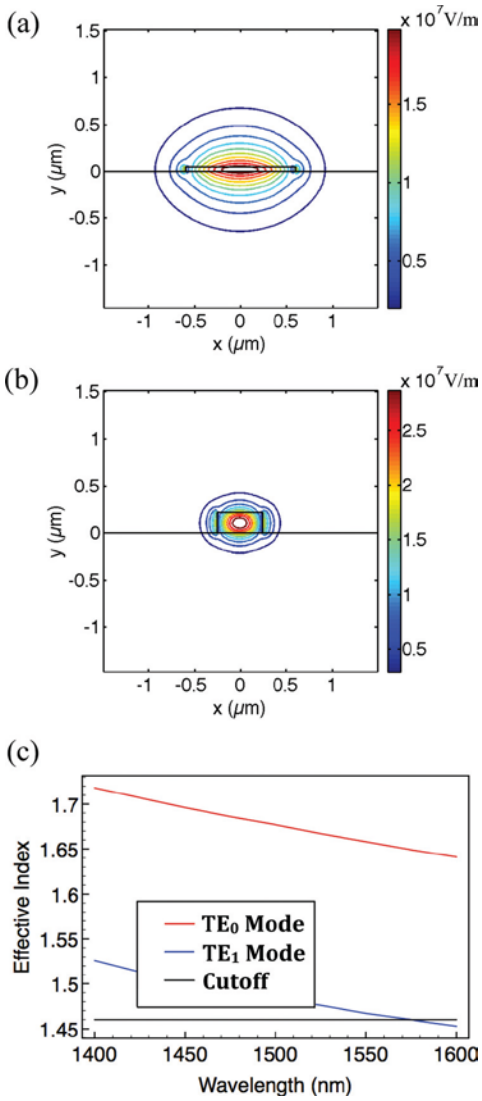

FIG. 1. Horizontal components of electric field (normalized to 1W) for fundamental mode of ultra-thin waveguide (a) and narrow strip waveguide (b). Dispersion diagram for the ultra-thin waveguide showing quasi-single mode behavior at 1.55 lm.

Example Papers from OpSIS Users:

66. Wesley D. Sacher, Tymon Barwicz, Benjamin J. F. Taylor, and Joyce K. S. Poon, "Polarization rotator-splitters in standard active silicon photonics platforms," Opt. Express 22, 3777-3786 (2014). (23 Google Scholar Citations)

Abstract: We demonstrate various silicon-on-insulator polarization management structures based on a polarization rotator-splitter that uses a bi-level taper TM0-TE1 mode converter. The designs are fully compatible with standard active silicon photonics platforms with no new levels required and were implemented in the IME baseline and IME-OpSIS silicon photonics processes. We demonstrate a

polarization rotator-splitter with polarization crosstalk < −13 dB over a bandwidth of 50 nm. Then, we improve the crosstalk to < −22 dB over a bandwidth of 80 nm by integrating the polarization rotator-splitter with directional coupler polarization filters. Finally, we demonstrate a polarization controller by integrating the polarization rotator-splitters with directional couplers, thermal tuners, and PIN diode phase shifters.

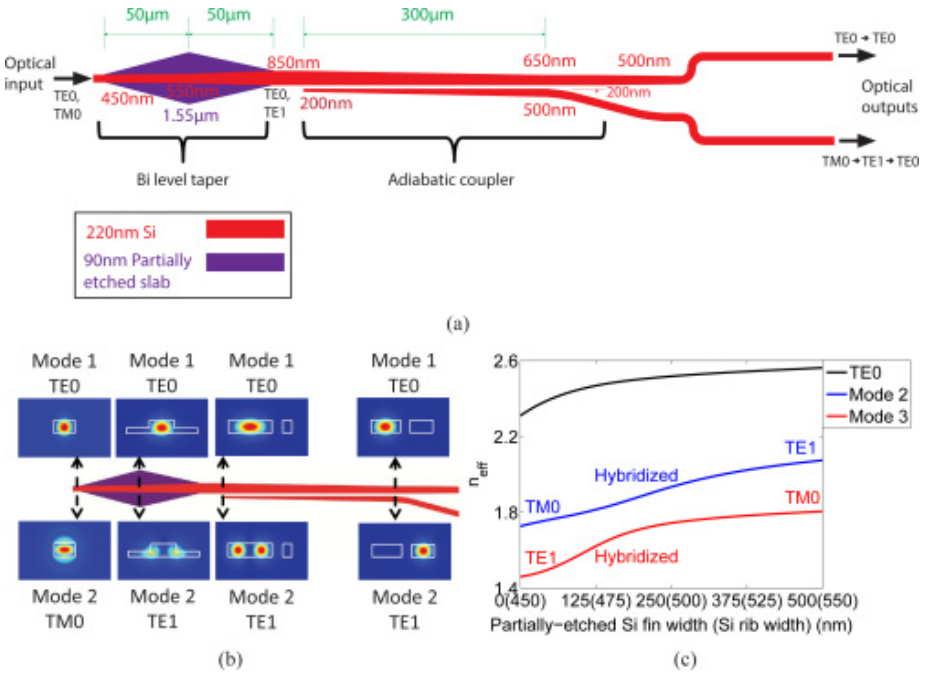

Fig. 1. (a) Schematic of the polarization rotator-splitter (PRS).Widths are labeled in red and purple; lengths use green labels. (b) Schematic showing the profiles of the modes with the first and second highest effective indices (i.e., "mode 1" and "mode 2") at different points along the PRS. In the adiabatic coupler, "mode 1" and "mode 2" refer to supermodes of the composite waveguide. (c) Effective indices along the first half of the bi-level taper for modes 1 to 3 at a wavelength of 1550 nm.

67. Runxiang Yu, Stanley Cheung, Yuliang Li, Katsunari Okamoto, Roberto Proietti, Yawei Yin, and S. J. B. Yoo, "A scalable silicon photonic chip-scale optical switch for high performance computing systems," Opt. Express 21, 32655-32667 (2013). (14 Google Scholar Citations)

Abstract: This paper discusses the architecture and provides performance studies of a silicon photonic chip-scale optical switch for scalable interconnect network in high performance computing systems. The proposed switch exploits optical wavelength parallelism and wavelength routing characteristics of an Arrayed Waveguide Grating Router (AWGR) to allow contention resolution in the wavelength domain. Simulation results from a cycle-accurate network simulator indicate that, even with only two transmitter/receiver pairs per node, the switch exhibits lower end-to-end latency and higher throughput at high (>90%) input loads compared with electronic switches. On the device integration level, we propose to integrate all the components (ring modulators, photodetectors and AWGR) on a CMOS-compatible silicon photonic platform to ensure a compact, energy efficient and cost-effective device. We successfully

demonstrate proof-of-concept routing functions on an 8 × 8 prototype fabricated using foundry services provided by OpSIS-IME.

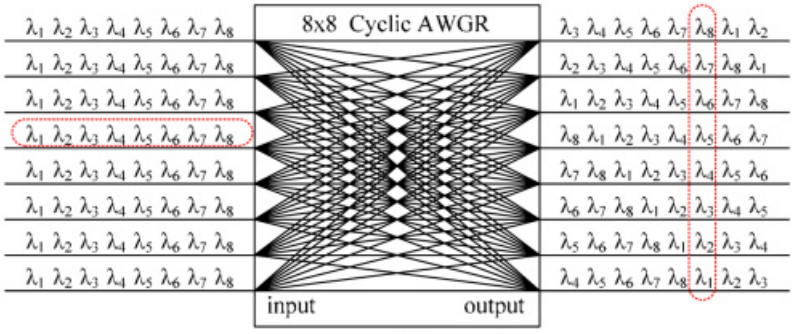

(a)

	Output 1	Output 2	Output 3	Output 4	Output 5	Output 6	Output 7	Output 8
Input 1	λ_3	λ_2	λ_1	λ_8	λ_7	λ_6	λ_5	λ_4
Input 2	λ_2	λ_1	λ_8	λ_7	λ_6	λ_5	λ_4	λ_3
Input 3	λ_1	λ_8	λ_7	λ_6	λ_5	λ_4	λ_3	λ_2
Input 4	λ_8	λ_7	λ_6	λ_5	λ_4	λ_3	λ_2	λ_1
Input 5	λ_7	λ_6	λ_5	λ_4	λ_3	λ_2	λ_1	λ_8
Input 6	λ_6	λ_5	λ_4	λ_3	λ_2	λ_1	λ_8	λ_7
Input 7	λ_5	λ_4	λ_3	λ_2	λ_1	λ_8	λ_7	λ_6
Input 8	λ_4	λ_3	λ_2	λ_1	λ_8	λ_7	λ_6	λ_5

(b)

Fig. 1 (a) the routing property and (b) the routing table of an 8 × 8 cyclic-frequency AWGR.

68. Jonathan Klamkin, Fabrizio Gambini, Stefano Faralli, Antonio Malacarne, Gianluca Meloni, Gianluca Berrettini, Giampiero Contestabile, and Luca Potì, "A 100-Gb/s noncoherent silicon receiver for PDM-DBPSK/DQPSK signals," Opt. Express 22, 2150-2158 (2014). (11 Google Scholar Citations)

Abstract: An integrated noncoherent silicon receiver for demodulation of 100-Gb/s polarization-division multiplexed differential quadrature phase-shift keying and polarization-division multiplexed differential binary phase-shift keying signals is demonstrated. The receiver consists of a 2D surface grating coupler, four Mach-Zehnder delay interferometers and four germanium balanced photodetectors.

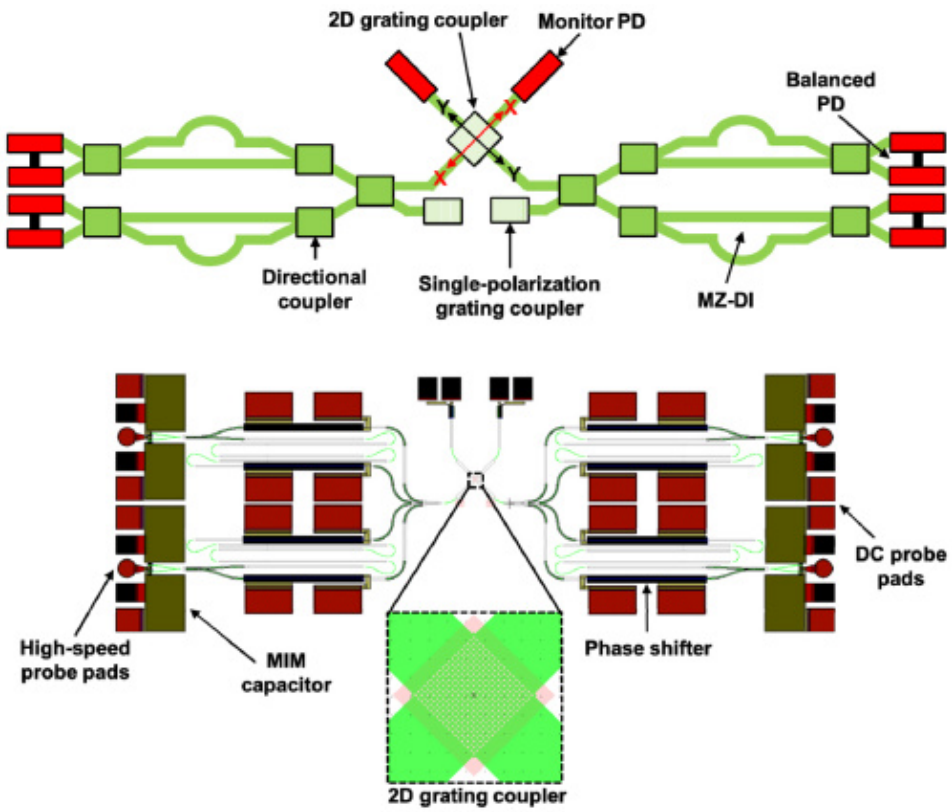

Fig. 1 Schematic (top) and mask layout (bottom) of integrated Si PDM-DBPSK/DQPSK receiver. A close-up of the layout of the 2D grating coupler is shown.

69. Malacarne, A.; Gambini, F.; Faralli, S.; Klamkin, J.; Poti, L., "High-Speed Silicon Electro-Optic Microring Modulator for Optical Interconnects," in *Photonics Technology Letters, IEEE* , vol.26, no.10, pp.1042-1044 (2014). (3 Google Scholar Citations)

Abstract: A silicon microring modulator for ON-OFF keying intensity modulation is presented and experimentally characterized. Modulation operation is based on carrier depletion effect in a p-n junction. The resonance wavelength shift is measured for bias voltages in the range between 0 and -7 V and modulation is demonstrated by employing electrical signals with data rates of 25 and 30 Gb/s and peak-to-peak voltage of 3.75 V. Performance in terms of bit error rate as a function of the optical signal-to-noise ratio for point-to-point transmission over 10 km of single mode fiber at both the data rates is experimentally evaluated, manifesting to be suitable for short- and medium-reach optical interconnects applications.

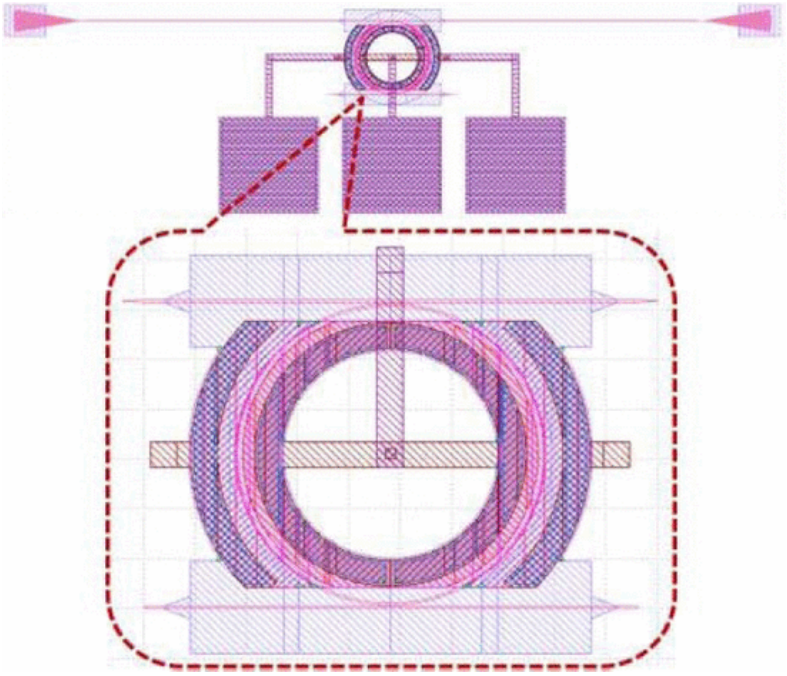

Fig. 1. Mask layout schematic of the microring modulator.

70. Doménech, J. D., Fandino, J. S., Banos, R., & Munoz, P. "Opto-electronic wavelength tracker in Silicon-on-Insulator," *European Conference on Integrated Optics* (2014).

Abstract: In this paper the experimental demonstration of a Silicon-on-Insulator opto-electronic wavelength tracker is reported. The device consist of a 2x3 Mach-Zehnder interferometer with 10 pm resolution and photo-detectors integrated on the same chip. The design provides three complementary, with 120◦ phase relations, responses. Optical input/output responses exhibit rejection as good as 15 dB, thanks to asymmetric design for the input coupler. Synchronized recorded DC electronic responses for the three photo-detector outputs reproduce the MZI de-phased characteristic, allowing for monitoring wavelength changes with sign.

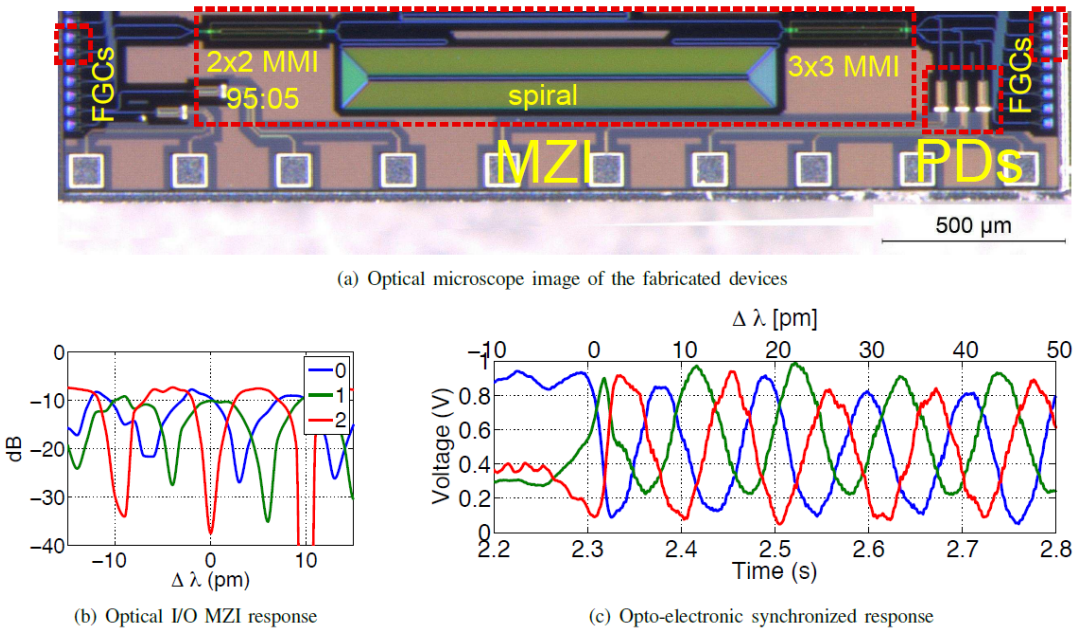

(a) Optical microscope image of the fabricated devices

(b) Optical I/O MZI response

(c) Opto-electronic synchronized response

Fig. 1. Optical microscope image of the fabricated device (a) MZI I/O spectral traces with respect of 1549.83 nm (b) and synchronized electronic traces (c) for the three WVLT channels.

71. Abiri, B., Aflatouni, F., & Hajimiri, A., "A self-equalizing photo detector," *Photonics Conference (IPC), IEEE*, pp. 196-197 (2014). (2 Google Scholar Citations)

Abstract: A self-equalizing photo-detector (SEPD) that mitigates the bandwidth limitations of electro-optical components of optical communication systems is demonstrated, enabling higher rate of data transmission, using slower components. Unlike other all-optical equalization schemes, SEPD is optically wide band, thus does not require wavelength tuning.

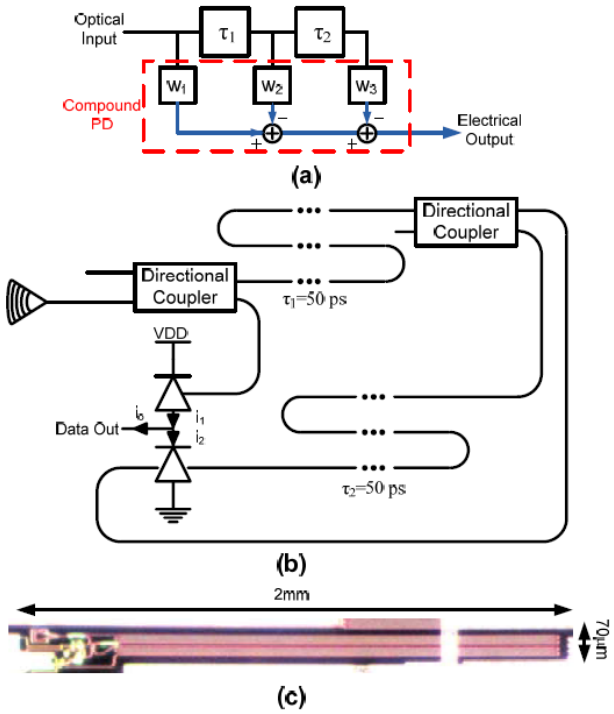

Figure 1. Proposed self-equalizing photo detector. (a) Conceptual block diagram, (b) detailed implemented block diagram, and (c) the die photo of fabricated detector

72. Jinsoo Rhim; Yoojin Ban; Jeong-Min Lee; Seong-Ho Cho; Woo-Young Choi, "A behavior model for silicon micro-ring modulators and transmitter circuit-level simulation using it," in *Group IV Photonics (GFP), 2014 IEEE 11th International Conference on* , vol., no., pp.7-8, 27-29 (2014). (2 Google Scholar Citations)

Abstract: We implement and verify Si micro-ring modulator (MRM) behavioral model based on the dynamic coupled-mode theory. We also perform circuit-level simulation of the entire Si photonic transmitter including the driver electronics and the Si MRM.

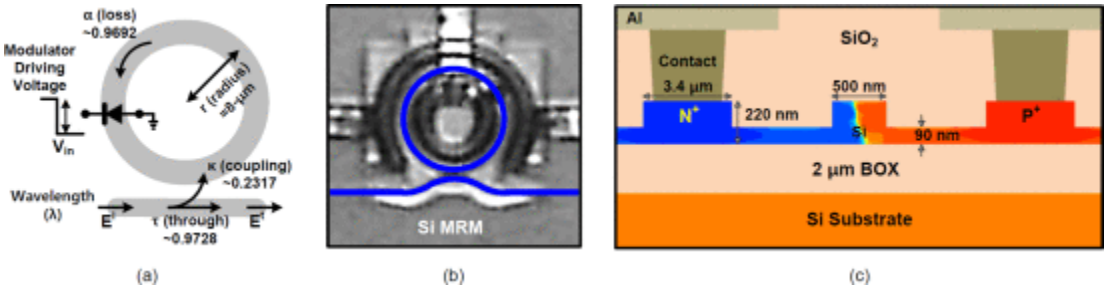

Fig. 1: Micro-ring modulator (a) structure (b) microphotograph (c) cross-sectional view

73. Yule Xiong; Ye, W.N., "Slotted silicon microring resonators with multimode interferometer couplers," in *Group IV Photonics (GFP), 2013 IEEE 10th International Conference on* , vol., no., pp.118-119, 28-30 (2013). (1 Google Scholar Citation)

Abstract: We demonstrate a SOI slotted microring resonator using a multimode interferometer (MMI) coupler. We achieved high bandwidth of 0.25 nm, and a quality factor Q of ~6000 for rings with a radius of 20 μm.

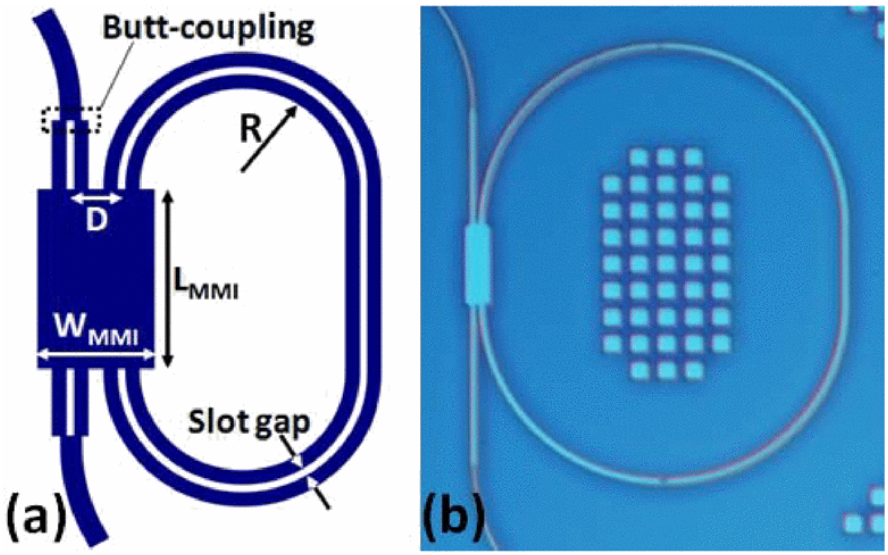

Fig 1. (a) Schematic of a MMI-coupled slot-waveguide-based ring resonator. (b) Microscopic image of the fabricated MMI-coupled slot ring resonator.

74. Saman Saeedi and Azita Emami, "Silicon-photonic PTAT temperature sensor for micro-ring resonator thermal stabilization," Opt. Express 23, 21875-21883 (2015).

Abstract: We present a scheme for thermal stabilization of micro-ring resonator modulators through direct measurement of ring temperature using a monolithic PTAT temperature sensor. The measured temperature is used in a feedback loop to adjust the thermal tuner of the ring. The closed-loop feedback system is demonstrated to operate in presence of thermal perturbations at 20Gb/s.

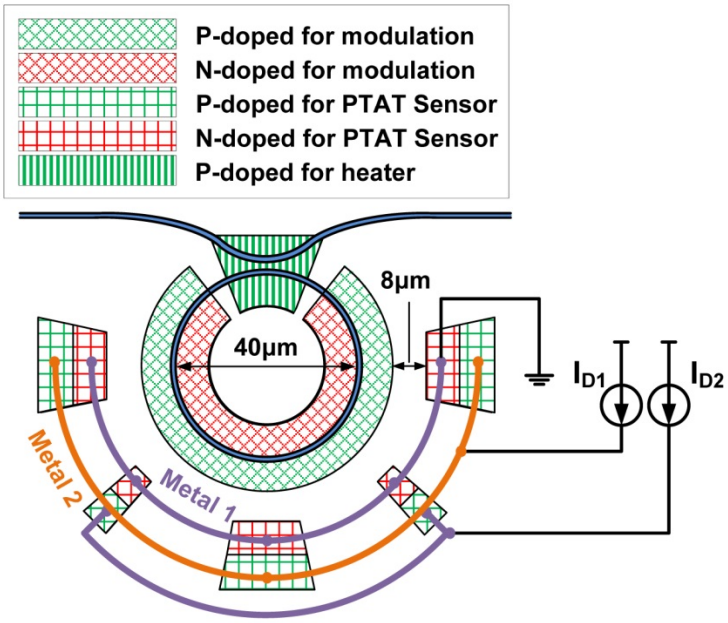

Fig. 1. Proposed structure of ring resonator with integrated heater and PTAT temperature sensor.

75. Doménech, J. D., Fandiño, J. S., Gargallo, B., Baños, R., & Muñoz, P., "Silicon opto-electronic wavelength tracker based on an asymmetric 2x3 Mach-Zehnder Interferometer."

Abstract: In this paper we report on the experimental demonstration of a Silicon-on-Insulator opto-electronic wavelength tracker for the optical telecommunication C-band. The device consist of a 2x3 Mach-Zehnder Interferometer (MZI) with 10 pm resolution and photo-detectors integrated on the same chip. The MZI is built interconnecting two Multimode Interference (MMI) couplers with two waveguides whose length difference is 56 mm. The first MMI has a coupling ratio of 95:05 to compensate for the propagation loss difference corresponding to the 56 mm. The wavelength tracker design provides three complementary, with 120◦ phase relations, responses. The MZI optical responses exhibit rejection as good as 15 dB, thanks to asymmetric design for the input coupler. Synchronized recorded DC electronic responses for the three photo-detector outputs reproduce the MZI de-phased characteristic, allowing for monitoring wavelength changes with sign.

Figure 1. Wavelength tracker concept (a) and sketch of a 2x3 Mach-Zehnder Interferometer based on Multimode Interference couplers (b).

76. Matiolli Machado, L.; Delrosso, G.; Borin, F.; Rodrigues Fernandes de Oliveira, J.; Corso, V.; Hecker de Carvalho, L.H.; Rodrigues Fernandes de Oliveira, J.C., "Advanced optical communication systems and devices," in *Electronics System-Integration Technology Conference (ESTC), 2014* , vol., no., pp.1-4, 16-18 (2014). (1 Google Scholar Citation)

Abstract: This paper shows recent developments and achievements at Centro de Pesquisa e Desenvolvimento em Telecomunicações (CPqD), Campinas, Brazil, concerning advanced photonic devices based respectively on Silicon Photonics (SiP) and Thin Film Polymer on Silicon (TFPS™) integration technologies to drive the next generation of ultra-fast optical communication networks. The Brazilian's first SiP-based 100G DP-QSPK modulator and a 100Gbps DP-QPSK Transmit Optical Sub-Assemblies (TOSA) module, suitable for CFP2 transceivers are reviewed. CPqD extensive research and development programme, the largest of its kind in Latin America, has produced ICT solutions for both private and public corporations in communications, multimedia, financial, utilities, industrial, defence and security sectors. Its Optical System Division is in charge of numerous projects in high capacity / ultra-fast optical systems and networks management, (software-defined networking and smart algorithms) as needed for the forthcoming future high-capacity elastic optical networks.

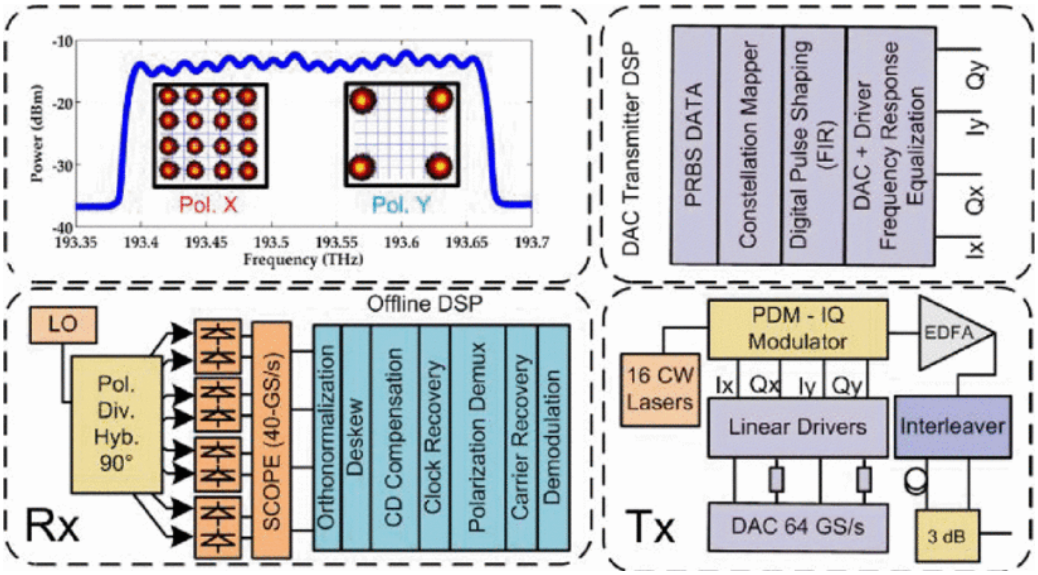

Figure 1: Details of the flexible transponder schematic, transmitter DSP and optical spectrum.

77. David Patel, Samir Ghosh, Mathieu Chagnon, Alireza Samani, Venkat Veerasubramanian, Mohamed Osman, and David V. Plant, "Design, analysis, and transmission system performance of a 41 GHz silicon photonic modulator," Opt. Express 23, 14263-14287 (2015). (4 Google Scholar Citations)

Abstract: The design and characterization of a slow-wave series push-pull traveling wave silicon photonic modulator is presented. At 2 V and 4 V reverse bias, the measured −3 dB electro-optic bandwidth of the modulator with an active length of 4 mm are 38 GHz and 41 GHz, respectively. Open eye diagrams are observed up to bitrates of 60 Gbps without any form of signal processing, and up to 70 Gbps with passive signal processing to compensate for the test equipment. With the use of multi-level amplitude modulation formats and digital-signal-processing, the modulator is shown to operate below a hard-decision forward error-correction threshold of 3.8×10^{-3} at bitrates up to 112 Gbps over 2 km of single mode optical fiber using PAM-4, and over 5 km of optical fiber with PAM-8. Energy consumed solely by the modulator is also estimated for different modulation cases.

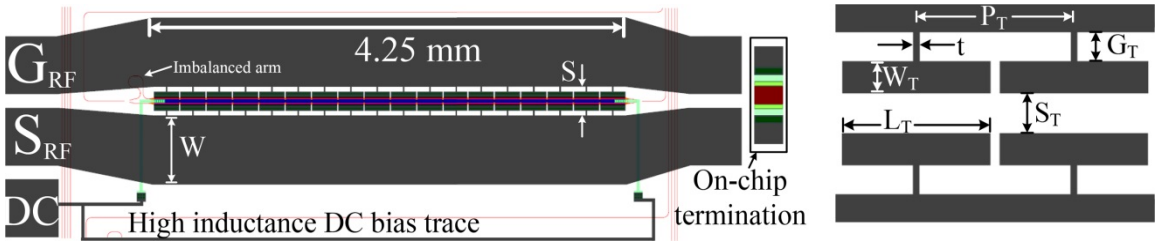

Fig. 1: *Layout schematic of the SPP TWMZM and a magnified view of the 'T'-shaped extensions (schematic not to scale). The dimensions are: W = 120 μm, S = 51 μm, t = 2 μm, S_T = 12.6 μm, G_T = 9.2 μm, W_T = 10 μm, L_T = 47 μm, and P_T = 50 μm.*

78. Jeong-Min Lee; Woo-Young Choi, "An equivalent circuit model for germanium waveguide vertical photodetectors on Si," in *Microwave Photonics (MWP) and the 2014 9th Asia-Pacific Microwave Photonics Conference (APMP), 2014 International Topical Meeting on* , vol., no., pp.139-141, 20-23 (2014).

Abstract: We present an equivalent circuit model for 1.55-μm germanium waveguide vertical photodetector on a Si-on- Insulator (SOI) substrate. The model has two current sources for modeling photogenerated carriers so that those carriers experiencing drift and diffusion within the Ge intrinsic layer can be independently modeled. The model provides photodetection frequency response simulation results that match very well with the measurement results. It should be very useful for designing integrated Si optical receiver.

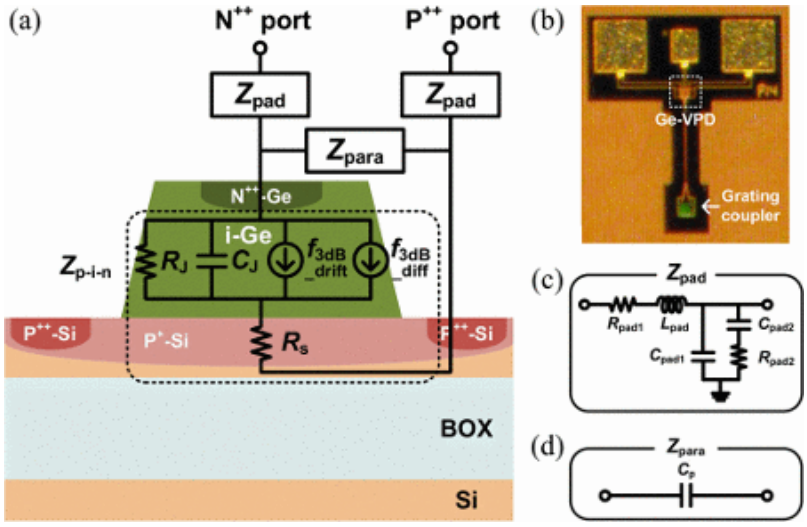

Fig. 1. (a) Cross-section and equivalent circuit model for Ge-Vpd. (b) Top view of the fabricated Ge-vpd. (c) Equivalent circuit model for pads and interconnection lines. (d) Equivalent circuit model for the parasitic elements.

79. Merget, F., Azadeh, S. S., Mueller, J., Shen, B., Nezhad, M. P., Hauck, J., & Witzens, J., “Novel Transmission Lines for 32 Gbit/s Si MZI Modulator.”

Abstract: We present MZI Silicon Photonics modulators with an advanced transmission line design which overcomes bandwidth limitations arising from crosstalk and improves linear RF-losses. A -3dBe electro-optic bandwidth of 16.2GHz with a 50□ matched dual drive voltage of 4V is experimentally validated for a 4mm long device.

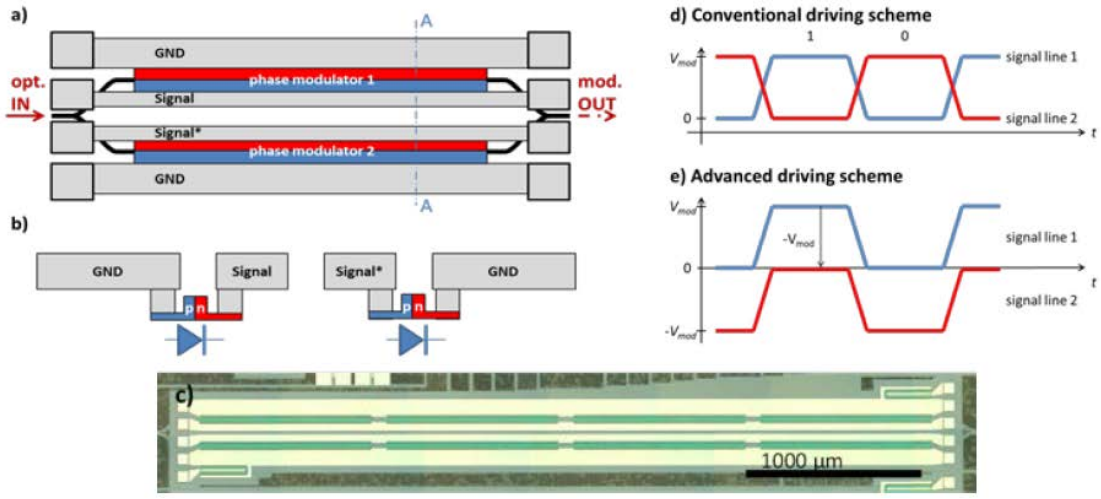

Fig. 1. Left: Top view (a), cross-sectional schematic (b) and microscope image (c) of the investigated modulator. Right: Signals for the conventional (d) and the advanced driving scheme (e).

80. R. Yu, S. Cheung, R. Proietti, Y. Li, K. Okamoto, and S. J. B. Yoo, "A Silicon Photonic Chip-Scale AWGR Switch for High Performance Computing Systems," in *CLEO: 2014*, OSA Technical Digest (online) (Optical Society of America, 2014), paper SM2G.7.

Abstract: This paper demonstrates a silicon-photonic AWGR-based optical switch for HPC systems. Simulations show high throughput and low latency even at high input load. A fabricated silicon-photonic AWGR switch with 32 Tx/Rx pairs showed error-free performance.

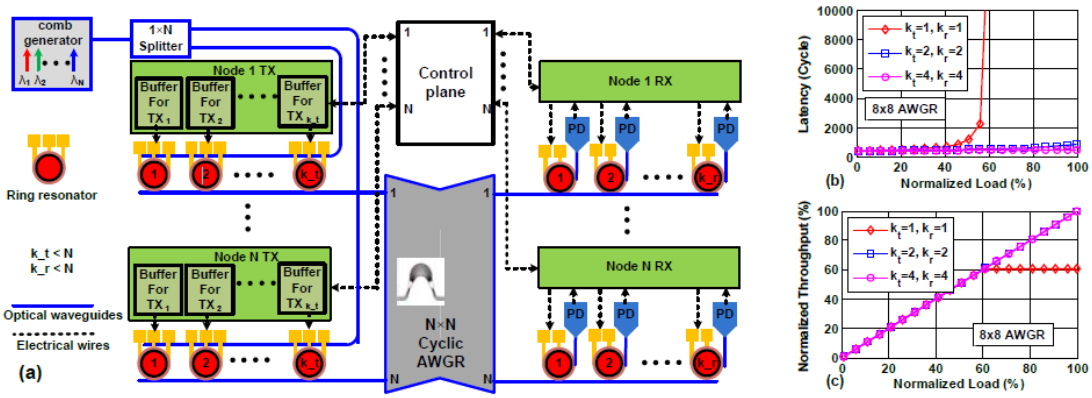

Fig. 1.(a) The proposed interconnect architecture for chip-scale high performance computing systems and performance study on (b) end-to-end latency and (c) throughput of the proposed architecture with 8 nodes under uniform random traffic.

81. Ciyuan Qiu, Weilu Gao, Robert Vajtai, Pulickel M. Ajayan, Junichiro Kono, and Qianfan, "Efficient Modulation of 1.55 μm Radiation with Gated Graphene on a Silicon Microring Resonator," Xu*Nano Letters* 2014 *14* (12), 6811-6815. (10 Google Scholar Citations)

Abstract: The gate-controllability of the Fermi-edge onset of interband absorption in graphene can be utilized to modulate near-infrared radiation in the telecommunication band. However, a high modulation efficiency has not been demonstrated to date, because of the small amount of light absorption in graphene. Here, we demonstrate a ~40% amplitude modulation of 1.55 μm radiation with gated single-layer graphene that is coupled with a silicon microring resonator. Both the quality factor and resonance wavelength of the silicon microring resonator were strongly modulated through gate tuning of the Fermi level in graphene. These results promise an efficient electro-optic modulator, ideal for applications in largescale on-chip optical interconnects that are compatible with complementary metal-oxide-semiconductor technology.

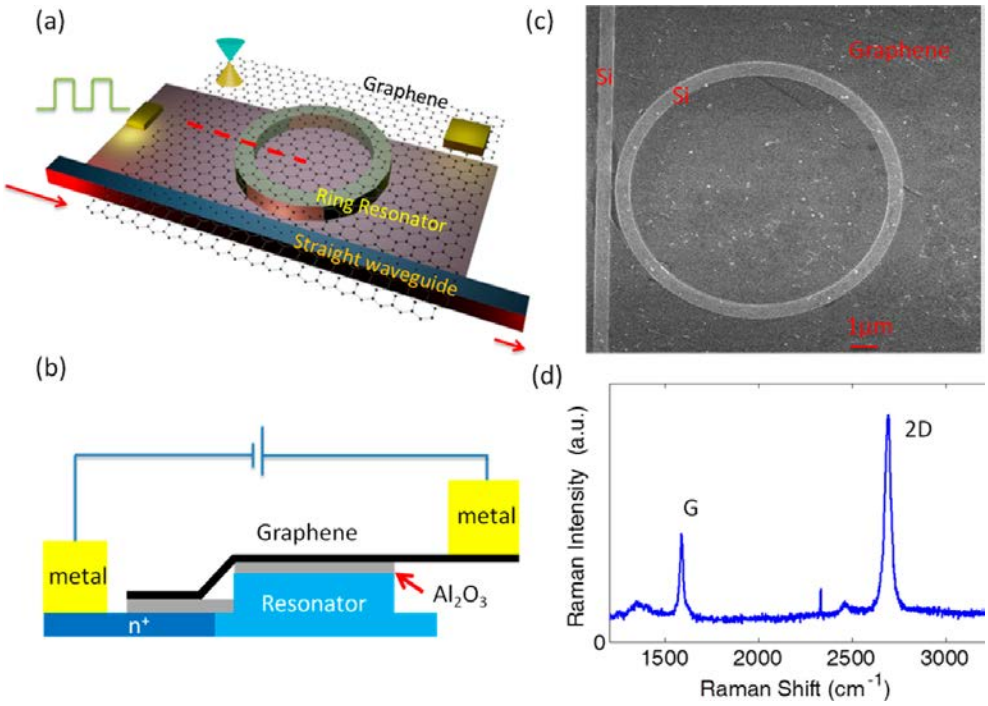

Figure 1. (a) Schematic diagram of graphene-modulated silicon microring modulator. (b) Cross-sectional diagram of the modulator corresponding to the red dashed line in (a). Al2O3 works as the gate dielectric material. The gate voltage is applied between the bottom n+-doped silicon slab and graphene layer. (c) Top-view scanning electron microscope picture of the modulator after graphene is transferred on top of the microring area. (d) Raman spectrum of transferred graphene.

82. S. Schneider, M. Lauermann, C. Weimann, W. Freude, and C. Koos, "Silicon Photonic Optical Coherence Tomography System," in CLEO: 2014, OSA Technical Digest (online) (Optical Society of America, 2014), paper ATu2P.4.

Abstract: A swept-source optical coherence tomography system is realized as a silicon photonic integrated circuit comprising passive components and germanium photo detector. Experiments show uniform sensitivity over 5 mm scanning range, enabling simple imaging demonstrations.

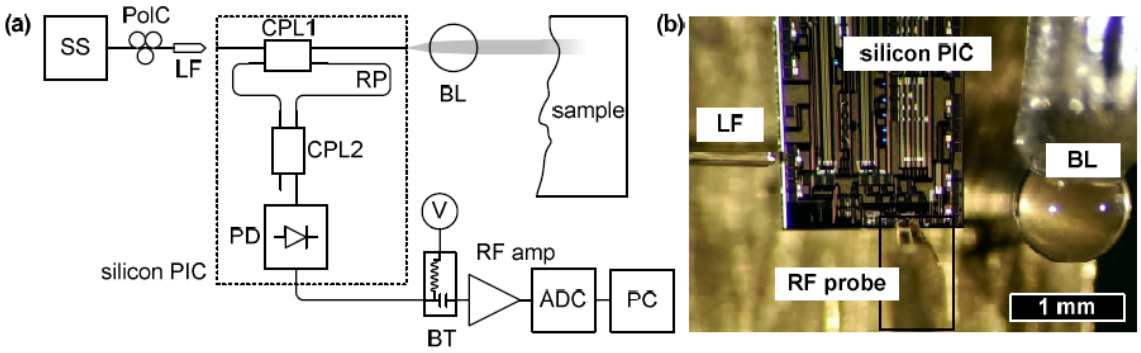

Fig. 1: Experimental setup and PIC structure. (a) Schematic of the setup. SS: swept-source laser, PolC: polarization controller, LF: lensed fibre, PIC: photonic integrated circuit, CPL: 3-dB-coupler, BL: ball lens, RP: reference path, PD: photo diode, BT: bias-T, V: bias voltage source, RF amp: RF amplifier, ADC: analogue-to-digital converter, PC: personal computer. (b) Microscope image showing the coupling configuration of the silicon chip. In all experiments, exact positioning of the ball lens is crucial to both beam collimation and beam angle.

83. Y. Painchaud ; M. Poulin ; F. Pelletier ; C. Latrasse ; J.-F. Gagné ; S. Savard ; G. Robidoux ; M. -. Picard ; S. Paquet ; C. -. Davidson ; M. Pelletier ; M. Cyr ; C. Paquet ; M. Guy ; M. Morsy-Osman ; M. Chagnon ; D. V. Plant; Silicon-based products and solutions. Proc. SPIE 8988, Integrated Optics: Devices, Materials, and Technologies XVIII, 89880L (March 8, 2014); doi:10.1117/12.2036355. (4 Google Scholar Citations)

Abstract: TeraXion started silicon photonics activities aiming at developing building blocks for new products and customized solutions. Passive and active devices have been developed including MMI couplers, power splitters, Bragg grating filters, high responsivity photodetectors, high speed modulators and variable optical attenuators. Packaging solutions including fiber attachment and hybrid integration using flip-chip were also developed. More specifically, a compact packaged integrated coherent receiver has been realized. Good performances were obtained as demonstrated by our system tests results showing transmission up to 4800 km with BER below hard FEC threshold. The package size is small but still limited by the electrical interface. Migrating to more compact RF interface would allow realizing the full benefit of this technology.

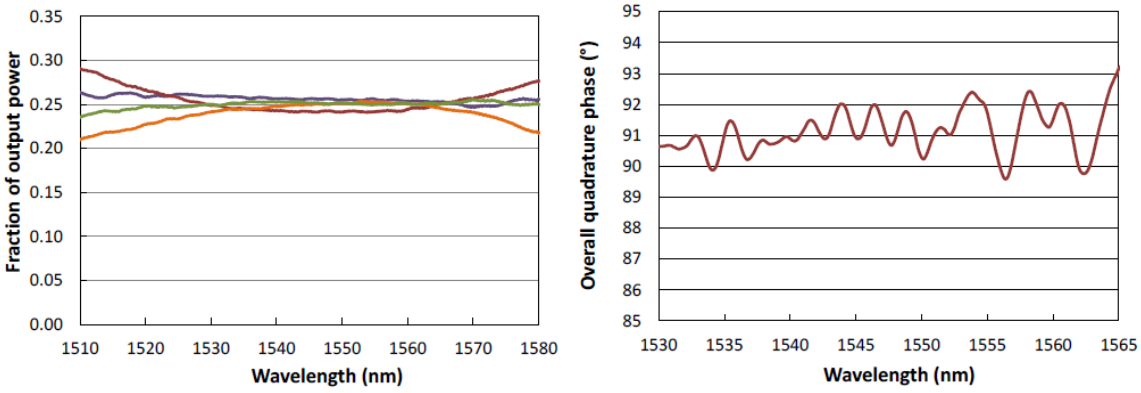

Figure 1. Proportion of the output power among the 4 outputs of a 4×4 MMI coupler (left) and overall quadrature phase of the four outputs (right).

84. W. Sacher, T. Barwicz, and J. Poon, "Silicon-on-Insulator Polarization Splitter-Rotator Based on TM0-TE1 Mode Conversion in a Bi-level Taper," in CLEO: 2013, OSA Technical Digest (online) (Optical Society of America, 2013), paper CTu3F.3. (5 Google Scholar Citations)

Abstract: The first demonstration of a silicon-on-insulator polarization splitter-rotator using TM0-TE1 mode conversion in a bi-level taper is reported. The device was fabricated in a foundry process and exhibits a polarization crosstalk < -13 dB.

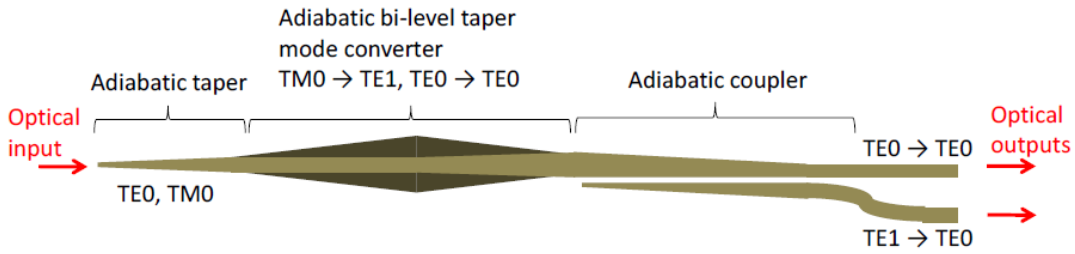

Fig. 1. Schematic of the PSR. The lighter regions represent Si with the full height, and the darker regions represent a partially etched level of Si

85. Júlio C. R. F. de Oliveira ; Alexandre P. Freitas ; Fellipe G. Peternella ; Leandro Matiolli ; Valentino Corso ; Flávio Borin ; Bernardo B. C. Kyotoku ; Neil Guerreiro-Gonzalez; "The first Brazilian integrated 100G DPQPSK transmitter on a 4×3 mm silicon photonic chip," Proc. SPIE 9010, Next-Generation Optical Networks for Data Centers and Short-Reach Links, 90100D (February 19, 2014); doi:10.1117/12.2040879. (2 Google Scholar Citations)

Abstract: The first Brazilian high speed integrated 100G-DPQPSK transmitter on a 4 x 3 mm silicon photonic chip is presented. The novel photonic component allows optical signal generation of advanced modulation formats in 25GHz bandwidth. Furthermore, in this paper we also present our vision on required integrated photonics targeting 400G optical transmission systems.

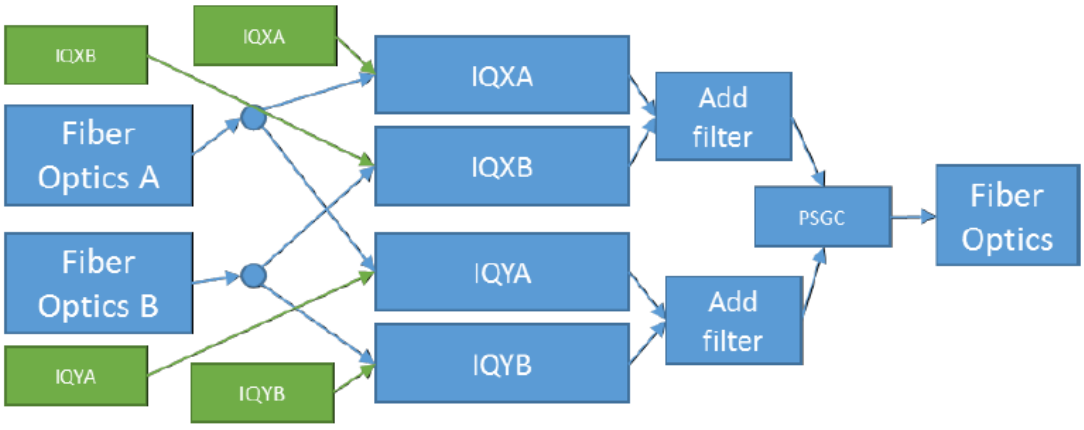

Figure 1: Diagram of the envisioned 400G transmitter. Green boxes refer to RF signals, blue boxes photonic component. Two wavelengths A and B are used. Each wavelength is modulated with an IQ modulator twice, one for each polarization (X and Y).

86. V. Kopp, J. Park, M. Wlodawski, E. Hubner, J. Singer, D. Neugroschl, and A. Genack, "Vanishing Core Optical Waveguides for Coupling, Amplification, Sensing, and Polarization Control," in Advanced Photonics, OSA Technical Digest (online) (Optical Society of America, 2014), paper SoW1B.3.

Abstract: Microformed, adiabatically tapered optical waveguides utilizing a "vanishing core" concept possess unique properties that make them useful for dense multichannel coupling, spatial division multiplexing for communications and sensing, polarization control, and amplification.

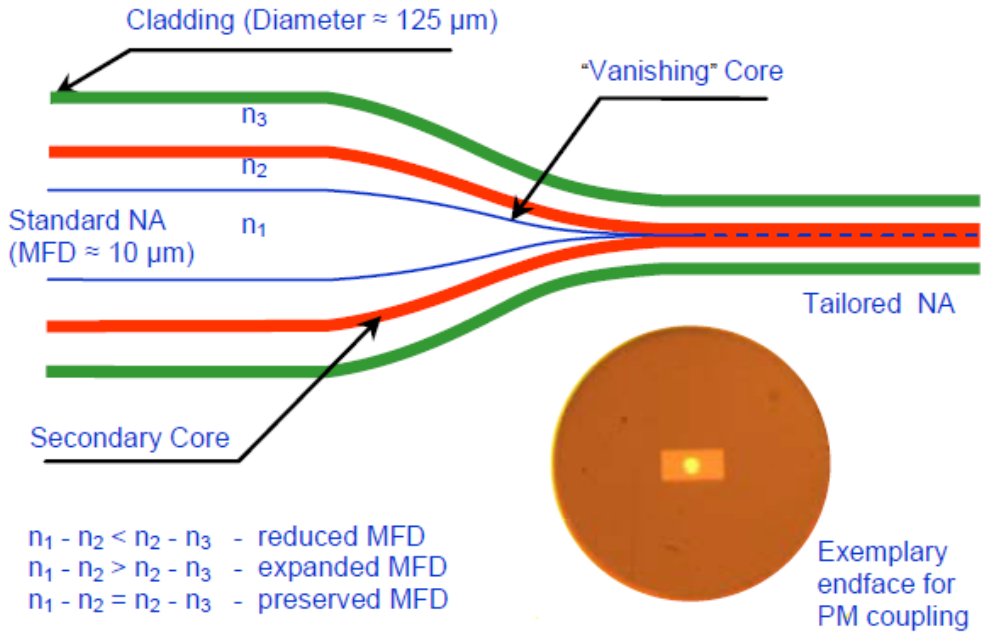

Fig. 1. "Vanishing Core" Concept. The inset showing the end face illustrates the ability to simultaneously modify both the mode field size and shape while maintaining light polarization.

1.

1. Report Type

Final Report

Primary Contact E-mail

Contact email if there is a problem with the report.

xuxd@uw.edu

Primary Contact Phone Number

Contact phone number if there is a problem with the report

206-543-8444

Organization / Institution name

University of Washington

Grant/Contract Title

The full title of the funded effort.

Optoelectronic Device Integration in Silicon (OpSIS)

Grant/Contract Number

AFOSR assigned control number. It must begin with "FA9550" or "F49620" or "FA2386".

FA9550-10-1-0439

Principal Investigator Name

The full name of the principal investigator on the grant or contract.

Xiaodong Xu

Program Manager

The AFOSR Program Manager currently assigned to the award

Dr. Gernot Pomrenke

Reporting Period Start Date

08/01/2010

Reporting Period End Date

07/31/2015

Abstract

This report summarizes achievements in Professor Hochberg's research group at the Universities of Washington and Delaware in the development of fundamental design tools and methodologies for optoelectronic devices in silicon photonics. We proposed to develop fundamental tools and methodologies that enable successful design of complex electronic-photonic integrated devices in silicon. We worked with a number of foundry partners, including BAE Systems, IME, and Luxtera, to develop leading-edge devices, including best-in-class modulators, couplers and detectors, and we prototyped integrated high-complexity devices that showcase these new design and layout capabilities. In particular we focused on devices that closely coupled electronics with photonics for low-loss data transmission, in order to realize multiple order-of-magnitude gains in performance and SWaP metrics. The goals of the project were to develop methodologies for designing and validating electronic-photonic integrated devices in silicon and to demonstrate leading-edge performance for a variety of device categories, including some fundamentally new device types. We developed a community of users for these processes, in order to enable the creation of a multi-project-wafer infrastructure for silicon photonics.

Distribution Statement

This is block 12 on the SF298 form.

Distribution A - Approved for Public Release

Explanation for Distribution Statement

If this is not approved for public release, please provide a short explanation. E.g., contains proprietary information.

SF298 Form

Please attach your SF298 form. A blank SF298 can be found here. Please do not password protect or secure the PDF The maximum file size for an SF298 is 50MB.

SF298 OPSIS Grant 10 13 2015.pdf

Upload the Report Document. File must be a PDF. Please do not password protect or secure the PDF . The maximum file size for the Report Document is 50MB.

OpSIS Final Report_10_14_15 (2).pdf

Upload a Report Document, if any. The maximum file size for the Report Document is 50MB.

Archival Publications (published) during reporting period:

Abdul-Majid, Sawsan, et al. "Photonic integrated interferometer based on silicon-on-insulator nano-scale MMI couplers." Photonics Conference (IPC), 2013 IEEE. IEEE, 2013.

Merget, Florian, et al. "Silicon photonics plasma-modulators with advanced transmission line design." Optics Express, Vol. 21, No. 17 (2013): 19593-19607. (2 citations)

Xiong, Yule, and W. Ye. "Silicon MMI-coupled slotted conventional and MZI racetrack microring resonators." Photonics Technology Letters, Vol. 25, No. 9 (2013): 1885-1888.

Sacher, Wesley, Tymon Barwicz, and Joyce K. Poon. "Silicon-on-Insulator Polarization Splitter-Rotator Based on TM0-TE1 Mode Conversion in a Bi-level Taper." CLEO: Science and Innovations. Optical Society of America (2013).

Simard, Alexandre D., Yves Painchaud, and Sophie LaRochelle. "Integrated Bragg gratings in spiral waveguides." Optics Express Vol. 21 No. 7 (2013): 8953-8963. (3 citations)

Zhu, Kehan, et al. "Design of a 10-Gb/s integrated limiting receiver for silicon photonics interconnects." Circuits and Systems (MWSCAS), 2013 IEEE 56th International Midwest Symposium on Circuits and System. IEEE, 2013.

Runxiang Yu, Stanley Cheung, Yuliang Li, Katsunari Okamoto, Roberto Proietti, Yawei Yin, and S. J. B. Yoo, "A scalable silicon photonic chip-scale optical switch for high performance computing systems," Optics Express Vol. 21 No. 26, (2013): 32655-32667.

Mohammed Shafiqul Hai, Meer Nazmus Sakib, and Odile Liboiron-Ladouceur, "A 16 GHz silicon-based monolithic balanced photodetector with on-chip capacitors for 25 Gbaud front-end receivers," Optics Express Vol. 21, No. 26, (2013): 32680-32689.

Yule Xiong; Ye, W.N., "Slotted silicon microring resonators with multimode interferometer couplers," Group IV Photonics (GFP), 2013 IEEE 10th International Conference on Group IV Photonics (2013): 118 - 119, 28-30 August 2013.

Merget, F., et al. "Novel Transmission Lines for Si MZI Modulators." Group IV Photonics (GFP), 2013 IEEE 10th International Conference on Group IV Photonics (2013): 61 – 62, 28-30 August 2013.

K Zhu, S Balagopal, V Saxena, W Kuang . “Design of a 10-Gb/s integrated limiting receiver for silicon photonics interconnects” Circuits and Systems (MWSCAS), 2013 IEEE 56th International Midwest

Symposium on Circuits and Systems (2013): 713 – 716, 4-7 August 2013.

Yi Zhang, Shuyu Yang, Hang Guan, Andy Eu-Jin Lim, Guo-Qiang Lo, Peter Magill, Tom Baehr-Jones, and Michael Hochberg, "Sagnac loop mirror and micro-ring based laser cavity for silicon-on-insulator," Optics Express 22, 17872-17879 (2014)

Y. Yang, C. Galland, Y. Liu, K. Tan, R. Ding, Q. Li, K. Bergman, T. Baehr-Jones, M. Hochberg. "Experimental demonstration of broadband Lorentz non-reciprocity in an integrable photonic architecture based on Mach-Zehnder modulators." Optics Express Vol. 22, No 14; 17409-17422 (2014).

Y. Liu, R. Ding, Y. Ma, Y. Yang, Z. Xuan, Q. Li, A. E.-J. Lim, P. G.-Q. Lo, K. Bergman, T. Baehr-Jones, M. Hochberg. "Silicon Mod-MUX-Ring transmitter with 4 channels at 40 Gb/s." Optics Express Vol. 22, No. 13; 16431-16438 (2014).

R. Ding, Y. Liu, Q. Li, Z. Xuan, Y. Ma, Y. Yang, A. E.-J. Lim, P. G.-Q. Lo, K. Bergman, T. Baehr-Jones, M. Hochberg. "A Compact Low-Power 320-Gb/s WDM Transmitter Based on Silicon Microrings." Photonics Journal Vol. 6, No. 3 (2014).

Y. Zhang, S. Yang, Y. Yang, M. Gould, N. Ophir, A. E.-J. Lim, P. G.-Q. Lo, P. Magill, K. Bergman, T. Baehr-Jones, M. Hochberg. "A high-responsivity photodetector absent metalgermanium direct contact." Optics Express, Vol. 22, No. 9; 11367-11375 (2014).

H. Guan, A. Novack, M. Streshinsky, R. Shi, Y. Liu, Q. Fang, A. E.-J. Lim, G.-Q. Lo, M. Hochberg, T. Baehr-Jones. "High-efficiency low-crosstalk 1310-nm polarization splitter and rotator built on a SOI platform." Photonics Technology Letters. Vol. PP, No. 99 (2014).

R. Ding, Y. Liu, Q. Li, Y. Ma, K. Padmaraju, A. E.-J. Lim, G.- Q. Lo, K. Bergman, T. Baehr-Jones, M. Hochberg. "Design and characterization of a 30-GHz bandwidth low-power silicon traveling-wave modulator." Optics Communications, Vol. 321; 124-133 (2014).

H. Guan, A. Novack, M. Streshinsky, R. Shi, Q. Fang, A. E.-J. Lim, P. G.-Q. Lo, T. Baehr-Jones, M. Hochberg. "CMOS-compatible highly efficient polarization splitter and rotator based on a double-etched directional coupler." Optics Express, Vol. 22, No. 3; 2489-2496 (2014).

S. Yang, Y. Zhang, D. Grund, G. Ejzak, Y. Liu, A. Novack, D. Prather, A. E.-J. Lim, P. G.-Q. Lo, T. Baehr-Jones, M. Hochberg. "A single adiabatic microring-based laser in 220 nm silicon-on-insulator." Optics Express Vol. 22. No. 1; 1173-1180 (2014).

M. Streshinsky, R. Shi, A. Novack, R. T. P. Cher, A. E.-J. Lim, P. G.-Q. Lo, T. Baehr-Jones, M. Hochberg. "A compact bi-wavelength polarization splitting grating coupler fabricated in a 220 nm SOI platform." Optics Express Vol. 21 No. 25; 31019-31028 (2013).

M. Streshinsky, R. Ding, Y. Liu, A. Novack, Y. Yang, Y. Ma, X. Tu, E. K. S. Chee, A. E.-J. Lim, P. G.-Q. Lo, T. Baehr-Jones, M. Hochberg. "Low power 50 Gb/s silicon traveling wave Mach-Zehnder Modulator near 1300 nm." Optics Express Vol. 21 No. 25; 30350-30357 (2013).

Y. Ma, Y. Zhang, S. Yang, A. Novack, R. Ding, A. E.-J. Lim, G.-Q. Lo, T. Baehr-Jones and M. Hochberg. "Ultralow loss single layer submicron waveguide crossing for SOI optical interconnect." Optics Express Vol. 21 No. 24; 29374-29382 (2013).

A. Novack, M. Gould, Y. Yang, Z. Xuan, M. Streshinsky, Y. Liu, G. Capellini, A. E.-J. Lim, G.-Q. Lo, T. Baehr-Jones and M. Hochberg. "Germanium photodetector with 60GHz bandwidth using inductive gain peaking." Optics Express Vol. 21 No. 23; 28387-28393 (2013).

Y. Liu, M. Hochberg, et. al. “Ultra-responsive Phase Shifters for depletion mode silicon modulators.” IEEE/OSA Journal of Lightwave Technology Vol. 31 No. 23; 3787-3793 (2013).

M. Streshinsky, R. Ding, Y. Liu, A. Novack, C. Galland, A.E.-J Lim, P.Guo-Qiang Lo, T. Baehr-Jones and M. Hochberg. “The Road to Affordable, Large -Scale Silicon Photonics.” Optics and Photonics News Vol. 24 No. 9; 32 – 39 (2013).

Changes in research objectives (if any):

Change in AFOSR Program Manager, if any:

Extensions granted or milestones slipped, if any:

AFOSR LRIR Number

LRIR Title

Reporting Period

Laboratory Task Manager

Program Officer

Research Objectives

Technical Summary

Funding Summary by Cost Category (by FY, $K)

	Starting FY	FY+1	FY+2
Salary			
Equipment/Facilities			
Supplies			
Total			

Report Document

Report Document - Text Analysis

Report Document - Text Analysis

Appendix Documents

2. Thank You

E-mail user

Oct 14, 2015 18:05:59 Success: Email Sent to: xuxd@uw.edu